University of Alberta

Salt-Inducible Kinase 1 and Transducer of Regulated CREB Activity 2 in the Rat Pineal Gland

by

Richard Kanyo

A thesis submitted to the Faculty of Graduate Studies and Research
in partial fulfillment of the requirements for the degree of

Doctor of Philosophy

Physiology

Spring 2014
Edmonton, Alberta

Abstract

In the rat pineal gland, the transcription of the melatonin-rhythm generating enzyme, arylalkyl-N-acetyltransferase (AA-NAT), is stimulated by norepinephrine (NE), acting through the cAMP → protein kinase A (PKA) → cAMP response element-binding protein (CREB) signalling pathway. Although the PKA-mediated phosphorylation of CREB is the main activation mechanism, the transcriptional activity of CREB can also be regulated by the salt-inducible kinase (SIK)/transducer of regulated CREB activity (TORC) pathway. Therefore, the objective of this study was to investigate the mechanisms involved in the regulation of SIK1 and TORC2 in the rat pineal gland and their roles in *Aa-nat* transcription.

We found a marked nocturnal induction of *Sik1* transcription in the rat pineal gland. In cultured pinealocytes, this induction is driven primarily by a β-adrenoreceptor/cAMP-dependent mechanism with a minor contribution from the α_1-adrenoreceptor/Ca^{2+}-pathway. Manipulating the level of *Sik1* expression in pinealocytes shows that endogenous SIK1 can function as a transcription repressor of *Aa-nat*. Studies on TORC2 show that although the TORC2 protein is dephosphorylated in the rat pineal gland with the onset of darkness and in pinealocytes within 15 min of NE stimulation, this occurs without any changes in the *Torc2* mRNA levels. The β-adrenoreceptor/cAMP-pathway and protein phosphatase 2A are involved in the NE-stimulated dephosphorylation of TORC2, which also result in its nuclear translocation. Elevating intracellular Ca^{2+} also

induces dephosphorylation of TORC2 but has no effect on its nuclear translocation. As for the role of TORC2 on *Aa-nat* transcription, whereas overexpression of TORC2 has an enhancing effect on the NE-stimulated *Aa-nat* expression, knockdown of TORC2 only has a small inhibitory effect. Finally, knockdown of endogenous *Sik1* has no effect on the phosphorylation status or cellular distribution of TORC2 under basal or stimulated conditions.

We show that the β-adrenoreceptor/cAMP signalling mechanism is the dominant pathway in inducing *Sik1* transcription and nuclear translocation of TORC2. However, the repressive effect of SIK1 on *Aa-nat* cannot be explained by regulating the cellular distribution of TORC2. Moreover, the phosphorylation status of TORC2 may not accurately reflect its activation and that TORC2 cellular distribution is not regulated solely by SIK1.

Acknowledgement

I would like to thank Dr. Ho and Dr. Chik for their patience and mentorship over the past years. I also would like to acknowledge former and current lab members who assisted me. These include: Dr. Donald Price, Wendy Dukewich, Nick Amyotte, Meghan Ferguson and James McTague.

I also appreciate the feedback from my supervisory committee. Finally, I like to thank the Government of Canada for the financial support through the Queen Elizabeth II Graduate Scholarship and the Canadian Institutes of Health Research.

Table of Contents

List of Tables Page

List of Figures

Chapter 1

Chapter 3

Chapter 4

List of Abbreviations

5-HT, 5-hydroxtryptamine

α_1-ADR, α_1-adrenergic receptor

AA-NAT, arylalkylamine-N-acetyltransferase

Ala, alanine

AKAP, A-kinase anchoring protein

AMPK, AMP-activated protein kinase

AP-1, activating protein-1

ATF, activating transcription factor

ATP, adenosine triphosphate

β-ADR, β-adrenergic receptor

bZIP, basic leucine zipper domain

CALY A, calyculin A

cAMP, cyclic adenosine monophosphate

CBP, CREB-binding protein

CBD, CREB-binding domain of TORC2

CEB, cytoplasmic extraction buffer

cGMP, cyclic guanosine monophosphate

CIP, calf intestinal alkaline phosphatase

CRE, cAMP response element

CREB, cAMP response element-binding protein

CREM, CRE-modulator

CSA, cyclosporine A

CYP11A1, side chain cleavage P450

DAG, diacylglycerol

dBcAMP, dibutyryl cAMP

dBcGMP, dibutyryl cGMP

Dio2, type 2 iodothyronine deiodinase

DMEM, Dulbecco's modified Eagle's medium

DRE, downstream regulatory element

DREAM, DRE antagonist modulator

E. coli, *Escherichia coli*

EBSS, Earle's balanced salt solution

FCS, fetal calf serum

FRA-2, fos-related antigen-2

G6Pase, glucose-6-phosphatase

GABA, γ-amino butyric acid

GAM, goat anti-mouse antibody

GAR, goat anti-rabbit antibody

GAPDH, glyceraldehyde-3-phosphate-dehydrogenase

GFP, green fluorescence protein

GTP, guanosine triphosphate

GTF, general transcription factor

h, hour(s)

HEK, human embryonic kidney

HIOMT, hydroxyindole-O-methyltransferase

H3, histone 3

HRP, horseradish peroxidise

ICER, inducible cAMP early repressor

IML, intermediolateral nucleus

IP_3, inositol 1,4,5-trisphosphate

ISO, isoproterenol

JDP, Jun dimerization protein

KID, kinase inducible domain

KIX, KID interacting domain

Lys, lysine

MAPK, mitogen-activated protein kinase

MARK, microtubule affinity-regulating kinase

min, minutes

Mkp-1, MAPK-phosphatase-1

nAchR, nicotinic acetylcholine receptors

NAS, N-acetylserotonin

NE, norepinephrine

NIF, nifedipine

OKA, okadaic acid

PACAP, pituitary adenylate cyclase-activating polypeptide

PBS, phosphate buffered saline

PCR, polymerase chain reaction

pCREB, phosphorylated CREB

PDE, phosphodiesterase

PE, phenylephrine

PEPCK, phosphoenolpyruvate carboxykinase

Pfu, *Pyrococcus furiosis*

PIC, preinitiation complex

PKA, cAMP-dependent protein kinase

PKC, protein kinase C

PKG, protein kinase G

PLCβ, the β isotype of PLC

PLC, phospholipase C

PIP_2, phosphatidylinositol 4,5-bisphosphate

PMA, 4β phorbol 12-myristate-13-acetate

PME-1, protein phosphatase methylesterase-1

Pol II, RNA-polymerase II

PP2A, protein phosphatase 2A

PP2B, protein phosphatase 2B

PRAZ, prazosin

PROP, propranolol

PSF, penicillin streptomycin amphotericin B

PVN, paraventricular nucleus

PVDF, polyvinylidene difluoride

RG, regulatory domain

RHT, retinohypothalamic tract

rpm, revolutions per minute

SCG, superior cervical ganglia

SCN, suprachiasmatic nucleus

SDS, sodium dodecyl sulfate

Ser, serine

SIK, salt-inducible kinase

Sik1-fl, adenovirus overexpressing the full-length *Sik1* transcript

Sik1-S577A, adenovirus overexpressing a mutated *Sik1* transcript (Ser577 substituted for Ala)

Sik1-fl-gfp, adenovirus overexpressing the *Sik1* transcript fused to *Gfp*

Sik1-sh, adenovirus expressing shRNAs against the *Sik1*transcript

shRNA, short-hairpin RNA

siRNA, small-interfering RNA

SNF, sucrose non-fermenting

StAR, steroidogenic acute regulatory protein

TAF, TBP-associating factors

Taq, Thermus aquaticus polymerase

TAU, tautomycin

TBP, TATA-binding protein

TBS, Tris-Cl buffered saline

TF, transcription factor

TORC, transducer of regulated CREB activity

Torc2-fl, adenovirus overexpressing the full-length *Torc2* transcript

Torc2-S171A, adenovirus overexpressing a mutated *Torc2* transcript (Ser171 substituted for Ala)

Torc2-sh, adenovirus expressing shRNAs against TORC2

TTBS, Tris-Cl buffered saline with Tween-20

VIP, vasoactive intestinal peptide

wk, week

ZT, Zeitgeber time

Chapter 1

Introduction

1.1 The Pineal Gland

A) The pineal gland and its hormone

The pineal gland, a pine cone shaped neuroendocrine organ (hence its name) is located near the center of the brain, between the two hemispheres. In the mammalian pineal gland, information on environmental lighting conditions that is neuronally encoded by the retina is converted into nocturnally elevated synthesis of the hormone melatonin (reviewed by Korf et al., 1998). Melatonin, a lipophilic hormone discovered by Aaron B. Lerner (1960) and the only known hormone produced by the pineal gland, is believed to have an important role in entraining circadian physiology (reviewed in Arendt, 1998). Since the nocturnal increase of melatonin is present in both diurnal and nocturnal animals, this molecule is also called the "hormone of darkness" (reviewed in Korf et al., 1998). The physiological function of melatonin is transduced via melatonin receptors that are able to respond to pmol concentration of this hormone (Reppert et al., 1995; Roca et al., 1996). The duration of nocturnally elevated melatonin levels varies across different seasons due to changes in day length. This hormonal message may provide a survival advantage by allowing the organism to adapt to seasonally related changes in environmental conditions such as temperature, rainfall and food availability. In seasonal animals, the duration of elevated circulating melatonin has been shown to regulate reproductive behaviours and pelage (coat growth or color; reviewed in Arendt, 1998). However, there is no clear evidence that melatonin is involved in regulating the reproductive axis in humans. Although changes in melatonin levels have been linked to metabolic disorders,

insomnia and depression in humans (reviewed in Arendt, 1998), it is unclear whether this is just an association or melatonin is of relevance to the pathogenesis of these conditions. In spite of this, melatonin has been used as a sleep aid and management of jet leg and the suppression of melatonin synthesis has been assumed to be one of the mechanism through which light-therapy alleviate seasonal affective disorder.

B) The neuronal pathways that regulate melatonin secretion in mammals

In lower vertebrates such as fish, amphibians, reptiles and avian species, the pineal gland itself is photosensitive. In comparison, the mammalian pineal gland does not detect light directly (reviewed by Korf et al., 1998). Instead, the pineal gland receives neuronal signals that are transmitted through multiple structures in the brain. Light is transduced into neuronal signals by the retina, which are then transmitted through the retinohypothalamic tract and projected to the suprachiasmatic nucleus (SCN) (Ebling, 1996). Gamma-aminobutyric acid (GABA)ergic and glutamatergic output from the SCN innervate the paraventricular nucleus (PVN) (Kalsbeek et al., 2000; Perreau-Lenz et al., 2003; Perreau-Lenz et al., 2004). During daytime, inhibitory GABAergic output from the SCN (Kalsbeek et al., 1999; Kalsbeek et al., 2000) overrides the stimulatory glutamatergic output signal to the PVN (Perreau-Lenz et al., 2003; Perreau-Lenz et al., 2004). During nighttime, the GABAergic signal is absent and the glutamatergic signal is transmitted to the PVN. From the PVN, neuronal signals are projected to the intermediolateral nucleus (IML) from which the signals are

transmitted to the superior cervical ganglia (SCG) (Klein et al., 1983; Moore and Klein, 1974). It is the postganglionic norepinephrine (NE)-containing fibres of the SCG that innervate the pineal gland (Fig. 1) (Klein et al., 1983; Moore and Klein, 1974) and stimulate the synthesis of melatonin at night. Melatonin, being lipophilic, is not stored in the pineal gland and is released after synthesis.

The rhythmic release of melatonin from the pineal gland is generated by the endogenous clock located in the SCN, which also controls the rhythmic responses of many other different tissues throughout the body (reviewed in Bass and Takahashi, 2010). Hence, the endogenous clock in the SCN is sometimes referred to as the "master circadian oscillator".

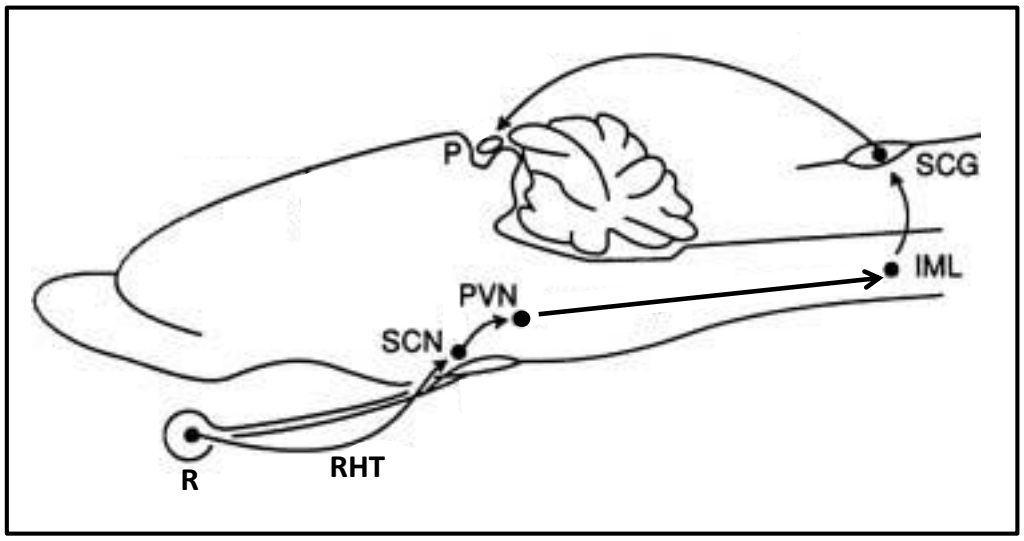

Figure 1: The neural circuitry from the retina to the pineal gland. Environmental lighting-status is transduced into neuronal signals by the retina (R). The neuronal signal travels from the retina through the retinohypothalamic tract (RHT) to the suprachiasmatic nucleus (SCN). The SCN is connected to the paraventricular nucleus (PVN), which then transmits the signal to the intermediolateral cell column (IML) in the spinal cord. From the IML, the signal is transmitted to the superior cervical ganglia (SCG), from which it is projected to the pineal gland (P) (figure modified from Ganguly et al., 2002).

C) The melatonin-rhythm generating enzyme: arylalkylamine N-acetyltransferase

At night, NE is released from the nerve terminals of the SCG that innervate the pineal gland and stimulates the synthesis of melatonin (Klein et al., 1983; Moore and Klein, 1974). Melatonin is hydrophobic and can diffuse through the cell membrane and blood-brain barrier. After being synthesized, this molecule is not stored at high concentration inside the pinealocyte and is released directly into the circulation. Therefore, the level of circulating melatonin is controlled by the enzymes involved in the biochemical pathway of melatonin synthesis. Transformation of melatonin into an inactive compound by the liver ensures that the circulating level of this hormone declines within 15 min once the synthesis of this molecule stops (Iguchi et al., 1982; Illnerova et al., 1978; Kopin et al., 1961).

In the pineal gland, melatonin is synthesized from serotonin in two biochemical steps. First, arylalkylamine N-acetyltransferase (AA-NAT) adds an acetyl-group to the serotonin molecule, converting serotonin into N-acetylserotonin (NAS; Fig. 2 left) (Klein et al., 1970a; Weissbach et al., 1960). This biochemical reaction is reflected in a decline of serotonin level and an increase of NAS level in the pineal gland at night (Fig. 2 right). The final enzymatic step involves the addition of a methyl group to NAS by hydroxyindole-O-methyltransferase (HIOMT) resulting in the formation of melatonin (Fig. 2 left) (Klein and Weller, 1970). In comparison to AA-NAT activity, which is undetectable at daytime and increases greatly at nighttime, HIOMT activity changes little between day and night (Klein et al., 1970b). Because NAS level is

low during daytime, melatonin synthesis by HIOMT is limited. With the nocturnal increase of AA-NAT activity, NAS synthesis is elevated resulting in increased synthesis of melatonin by HIOMT. Hence, the daily rhythm of circulating melatonin is generated by regulating the daily rhythm of AA-NAT activity through the release of NE from the nerve terminals innervating the pineal gland. The daily variation of circulating adrenaline level has no impact on the AA-NAT rhythm.

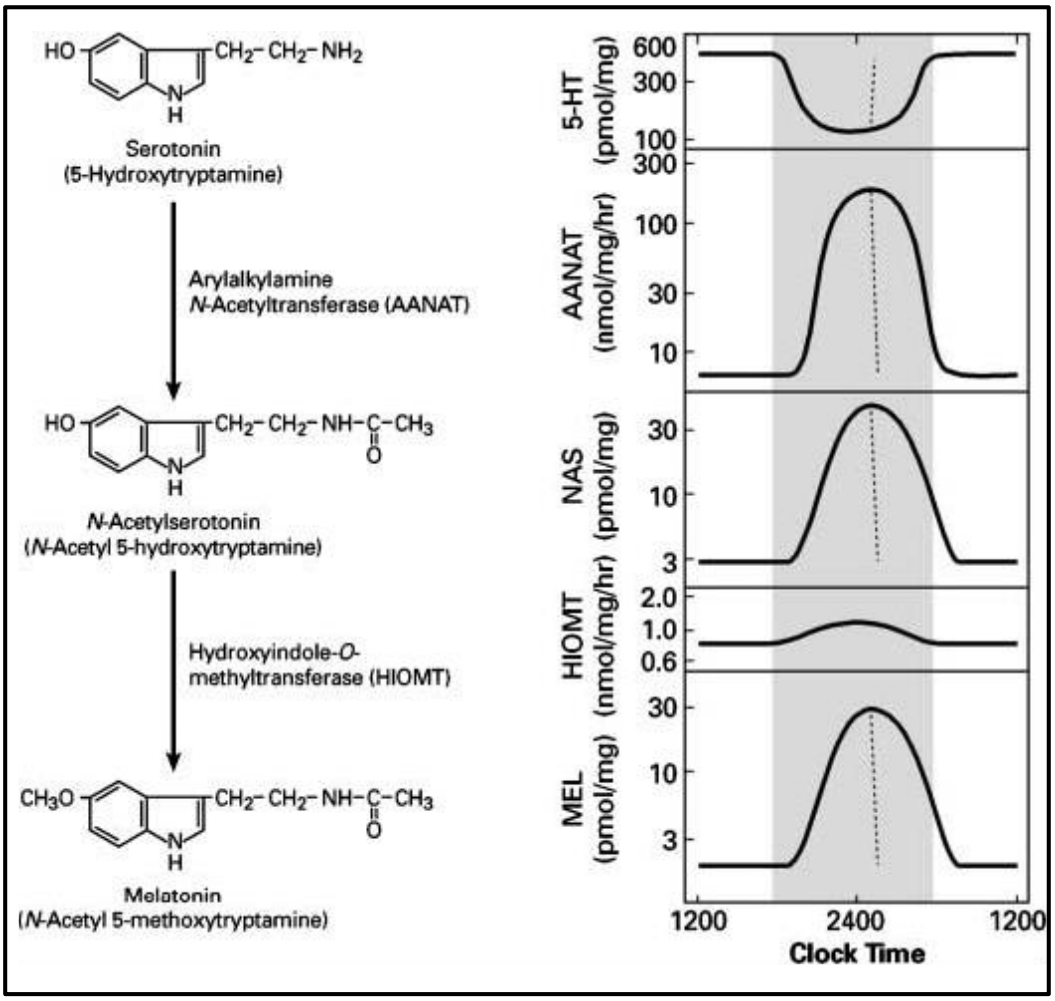

Figure 2: The role of arylalkylamine N-acetyltransferase (AA-NAT) in melatonin synthesis. On the left: The biosynthesis of melatonin (MEL) occurs in two major enzymatic steps: First, the conversion of serotonin (5-hydroxytryptamine; 5-HT) into N-acetylserotonin (N-acetyl 5-hydroxytryptamine; NAS) by AA-NAT. Then, NAS is converted into MEL (N-acetyl 5-methoxytryptamine) by hydroxyindole-O-methyltransferase (HIOMT). On the right: During night (grey area), while the amounts of 5-HT decrease, AA-NAT enzymatic activity, NAS and MEL increase. However, relative to the increases in AA-NAT and NAS, little change in HIOMT activity is observed (figure from Ganguly et al., 2002).

1.2 Signal transduction pathways regulating AA-NAT in the rat pineal gland

Environmental lighting synchronizes the endogenous clock in the SCN, which send signals to the pineal gland and ensures that AA-NAT synthesis is induced only at night. At night, NE is released from the sympathetic nerve terminals that innervate the pineal gland and stimulates both β- and α_1-adrenergic receptors (Axelrod, 1974; Vanecek et al., 1985). Stimulation of the β-adrenergic receptor initiates the synthesis of the second messengers, cAMP and cGMP (Ho et al., 1987a; Sugden and Klein, 1987). Stimulation of the α_1-adrenergic receptor activates phospholipase C (PLC) (Ho et al., 1988a; Ho and Klein, 1987) and protein kinase C (PKC) (Sugden et al., 1985), and elevates intracellular Ca^{2+} (Sugden et al., 1987). Although AA-NAT expression is induced mainly through the cAMP pathway (Ganguly et al., 2001; Gastel et al., 1998; Roseboom et al., 1996; Roseboom and Klein, 1995), other signalling pathways have also been shown to modulate the NE-stimulated AA-NAT level (reviewed by Ho and Chik, 2010).

A) Role of β-adrenergic receptor stimulation

Regulation of cAMP and cGMP

The synthesis of intracellular cAMP and cGMP can be stimulated through the β-adrenergic receptor, which is coupled to a (GTP)-binding protein (G_s-protein). The G_s-protein consists of three subunits: $G_s\alpha$, Gβ and Gγ. When the agonist binds to the receptor, the $G_s\alpha$-subunit dissociates from the Gβγ complex and binds to adenylyl cyclase (reviewed in Gilman, 1987). Adenylyl cyclase is

activated by the association to the $G_s\alpha$-subunit and starts converting ATP to cAMP (reviewed in Wettschureck and Offermanns, 2005). Intracellular cGMP levels are stimulated by activating guanylyl cyclase which converts GTP to cGMP (reviewed in Hurley, 1998).

In the rat pineal gland, stimulation of the β-adrenergic receptor is an absolute requirement for elevation of intracellular cAMP and cGMP levels (Ho et al., 1987a; Sugden and Klein, 1987) (Fig. 3). However, simultaneous α_1-adrenergic receptor stimulation can further increase cAMP and cGMP levels induced by activation of the β-adrenergic receptor (described in *Section 1.2 B*).

The intracellular cAMP level is controlled by synthesis via the adenylyl cyclase and its degradation via phosphodiesterases (PDEs). Whereas a rhythm of PDE activity in the pineal has been known for a long time (Minneman and Iversen 1976), the molecular basis for this rhythm was only established 30 years later (Kim *et al.* 2007a). The nocturnal elevation of PDE activity in the pineal gland is due to an increase in the transcription of *Pde4b2* followed by a corresponding increase in protein and enzyme activity (Kim *et al.* 2007). This induction of PDE4B2 may function as a negative feedback signal that limits the synthesis of cAMP and therefore the duration of AA-NAT induction (Kim et al., 2007).

Downstream effect of intracellular cAMP elevation

Increases of intracellular cAMP levels activate protein kinase A (PKA; Fig. 3 Bottom), which consists of four subunits: two regulatory- and two catalytic-subunits (reviewed in Francis and Corbins, 1999). Following elevation of

intracellular cAMP, two cAMP molecules bind to each of the regulatory subunits. The conformational change initiated by the binding of cAMP causes the detachment of the two catalytic subunits which are then distributed in the cytoplasm and the nucleus.

In the rat pineal gland, the NE-stimulated induction of AA-NAT is mainly controlled by activation of the cAMP/PKA pathway (Ganguly et al., 2001; Gastel et al., 1998; Roseboom and Klein, 1995). In the nucleus, PKA activates the transcription of *Aa-nat* by phosphorylating the cAMP response element-binding protein (CREB) (Baler et al., 1997; Roseboom and Klein, 1995) (Fig. 4 page 17; also described in *Section 1.3*). In the cytoplasm, PKA-mediated phosphorylation of AA-NAT protects the protein from degradation by the proteasome (Ganguly et al., 2001; Gastel et al., 1998). The protection from the proteasome is due to the interaction of phosphorylated AA-NAT with a scaffolding protein, 14-3-3 (Ganguly et al., 2001).

Other cAMP-mediated pathways are also involved in modulating AA-NAT expression. The involvement of members of the mitogen-activated protein kinase (MAPK) family in regulating gene transcription is well established (reviewed in Kyriakis and Avruch, 2001). Studies in the rat pineal gland show increased phosphorylation of p38MAPK following the activation of the PKA signalling pathway (Chik *et al.* 2004). Studies with p38MAPK inhibitors suggest that this kinase likely has a modulating effect on the amplitude and duration of the AA-NAT response (Man *et al.* 2004).

Post-translational modifications of histone have also been found to regulate gene expression (reviewed by Grunstein *et al.* 1997; Jenuwein and Allis, 2001) and have been investigated in the pineal gland. Activation of the cAMP/PKA-pathway also leads to phosphorylation of the Ser10 residue on histone H3. The NE-stimulated increase of H3Ser10 phosphorylation precedes the induction of *Aa-nat* (Chik et al., 2007a). Inhibition of Aurora C, a histone kinase, which is activated through the cAMP pathway, not only reduces the NE-stimulated H3Ser10 phosphorylation but also the NE-stimulated *Aa-nat* expression (Price et al., 2009). This suggests that phosphorylation of H3Ser10 may also modulate NE-stimulated *Aa-nat* transcription. In addition to phosphorylation, histone H3 acetylation was also investigated in the pineal gland, but is likely not regulated by the cAMP-pathway (Ho et al., 2007a).

Downstream effect of intracellular cGMP elevation

Less is known about the role of cGMP in modulating AA-NAT expression compared to cAMP and Ca^{2+}. In general, the main function of cGMP is to activate protein kinase G (PKG; reviewed in Francis and Corbin, 1999). In rat pinealocytes, cGMP has been shown to stimulate the phosphorylation-dependent activation of p42/44MAPK (Ho et al., 1999). Activation of p42/44MAPK occurs during the early part of night which precedes the activation of p38MAPK (Ho *et al.* 2003, Chik *et al.* 2004). Studies with selective MAPK inhibitors reveal the involvement of p42/44MAPK in the early induction of AA-NAT (Ho *et al.* 2003; 2006; Man *et al.* 2004). Moreover, cGMP has been shown to modulate the L-type

Ca^{2+} channel currents in rat pinealocytes, causing inhibition of this current (Chik *et al.* 1995).

B) Role of α_1-adrenergic receptor stimulation

Regulation of intracellular Ca^{2+}elevation and PKC activation

In the rat pineal gland, stimulation of the α_1-adrenergic receptor activates PLC (Ho et al., 1988a; Ho and Klein, 1987), PKC (Sugden et al., 1985) and elevates intracellular Ca^{2+} (Sugden et al., 1987). The α_1-adrenergic receptor is coupled to a G_q-protein, which activates PLCβ once the receptor is stimulated. Activated PLC degrades phospholipids converting phosphatidylinositol 4,5-bisphosphate (PIP_2) into diacylglycerol (DAG) and inositol 1,4,5-trisphosphate (IP_3) (reviewed in Rhee, 2001). Whereas DAG is involved in PKC activation (reviewed in Nishizuka, 1995), IP_3 causes elevation of intracellular Ca^{2+} level by releasing Ca^{2+} from the intracellular Ca^{2+} stores. The increases of intracellular Ca^{2+} mediated through α_1-adrenergic receptors are due to both IP_3-sensitive intracellular stores (Saez et al., 1994; Schomerus et al., 1995) and the influx of Ca^{2+} from the extracellular space (Sugden et al., 1987) through store-operating Ca^{2+}channels (Lee et al., 2006; Zemkova et al., 2011). As described below, intracellular Ca^{2+} elevation is of importance to the activation of the PKC (Ho et al., 1988b) and the Ca^{2+}/calmodulin pathway (Ho et al., 1991).

The mechanism of PKC activation has been well established (reviewed in Nishizuka, 1995). In general, DAG and Ca^{2+} synergistically activate PKC. Intracellular DAG elevation increases the affinity of PKC to Ca^{2+} and causes the

translocation of PKC from the cytosol to the plasma membrane where the active enzyme becomes stabilized by interacting with membrane phospholipids (reviewed in Nishizuka, 1995 and Webb et al., 2000).

In the rat pinealocyte, mimicking an increase in DAG concentration with the addition of a DAG-analogue, phorbol 12-myristate 13-acetate (PMA), can activate PKC in the presence of basal Ca^{2+} concentration (Ho et al., 1988b). In addition, the basal DAG concentration in the rat pinealocyte is at a sufficient threshold so that intracellular Ca^{2+} elevation alone can also cause the membrane translocation and activation of PKC (Ho et al., 1988b). It is likely that during NE stimulation, both increases in DAG and intracellular Ca^{2+} are involved in activating PKC in rat pinealocytes.

Besides activating PKC, intracellular Ca^{2+} elevation can also activate the Ca^{2+}/calmodulin-dependent pathway in rat pinealocytes (Ho et al., 1991). The mechanism of activation of the calmodulin-dependent pathway involves the direct interaction of elevated intracellular Ca^{2+} with the calmodulin. Ca^{2+}/calmodulin can interact with Ca^{2+}/calmodulin-dependent kinases (reviewed in Chin and Means, 2000; Braun and Schulman, 1995) and protein phosphatase 2B (PP2B; also known as calcineurin) (reviewed in Shi, 2009).

Downstream effect of PKC activation and intracellular Ca^{2+} elevations

Although stimulation of the β-adrenergic receptor can signal the increase in cAMP and cGMP in the rat pinealocyte, simultaneous activation of the α_1-adrenergic receptor can potentiate the effects of the stimulated β-adrenergic

receptor and further elevates cAMP and cGMP levels by 10- and 200-folds, respectively (Vanecek et al., 1985). α_1-Adrenergic receptor-mediated PKC activation is sufficient to potentiate the β-adrenergic-stimulated intracellular cAMP level (Sugden et al., 1985) and also translates into increased AA-NAT activity (Sugden et al., 1985; Zatz, 1985). However, the full potentiation of β-adrenergic-stimulated intracellular cGMP is different in that it requires both activation of PKC and simultaneous elevation of intracellular Ca^{2+} (Ho et al., 1987a). This probably reflects that the Ca^{2+}/calmodulin-dependent pathway is also involved in regulating cGMP level and, to a lesser degree, cAMP (Ho et al., 1991).

Other downstream effects of PKC activation and intracellular Ca^{2+} elevation include regulation of the protein stability of one of the cAMP inducible gene products, MAPK-phosphatase-1 (MKP-1) (Price et al., 2004a; Price et al., 2004b). Although the mechanism by which PKC and Ca^{2+} stabilizes the MKP-1 protein remains to be determined, knockdown of endogenous *Mkp-1* expression enhances p42/44MAPK phosphorylation and increases the NE-stimulated AA-NAT protein level (Price et al., 2007). This suggests that MKP-1 can modulate AA-NAT activity by reversing the phosphorylation-dependent activation of p42/44MAPK.

C) Other Receptors

NE is accepted to be the main neurotransmitter that signals intracellular elevations of cAMP, cGMP and Ca^{2+} levels in the rat pinealocyte. However,

many other receptors are also expressed in the rat pineal gland (Bailey et al., 2009). The effects of peptide hormones, vasoactive intestinal peptide (VIP) and pituitary adenylate cyclase-activating polypeptide (PACAP), in the rat pineal gland have been investigated. Stimulation of either PACAP or VIP receptors can elevate cAMP (Chik and Ho, 1995; Chik et al., 1988; Ho et al., 1987b). Although PACAP and VIP receptors belong to the same peptide receptor family, only activation of VIP receptors can elevate cGMP (Chik and Ho, 1995). The VIP-stimulated cAMP and cGMP responses can be potentiated by activation of α_1-adrenergic receptors (Chik et al., 1988; Ho et al., 1987b). Receptors that can elevate intracellular Ca^{2+} have also been found. Stimulation of the nicotinic subtype of acetylcholine receptors (nAchR) increases intracellular Ca^{2+} levels through depolarization, probably through the opening of voltage-gated L-type Ca^{2+} channels (Letz et al., 1997).

Although many other receptors are expressed in the rat pineal gland (Bailey et al., 2009), only NE-containing nerve fibers have been found to innervate the pineal gland and regulate AA-NAT activity (Klein et al., 1983; Moore and Klein, 1974). This suggests that the major changes of intracellular cAMP, cGMP and Ca^{2+} levels, which control the AA-NAT response, are mediated by NE stimulation through the β- and α_1-adrenergic receptors. Therefore, only NE-stimulated pathways will be investigated in this study.

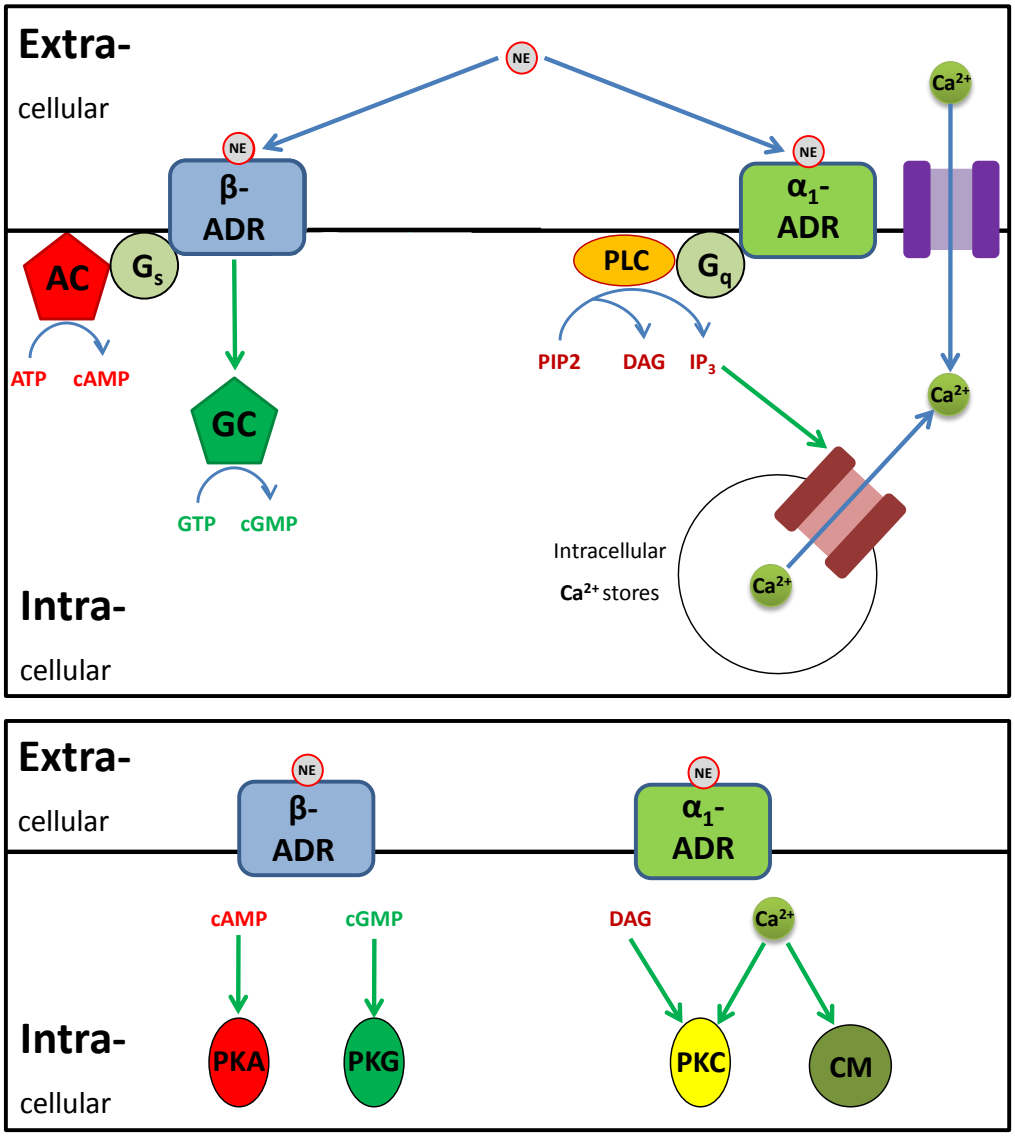

Figure 3: Transmembrane signal transduction in the rat pineal gland. Top, NE activates both β-adrenergic receptor (β-ADR; coupled to a G_s-protein) and α_1-ADR (coupled to a G_q-protein). Stimulation of β-ADR activates adenylyl cyclase (AC) and guanylyl cyclase (GC) which converts ATP to cAMP and GTP to cGMP, respectively. Stimulation of the α_1-ADR activates phospholipase C (PLC) which cleaves phosphatidylinositol 4,5-bisphosphate (PIP_2) into diacylglycerol (DAG) and inositol 1,4,5-trisphosphate (IP_3). α_1-ADR activation also initiates increases in intracellular elevation of Ca^{2+}. Intracellular elevation of Ca^{2+} involves influx of extracellular Ca^{2+} through store-operated Ca^{2+}channels (purple) and depletion of intracellular Ca^{2+} stores through Ca^{2+}channels sensitive to IP_3 (brown; green arrow). **Bottom**, cAMP activates protein kinase A (PKA), cGMP activates PKG and Ca^{2+} activates calmodulin (CM). PKC is activated by DAG and Ca^{2+}.

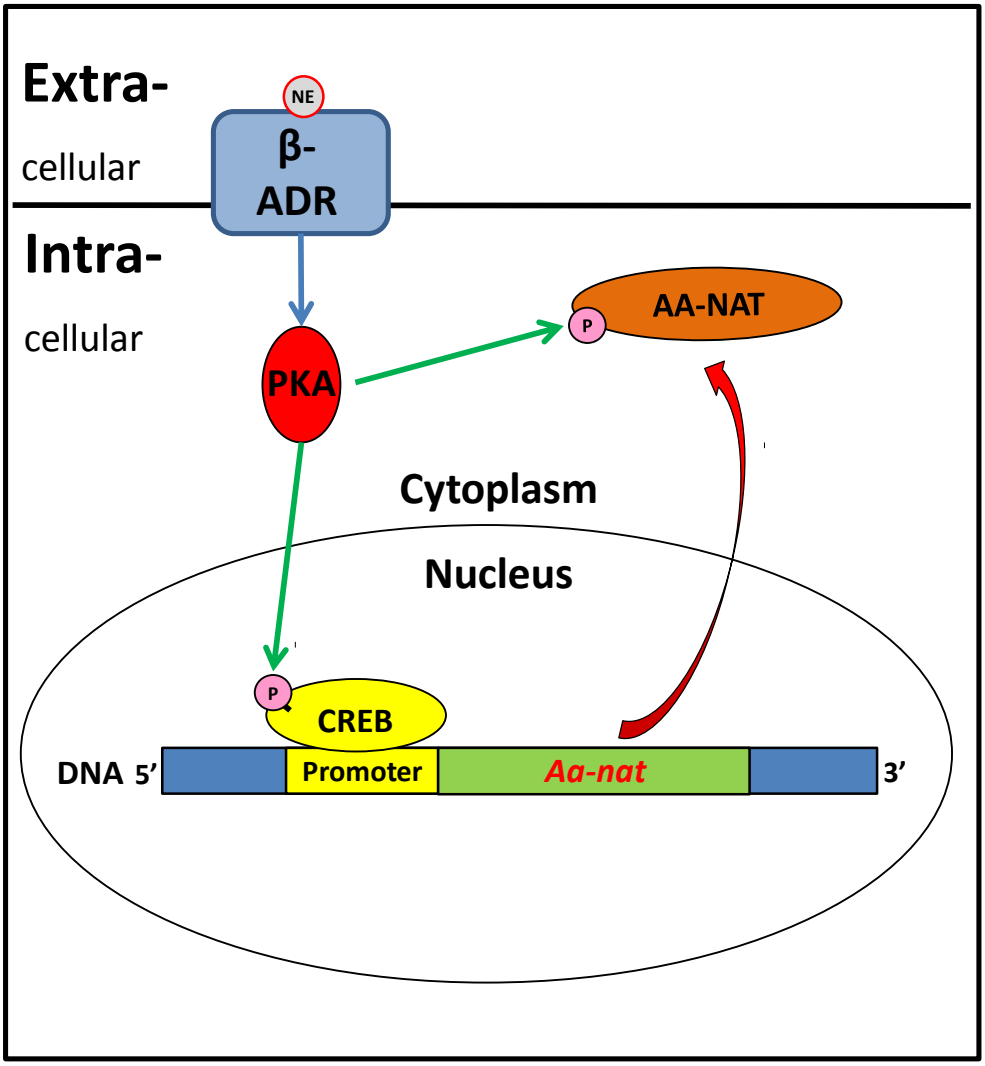

Figure 4: PKA downstream mechanisms. NE activates the β-adrenergic receptor (β-ADR) which in turn leads to the activation of protein kinase A (PKA). In the nucleus, PKA phosphorylates the cAMP response element-binding protein (CREB), which is bound to the promoter of *Aa-nat*. *Aa-nat* is transcribed and translated into the AA-NAT protein (red arrow). In the cytoplasm, PKA phosphorylates AA-NAT directly, which prevents AA-NAT from proteolytic degradation. Green arrows highlight the actions of PKA.

1.3 Regulation of CREB-mediated *Aa-nat* transcription

In the rat pineal gland, the daily rhythm of circulating melatonin is driven by CREB-mediated transcription of the *Aa-nat* gene (Roseboom et al., 1996; Roseboom and Klein, 1995). In general, genes are transcribed by the preinitiation complex (PIC) consisting of the RNA polymerase II (Pol II) and general transcription factors (GTFs) (reviewed in Smale and Kadonaga, 2003). The PIC is assembled at the promoter of the gene, which contains different elements. These promoter elements serve as binding sites for GTFs and additional transcription factors that can regulate gene transcription, such as activators and repressors (reviewed in Lee and Young, 2000). Whereas activators help the assembling of PIC, repressors inhibit this process. Coactivators, such as the CREB-binding protein (CBP), can also regulate gene transcription. Instead of interacting with DNA directly like activators and repressors, coactivators bind to the activator.

A) The promoter-region of Aa-nat

The promoter region of *Aa-nat* was found to contain two basic transcription elements, a TATA box, consisting of alternating thymine and adenine nucleotides, and an initiator motif, consisting of alternate purine-pyrimidine repeat (Baler et al., 1997). Both the initiator motif and the TATA box are important for the assembling of the PIC at the promoter-region in general (reviewed in Smale and Kadonaga, 2003). The TATA box is recognized by the

GTF, TFIID, which is accepted to be critical in the recruitment of Pol II (Felinski et al., 2001).

Several elements that can be targeted by activators and repressors have also been identified in the promoter region of *Aa-nat* (Baler et al., 1997). These include a cAMP response element (CRE), an activating protein-1 (AP-1)-like element (Baler et al., 1997) and two downstream regulatory elements (DREs) (Link et al., 2004). The CRE-site of *Aa-nat* (TGACGCCA) closely resembles the perfect CRE consensus-site (TGACGTCA) (Baler et al., 1997). The interaction of phosphorylated CREB (pCREB) with the CRE-site is of importance to the activation of *Aa-nat* transcription, but other elements may also be involved in modulating *Aa-nat* expression.

In general, activators and repressors interact with the DNA directly at elements, including the ones described above. They consist of at least two domains, a stimulus-sensitive domain and a DNA-element interacting domain (reviewed in Lee and Young, 2000). Element-specific activators and repressors ensure that only genes that contain the corresponding element will be turned on or off, respectively (reviewed in Lee and Young, 2000; Gaston and Jayaraman, 2003). Therefore, an external stimulus can regulate the transcription of some genes without influencing the expression of others. In addition, one gene can be regulated by many different activators and/or repressors if the promoter contains the corresponding elements.

B) Modulation of Aa-nat gene transcription via CREB phosphorylation

In the rat pineal gland, the CREB-driven transcription of *Aa-nat* has been well investigated using pharmacological agents and organ cultures. At night, *Aa-nat* transcription is activated via PKA-mediated phosphorylation of CREB following the NE stimulation of the β-adrenergic receptor/cAMP-pathway (Roseboom and Klein, 1995). The basal *Aa-nat* transcription is low during the day and elevated by over 150-folds at night. This large induction drives the daily rhythm of circulating melatonin (Roseboom et al., 1996). Therefore, regulating the NE-stimulated transcription of *Aa-nat* through CREB can control melatonin synthesis at night.

The accepted mechanism by which CREB-dependent gene transcription is activated in general is through PKA-mediated phosphorylation of Ser133 on CREB (Gonzalez and Montminy, 1989). The CREB-coactivator, CBP, interacts with the phosphorylated Ser133 residue on CREB (Chrivia et al., 1993; Radhakrishnan et al., 1997) and promotes CREB-dependent transcription by acetylating histones (Bannister and Kouzarides, 1996; Kwok et al., 1994; Martinez-Balbas et al., 1998; Ogryzko et al., 1996). Acetylation of the histone N-terminal neutralizes the nucleosome by removing the positive charge from the histones (reviewed in Grunstein, 1997). This causes the "loosening" of the negatively charged chromatin fiber that wraps around the nucleosome, making the promoter more accessible to other activators and GTFs (reviewed in Grunstein, 1997).

1.4 The transcriptional activator, CREB

CREB is an important transcriptional activator that has been linked to many physiological functions including memory formation (Bourtchuladze et al., 1994; Kaang et al., 1993; Yin et al., 1994), glucose metabolism (Herzig et al., 2001), steroidogenesis (Inoue et al., 1991; Manna et al., 2002), immune function (Gubina et al., 2001), cell proliferation, cell survival and cell differentiation (reviewed in Wen et al., 2010). In mammals, this activator is evolutionarily conserved with homologs present in many different species including humans, mice, *Drosophila melanogaster* (Yin et al., 1994) and yeast (Fimia et al., 1999). Members of the CREB family, such as CREM and ATF1, are characterized by a basic leucine zipper (bZIP) domain (reviewed in Mayr and Montminy, 2001). The CREB protein is composed of two hydrophobic glutamine rich sequences (Q1 and Q2, starting from the N-terminus) separated by the kinase-inducible domain (KID; Fig. 5A). The Q2-sequence is then followed by the bZIP domain (Fig. 5A) (reviewed in Mayr and Montminy, 2001).

The roles of the CREB domains, Q2, KID and bZIP, are highlighted in Figure 5. The Q2 domain promotes gene transcription by interacting with TAF130, a component of TFIID (Ferreri et al., 1994; Saluja et al., 1998). TFIID in turn can recruit Pol II, which then starts transcription (Felinski et al., 2001). As already mentioned, phosphorylation of the Ser133 residue of CREB (located in KID) by PKA is considered to be the key event in activating transcription (Fig. 5) (Gonzalez and Montminy, 1989; Mayr and Montminy, 2001). The PKA-dependent phosphorylation of CREB leads to the interaction of CREB with the

KID-interacting (KIX) domain of CBP (Chrivia et al., 1993; Radhakrishnan et al., 1997), the coactivator and histone acetyltransferase (Fig. 5B) (Bannister and Kouzarides, 1996; Kwok et al., 1994; Martinez-Balbas et al., 1998; Ogryzko et al., 1996). The bZIP domain is responsible for the promoter binding and dimerization of CREB (Fig. 5) (Schumacher et al., 2000).

Although phosphorylation of Ser133 is considered to be the main activating mechanism of CREB-dependent gene transcription, other Ser residues in KID can also be phosphorylated and play a role in CREB-driven gene expression. For example, phosphorylation of Ser142 mediated by Ca^{2+}/ calmodulin-dependent kinase II prevents the recruitment of CBP to phosphorylated Ser133 (Sun et al., 1994). This mechanism appears to be important to ensure that only cAMP activates CREB-dependent transcription. Therefore, when intracellular elevation of Ca^{2+} activates PKC, which can also phosphorylate Ser133 (Wagner et al., 2000), CREB-dependent transcription remains inactive (reviewed in Mayr and Montminy, 2001).

The CREB bZIP domain interacts with the CRE-site located in the promoter of CREB-target genes (Fig.5A) (Fink et al., 1988; Montminy et al., 1986; Schumacher et al., 2000; Yamamoto et al., 1988). The CRE-site consists of either a full palindrome, (TGACGTCA), or a less active half-site, (CGTCA/TGACG) (Craig et al., 2001; Fink et al., 1988; Yamamoto et al., 1988). For example, the promoter of *Aa-nat* contains a CRE half-site (TGACG<u>C</u>CA) which differs from the full palindrome by only one nucleotide substitution (Baler et al., 1997).

As described in *section 1.3A*, most activators consist of at least two domains, a domain that responds to a stimulus and a DNA-interacting domain (reviewed in Lee and Young, 2000). In case of CREB, KID is the main stimulus-sensitive domain. However, the DNA-interacting domain, bZIP, may also play an important role in the regulation of CREB-driven gene expression. Salt-inducible kinase 1 (SIK1) has been shown to repress CREB-target gene expression via the bZIP domain (Doi et al., 2002). Considering the importance of CREB in the nocturnal induction of *Aa-nat* transcription, this mechanism may also function in the rat pineal gland.

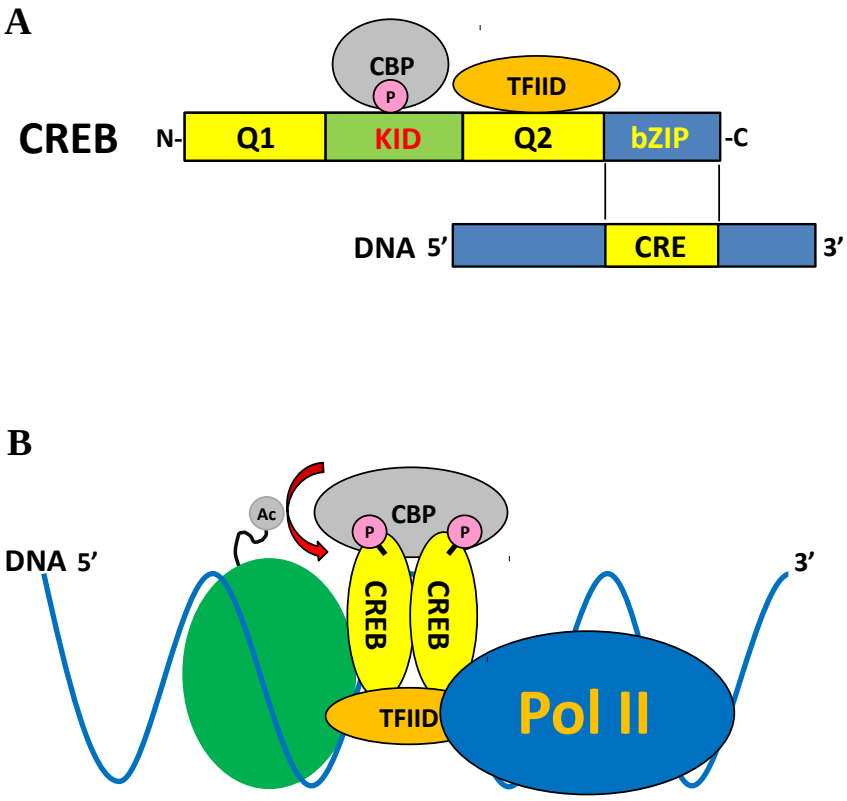

Figure 5: The cAMP response element-binding protein (CREB). A, The CREB structure includes the following domains starting from the N-terminus: The glutamine-rich Q1 domain; the kinase-inducible domain (KID; phosphorylation of the Ser133 residue will lead to recruitment of the CREB-binding protein (CBP; grey); the glutamine-rich Q2 domain (responsible to recruit the transcription factor IID (TFIID)); and the bZIP domain that will bind to the cAMP response element (CRE) within the promoter. **B**, The chromatin/DNA (blue) is wrapped around the nucleosome (green; composed of histones). When transcription is induced, the phosphorylated and dimerized CREB (yellow) interacts with CBP, TFIID (orange), and the DNA. CBP will acetylate histones (red arrow) whereas TFIID will recruit the RNA polymerase II (Pol II; dark blue).

1.5 Salt-inducible kinase 1

SIK1 was first identified in adrenal glands of rats fed with a high salt (Na^+, K^+)-diet (Wang et al., 1999). Homologs of SIK1 have been identified in different organisms including *Drosophila melanogaster*, *Caenorhabditis elegans, Saccaromyces cerevisiae*, rats and humans suggesting that this kinase is evolutionary conserved (Choi et al., 2011; Hardie, 2007; van der Linden et al., 2008; Wang et al., 1999). This kinase has also been shown to be expressed in a range of different tissues, with especially high levels in adrenal glands and the brain (Horike et al., 2003). The wide distribution of SIK1 across different organisms and different tissues suggests its potential importance in various physiological processes.

The sequence characteristic of SIK1 suggests that this kinase is a member of the sucrose non-fermenting (SNF)/AMP-activated protein kinase (AMPK) family (Wang et al., 1999). In addition to SIK1, there are two other SIK isoforms, SIK2 and SIK3 (Katoh et al., 2004a). SIK2 is highly expressed in adipocytes (Horike et al., 2003) whereas SIK3 is expressed ubiquitously (Katoh et al., 2004a). Most members in the AMPK family are studied in connection with energy storage and are in general activated by high levels of intracellular AMP and inhibited by high levels of intracellular ATP (reviewed in Hardie, 2007). Most AMPKs consist of three protein units, α, β and γ. All three units are important in stabilizing the heterotrimeric complex. The α-subunit is the catalytic subunit and the γ-subunit detects changes in the ratios of AMP and ATP. In comparison, SIKs are insensitive to the changing ratios of AMP and ATP directly

due to a lack of the β and γ subunits. Instead, SIKs function as a single unit and are homologous to the α-subunit (Fig. 6A) (reviewed in Hardie, 2004).

Figure 6A highlights the structure of SIK1, which contains the kinase domain in the N-terminus and the regulatory domain. The regulatory domain contains a PKA phosphorylation site and an arginine- and lysine-rich nuclear import region (Katoh et al., 2004b). PKA-mediated phosphorylation of the Ser577-site causes the nuclear export of SIK1 (Fig. 6B) (Takemori et al., 2002). The import region is important in controlling the cellular location of SIK1, since deletion of this region maintains most of the SIK1 protein in the cytoplasm under basal and stimulated conditions (Katoh et al., 2004b). Determining the cellular location may not be the only mechanism by which the function of SIK1 is regulated. Studies using Y1 (a mouse adrenocortical tumor cell line) and PC12 (a rat pheochromocytoma cell line) cells indicate that *Sik1* transcription can be induced by intracellular elevations of Ca^{2+} and cAMP (Feldman et al., 2000; Lin et al., 2001).

Since SIK1 may be important for different physiological processes, investigators have begun to study the function of this kinase. As knock-out animal model for SIK1 has not been established, most of these earlier studies were based on transient knockdown or overexpression of SIK1 in various cell cultures. SIK1 has been first studied in connection with steroidogenesis (Doi et al., 2002) and gluconeogenesis (Koo et al., 2005). By using luciferase gene reporter assays and the promoters of established CREB-target genes involved in steroidogenesis, SIK1 has been shown to repress the transcription of the *steroidogenic acute*

regulatory protein (*StAR*) and *side chain cleavage P450* (*CYP11A1*), two CREB-target genes (Doi et al., 2002; Lin et al., 2001; Takemori et al., 2002). However, SIK1 does not phosphorylate CREB directly and represses gene expression through the bZIP-domain of CREB (Doi et al., 2002; Lin et al., 2001). In addition, expressing a mutated SIK1 which is only detectable in the cytoplasm remains effective in repressing CREB-target gene expression, suggesting the involvement of shuttling an intermediate protein in this mechanism (Doi et al., 2002; Katoh et al., 2004b). Indeed, this kinase has been shown to regulate the cellular distribution of a member of the CREB-coactivator family, the transducer of regulated CREB activity (TORC) (Katoh et al., 2006; Katoh et al., 2004b), which will be described more in detail in *section 1.7*.

A

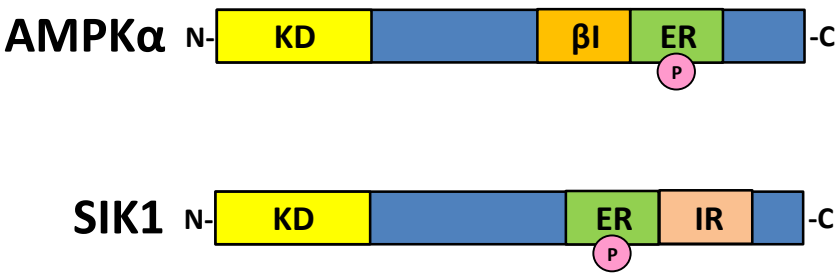

B

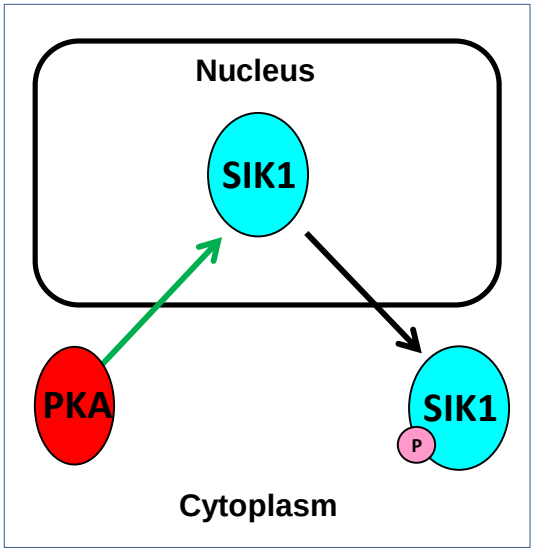

Figure 6: Salt-Inducible Kinase 1 (SIK1). **A**, Structures of the catalytic subunit of AMP-activated protein kinase α (AMPKα) and SIK1 including the following domains and regions: The kinase domain (KD); the export region (ER; can be phosphorylated by PKA), the import region (IR; in case of SIK1) and the β-subunit interacting region (βI; in case of AMPKα). **B**, PKA can phosphorylate SIK1, which in turn causes the export of SIK1 from the nucleus.

1.6 Transducer of regulated CREB activity 2

Considering the importance of CREB in a wide range of physiological processes (see *section 1.4*), additional mechanisms that can regulate CREB-target gene expression have been investigated. By using high-throughput screens for modulators of a CRE-luciferase reporter, two independent groups identified the TORC family of CREB-coactivators (Conkright et al., 2003; Iourgenko et al., 2003). Homologs of TORCs are expressed in many different species including humans, other mammals, *Drosophila melanogaster* (Wang et al., 2008) and *Caenorhabditis elegans* (Mair et al., 2011) suggesting that these coactivators are evolutionary conserved. The TORC family consists of three isoforms: TORC1, TORC2 and TORC3 (Conkright et al., 2003; Iourgenko et al., 2003). All three TORCs are similar in structure consisting of a CREB-binding domain (CBD) at the N-terminus and a regulatory domain, which is subject to phosphorylation (Fig. 7A) (Conkright et al., 2003; Screaton et al., 2004). The similarity in the structure of all three TORCs suggests that their mechanisms of regulating CREB-target gene expression may be similar.

The tissue distribution of the three TORC isoforms is different. In comparison to TORC2, which is expressed ubiquitously, TORC1 is expressed predominantly in brain tissue (Altarejos et al., 2008; Wu et al., 2006) whereas TORC3 is detected predominantly in white and brown adipocytes (Song et al., 2010). TORC2 has been studied mostly in connection with gluconeogenesis (Dentin et al., 2007; Koo et al., 2005; Liu et al., 2008). Many genes encoding enzymes that are important in the gluconeogenic pathway, such as *glucose-6-*

phosphatase (*G6Pase*) and *phosphoenolpyruvate carboxykinase* (*Pepck*), are established CREB-target genes (Herzig et al., 2001; Quinn and Granner, 1990; Wynshaw-Boris et al., 1986). Knockdown of TORC2 in mouse hepatocytes has been shown to reduce the expressions of *G6Pase*, *Pepck* and other CREB-target genes (Koo et al., 2005). Given that TORC2 is expressed in all tissues investigated so far, this TORC isoform is more likely to function in the pineal gland.

The mechanism by which TORCs are believed to function is by providing binding sites for GTFs and/or stabilizing the PIC (Conkright et al., 2003). It is accepted that four TORC2 proteins form a tetramer and interact with the bZIP domain of CREB (Conkright et al., 2003). This interaction enhances the association of CREB with TAF130 (part of TFIID; Fig. 7A). In addition to providing binding sites for GTFs, TORC2 has also been shown to cooperatively interact with CBP and enhancing its recruitment to CREB (Ravnskjaer et al., 2007; Xu et al., 2007). Overall, the above studies suggest that the interaction of TORC2 with the bZIP domain of CREB helps the formation of PIC by enhancing the recruitment of CBP and GTFs.

The function of TORC2 is reported to be controlled by its location within the cell (Bittinger et al., 2004; Screaton et al., 2004). The cellular distribution of this coactivator is regulated by a phosphorylation-dependent shuttling mechanism that traffics TORC2 between the cytoplasm and the nucleus (Fig. 7B). Under basal conditions, TORC2 is phosphorylated and is sequestered in the cytoplasm by binding to 14-3-3, a scaffolding protein (Screaton et al., 2004). Additional

studies report that with the elevation of intracellular cAMP and Ca^{2+}, TORC2 is dephosphorylated and translocates into the nucleus where it functions as a coactivator of CREB (Bittinger et al., 2004; Screaton et al., 2004). Since it has been suggested that simultaneous elevations of intracellular cAMP and Ca^{2+} cause the nuclear translocation of this coactivator, TORC2 has been referred to as a Ca^{2+}- and cAMP-sensitive coincidence detector (Screaton et al., 2004).

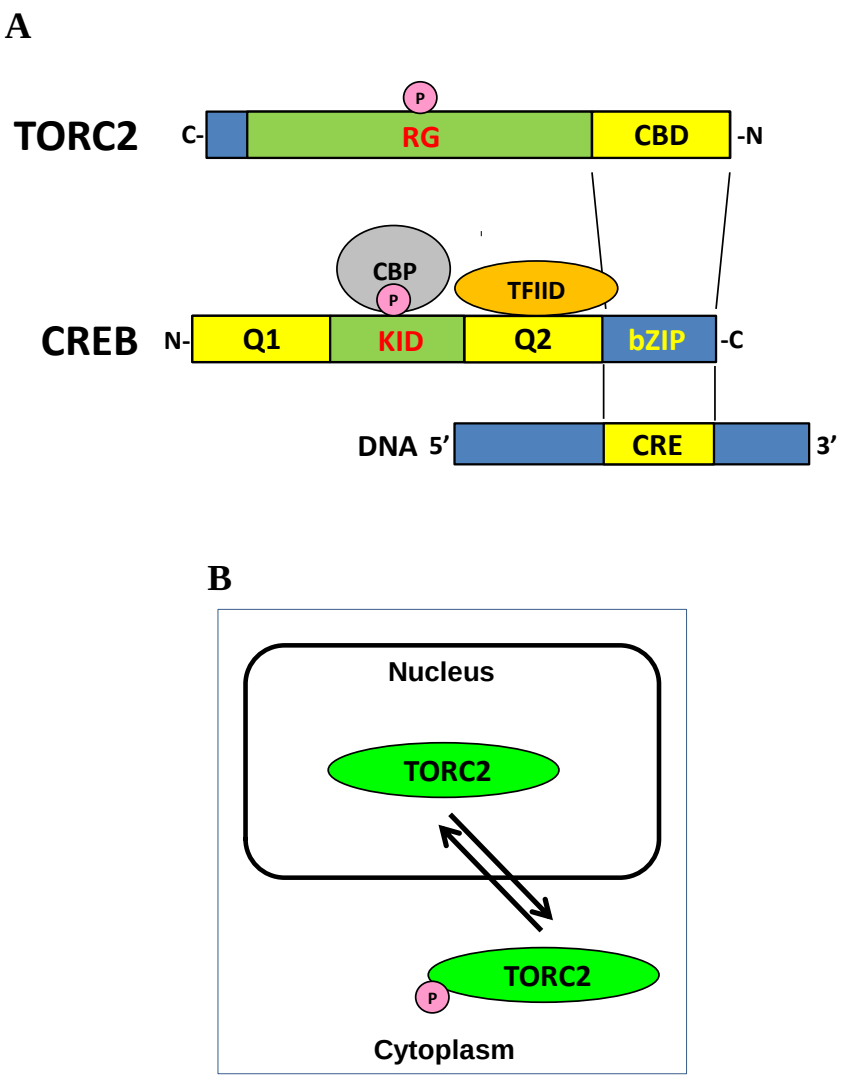

Figure 7: Transducer of regulated CREB activity 2 (TORC2). **A**, The interaction of CREB with TORC2.The CREB structure includes, the Q1 domain, the kinase-inducible domain (KID; phosphorylation of KID will lead to recruitment of the CREB-binding protein (CBP)), the Q2 domain (responsible to recruit TFIID); and the bZIP domain that will bind to cAMP response element (CRE) and the CREB-binding domain (CBD) of TORC2. Besides CBD, the TORC2 also contains a regulatory domain (RG) that is subject to phosphorylation. **B**, The phosphorylation-status determines the cellular distribution of TORC2. When TORC2 is dephosphorylated it translocates into the nucleus and functions as a coactivator of CREB. Phosphorylation of TORC2 will cause the export of TORC2 from the nucleus.

1.7 SIK-mediated regulation of TORC2

The SIK-mediated export of TORC2 is the current working model by which SIKs are believed to repress CREB-target gene expression (Katoh et al., 2004b; Koo et al., 2005; Screaton et al., 2004). Whereas PP2B can dephosphorylate TORC2 (Screaton et al., 2004), SIK1 has been shown to phosphorylate this coactivator (Katoh et al., 2006; Katoh et al., 2004b). Controlling the phosphorylation-dependent cellular distribution of TORC2 is believed to be the mechanism that regulates the TORC2-mediated effect on CREB-target gene expression.

Screaton *et al.* (2004) suggests that TORC2 is regulated by the combined actions of SIK (described in *section 1.5*) and PP2B. Intracellular elevation of Ca^{2+} activates PP2B, which can function as a phosphatase for TORC2. How intracellular cAMP promotes dephosphorylation of TORC2 is not clear, but it has been speculated that whereas the activity of SIK is inhibited by intracellular elevation of cAMP, PP2B can dephosphorylate TORC2. Once TORC2 is dephosphorylated, it translocates to the nucleus where it enhances CREB activity (Screaton et al., 2004). This would also imply that following decreases in intracellular cAMP levels, SIK may again become active leading to the phosphorylation-mediated nuclear export of TORC2 and termination of TORC2 coactivation activity. This inhibition of TORC2 activity by SIK may also represent a mean to limit the duration of CREB-stimulated gene transcription, and thus controls the temporal profile of the stimulated response.

As already described, *Aa-nat* is a CREB-target gene (Baler et al., 1997; Roseboom and Klein, 1995) and it is unknown whether SIK1 and TORC2 can regulate the NE-stimulated *Aa-nat* expression that drives the daily rhythm of circulating melatonin in rats. Therefore, how SIK1 and TORC2 are regulated in the pineal gland and how they can impact on *Aa-nat* transcription, in particular its temporal profile, will be a focus of this study.

1.8 The goal of the study

Regulating inducible gene transcription can control the synthesis of hormones, growth factors and other signalling molecules. As reviewed previously, in the rat pineal gland, *Aa-nat* expression (a CREB-target gene) is induced by over 150-folds and is important in driving the daily rhythm of circulating melatonin (Roseboom et al., 1996; Roseboom and Klein, 1995). At night, NE released from the nerve terminal stimulates both β- and α_1-adrenergic receptors, which leads to intracellular elevation of the common second messengers, cAMP, cGMP and Ca^{2+} (reviewed in Chik and Ho, 1989). It is generally accepted that the activation of CREB-dependent gene transcription occurs via the PKA-mediated phosphorylation of CREB through the cAMP-pathway (Gonzalez and Montminy, 1989; Mayr and Montminy, 2001). However, other signalling pathways may also modulate the expression of CREB-target genes. SIK1 has been shown to repress CREB-driven gene expression through phosphorylation-dependent nuclear export of the CREB-coactivator TORC2 (Katoh et al., 2006; Katoh et al., 2004b). Due to the importance of the

SIK1/TORC2 signalling pathway in CREB-driven gene expression, and the potential impact on the temporal profile of the response, it is imperative to determine the role of SIK1 and TORC2 in the NE-stimulated *Aa-nat* transcription in the rat pineal gland.

Cultured rat pinealocytes provide an excellent model system to investigate how multiple signalling mechanisms are integrated to regulate cellular processes, such as inducible gene transcription or protein phosphorylation. Most second messenger pathways involved in the adrenergic regulation of pineal function have been well characterized (reviewed in Chik and Ho, 1989). By using established selective activators and inhibitors of NE-stimulated signalling pathways, one can establish the transduction pathways involved in the regulation of SIK1 and TORC2. Moreover, to demonstrate the involvement of SIK1 and TORC2 in a signalling pathway, established protocols of viral transfection have been developed to manipulate the levels of protein expression (Ho et al., 2007b). Given the large magnitude of the NE-induced *Aa-nat* expression, changes in the amplitude and duration of its expression can be easily measured. In addition, cellular processes, such as gene expression, can differ between normal and cancer cells (Zhang et al., 1997). Therefore, studies using cultured pineal cells are likely more relevant to cellular processes than studies performed in tumor cell lines.

The objective of the thesis is to investigate the role of SIK1 and TORC2 on the adrenergic-regulated AA-NAT synthesis in the rat pineal gland. To achieve this objective, the following studies were performed:

a) The mechanism involved in regulating the expression of *Sik1*

b) The effect of SIK1 on NE-stimulated *Aa-nat* transcription

c) The mechanism involved in regulating the expression and cellular distribution of TORC2

d) The impact of TORC2 on NE-stimulated *Aa-nat* transcription

e) The effect of SIK1 on the cellular distribution of TORC2

Chapter 2

Materials and Methods

2.1 Materials

Cycloheximide, dibutyryl-cAMP (dBcAMP), dibutyryl-cGMP (dBcGMP), isoproterenol, NE, phenylephrine, 4β phorbol 12-myristate 13-acetate (PMA), nifedipine, prazosin, and propranolol were obtained from Sigma-Aldrich Co. (St. Louis, MO). Ionomycin was obtained from Calbiochem-Novabiochem Corp. (San Diego, CA). Monoclonal anti-glyceraldehyde-3-phosphate-dehydrogenase (GAPDH) serum was obtained from Ambion Inc. (Austin, TX). Polyclonal anti-green fluorescence protein (GFP) serum was from Abcam (Cambridge, MA). Polyclonal anti-TORC2 serum was obtained from Calbiochem-Novabiochem Corp. (San Diego, CA). Rabbit monoclonal anti-phospho-CREB (Ser133) serum was obtained from Cell Signaling Technology (Beverly, MA). Rabbit polyclonal anti-histone H3 serum was obtained from Upstate Biotechnology (Lake Placid, NY). Polyclonal anti-AA-NAT 25–200 (AB3314) serum was a gift from Dr. D.C. Klein (National Institute of Child Health and Human Development, National Institutes of Health, Bethesda, MD). Oligonucleotides were obtained from Sigma-Aldrich Co. and are listed in tables 1, 2 and 4. All other chemicals were of the purest grades available commercially.

2.2 Animal handling and pineal gland isolation

Animal handling procedures were reviewed and approved by the Health Sciences Animal Policy and Welfare Committee of the University of Alberta. Sprague Dawley rats (male, weighing ~150 g) were obtained from the University of Alberta animal unit and were housed under a lighting regimen providing 12 h

of light every 24 h with lights on at 0600 h unless otherwise indicated. For pinealocyte cell culture preparation, 12–15 animals were killed 3 h after the onset of light and intact pineal glands, which locate at the top of the brain between the cerebral cortex and the cerebellum, were removed and placed in ice-cold phosphate buffered saline (PBS) until enzymatic digestion. To determine if there are diurnal rhythms in the mRNA and protein levels of TORC2, pCREB and AA-NAT, groups of animals (n = 3) were conditioned for 1 wk under 14 h of light every 24 h and killed at various time-points as indicated. Pineal glands were collected, cleaned in ice-cold PBS, flash frozen on dry ice, and stored at -75^{o}C until preparation for RNA extraction or Western blot analysis. A dim red light was used when animals were killed during the dark period.

2.3 Preparation of cultured rat pinealocytes and drug treatment

Pinealocytes were prepared from isolated pineal glands using a papain dissociation system from Worthington Biochemical Corp. (Lakeway, NJ) as previously described (Terriff et al., 2005). Freshly harvested rat pineal glands were washed three times with PBS. Glands were incubated in 2 ml of papain solution (17 units of papain dissolved in Earle's balanced salt solution (EBSS) containing 170 units of DNase for 40 min at 37^{o}C with gentle vortexing every 10 min during the enzymatic treatment. Next, 350 µl of fetal calf serum (FCS) was gently mixed into the suspension containing the glands, which were then centrifuged at 1300 x g for 10 min at room temperature. The supernatant was replaced with 1.8 ml of pineal media (DMEM + 10 % FCS + ascorbic acid (100

mg/l) + 1 % penicillin, streptomycin, and amphotericin B (PSF)) containing 1000 units DNase (Sigma-Aldrich Co.). The digested glands were dissociated by pipette trituration and the dissociated cells were pelleted by centrifugation at 1300 x g for 10 min at room temperature. The cell pellet was then resuspended in a solution containing a mixture of 900 µl EBSS, 100 µl albumin-protease inhibitor solution and 100 units of DNase. A discontinuous density gradient was prepared by layering the cell suspension onto 2 ml of the albumin-protease solution and centrifuged at 500 x g for 8 min at room temperature. After removing the supernatant, the cell pellet was washed twice with 6 ml of pineal medium and resuspended in 10 ml of the same medium. The cell count and viability were determined using a hemocytometer after mixing 20 µl of the cell suspension with 20 µl of tryptan blue solution (0.04 %; Sigma-Aldrich Co.). The cells were maintained in pineal medium at 37^{o}C in an atmosphere of 95 % air and 5 % CO_2 and incubated for at least 18 h before experiments. During this incubation, while other cell types became attached to the flask, pinealocytes remain in suspension and were collected by centrifugation. Cell yield was approximately 7 x 10^5 pinealocytes per gland.

2.4 Construction of the *Sik1* and *Torc2* overexpression adenoviral constructs

A) Wild-type Sik1-full-length (fl) and Torc2-fl adenoviral constructs

Primers for amplification of the full-length *Sik1* and *Torc2* cDNA were designed with *Primer 3* (Rozen and Skaletsky, 2000) from the *Sik1* (accession no. NM_021693) and *Torc2* (*Crtc2*; accession no. DQ185515.1) cDNA sequences

obtained from BLAST and are shown in table 1. The cDNAs were amplified by polymerase chain reaction (PCR) from a cDNA collection obtained from rat pinealocytes as described in *section 2.7*. Two µl of cDNA was used as template in a 30 µl-PCR reaction containing 1 x PCR buffer (10 mM Tris (pH 8.8), 50 mM KCl, 1.5 mM $MgCl_2$, 0.008 % of Nonidet P-40 (Sigma-Aldrich Co.) and 200 µM dNTPs) and 1 µM forward and reverse primers. To avoid mutations in the PCR product, a 10:1 mixture of *Thermus aquaticus* polymerase (*Taq*; Perkin-Elmer Cetus, Emerville, CA) and *Pyrococcus furiosis* (*Pfu*; Invitrogen Corp.) proofreading polymerase was used in the reaction. To further reduce the probability of mutations, the *Sik1* and *Torc2* cDNAs were amplified with the minimum required cycle number. The program was set for 12 cycles and run twice with 0.5 µl of fresh enzyme added after the first run. To amplify the *Sik1* cDNA, the PCR cycling conditions were as follows: denaturing at 94^{o}C for 30 sec; annealing at 63^{o}C for 15 sec and extension at 72^{o}C for 3 min. The initial denaturing segment ran for 3.5 min and the final extension segment ran for 8 min. To amplify the *Torc2* cDNA, the PCR cycling conditions were as follows: denaturing at 93^{o}C from 1 min; annealing at 58^{o}C for 1 min and extension at 72^{o}C for 6 min. The initial denaturing segment ran for 3 min and the final extension segment ran for 10 min. The PCR product was visualized on a 0.8 % ethidium bromide-stained agarose gel and extracted using the *Qiagen Qiaex II kit* (Qiagen, Mississauga, ON).

The purified *Sik1* or *Torc2* PCR products were inserted into the *pCR8/GW/TOPO* entry vector in a 30 min ligation reaction at room temperature.

The *pCR8/GW/TOPO* construct (containing the *Sik1* or *Torc2* insert) was then transformed into competent DH5α strains of *Escherichia coli* (*E.coli)* cells and plated on spectinomycin (100 µg/ml) LB-agar plates. The integrity and correct orientation of the insert in the *pCR8/GW/TOPO* entry vector was determined by sequencing using the *DYNnamic ET Terminator Cycle Sequencing Kit* by Amersham Biosciences (Piscataway, NJ).

Next, the *Sik1* and *Torc2* inserts from the entry vector were recombined into a *pAD/CMV/V5-DEST* destination vector according to the manufacturer's instruction as follows (Invitrogen Corp.). First, a recombination reaction was set up with Gateway LR Clonase by incubating the *pCR8/GW/TOPO* construct with the insert and the *pAD/CMV/V5-DEST* destination vector for 2 h at room temperature. Four µl of the recombination reaction was used for transformation into DH5α *E. coli* strains, which were then spread on ampicillin (100 µg/ml) LB-agar plates. Several ampicillin resistant colonies were selected and the *pAD/CMV/V5-DEST* construct with the insert was isolated using the *GenElute Plasmid Miniprep kit* from Sigma-Aldrich Co. The ampicillin resistant colonies were also plated on chloramphenicol (30 µg/ml) LB-agar plates to test for chloramphenicol sensitivity. Sensitivity to chloramphenicol confirms that the genes for chloramphenicol resistance and *ccdB* (expresses a protein that is toxic to the DH5α *E. coli* strains) on the *pAD/CMV/V5-DEST* destination vector were replaced by the insert through successful recombination.

In order to expose the inverted terminal repeats of the viral DNA, 5 µg of the isolated *pAD/CMV/V5-DEST* construct containing the insert was digested with

Pac I (New England BioLabs Ltd, Pickering, Ontario) in a 50 µl digestion reaction for 1 h at 37^{o}C. Digestion was confirmed by running 5 µl of the digest on a 0.8 % ethidium bromide-stained agarose gel. The digested *pAD/CMV/V5-DEST* construct (33 kb band) with the insert was then purified using *Qiagen Qiaex II kit* (Quiagen) and transfected into human embryonic kidney (HEK) 293A cells. For transfection, 1 µg of the eluted *Pac I* digested *pAD/CMV/V5-DEST* construct was added to 250 µl of serum reduced Opti-MEM media (Gibco, Grand Island, N.Y.). Separately, 4 µl of Lipofectamine complex 2000 was diluted in 250 µl of serum reduced Opti-MEM media and incubated for 5 min at room temperature. The diluted *Pac I* digest was mixed gently with the Lipofectamine complex 2000 dilution and incubated for 20 min at room temperature. The mixture was then added drop wise to 80 % confluent HEK 293A cells grown on 3 cm 6-well plates. The cells were maintained in an atmosphere of 95 % air and 5% CO_2 at 37^{o}C in HEK medium (DMEM + 10 % FCS + 1 % non-essential amino acids) for 48 h and then replated onto 10 cm plates. The medium was replaced every two days until plaque formation.

A crude lysate containing virus particles was harvested when about 80 % of the cells were detached due to plaque formation. The harvested cells were lysed with three freeze/thaw cycles using dry ice and a 37^{o}C water bath. The crude lysate was then harvested by pelleting the cell debris at 2000 g for 15 min and the supernatant collected. To amplify the virus, 100 µl of crude lysate containing the intact virus was added to 80 % confluent HEK 293A cells grown on 10 cm plates. Amplified virus was extracted using same method as for the

crude lysate. Finally, the lysate was further purified with a 45 µm syringe filter and infectious units were determined with the QuickTiter™ Adenovirus Titer Immunoassay of Cell Biolabs, Inc (San Diego, CA). The viruses were then stored at -75°C until ready for use.

B) Mutant Sik1-S577A and Torc2-S171A adenoviral constructs

Mutant *Sik1*-S577A and *Torc2*-S171A adenoviral constructs that had phosphorylation sites of interest abolished were also generated. Ser577 and Ser171 residues on SIK1 and TORC2, respectively, were converted into an alanine (Ala) residues by site-directed mutagenesis as described previously (Fisher and Pei, 1997). Mutagenic primers were selected using the online primer design tool of Stratagene, Inc (La Jolla, CA) and shown in table 1.

Fifteen nanograms of *pCR8/GW/TOPO* containing the wild-type *Sik1* or *Torc2* insert was used as starting template for the mutagenesis reaction. The 50 µl mutagenesis reactions were set up in 1x *Pfu* buffer (20 mM Tris-HCl (pH 8.8), 10 mM $(NH_4)_2SO_4$, 10 mM KCl, 0.1 % (v/v) Triton X-100, 0.1 mg/ml BSA) containing 2 mM of $MgSO_4$, mutagenic primers at 25 µM, dNTPs at 10 mM and 2.5 units of *Pfu* polymerase. To amplify the mutated construct, 18 cycles were used with the following PCR cycling conditions: denaturing at 95°C for 30 sec, annealing at 55°C for 60 sec and extension at 68°C for 6 min with 30 sec initial denaturing and 6 min final extension steps. Completed mutagenesis reactions were treated with 10 units of *DpnI* (Invitrogen Corp.) at 37°C for 1 h to digest the parent plasmid DNA. One µl of digested reaction was then transformed into

DH5α *E. coli* cells. Cloned mutations were confirmed by sequencing and adenoviruses expressing the *Sik1*-S577A or *Torc2*-S171A constructs were prepared as described previously for the wild-type *Sik1*-fl and *Torc2*-fl adenoviral constructs.

C) Sik1-fl-gfp fusion adenoviral construct

The *Sik1-fl-gfp* fusion was generated using a PCR-ligation-PCR approach (Ali and Steinkasserer, 1995). A vector encoding *Gfp* (pEGFP-N1; *Becton Dickinson*, Franklin Lakes, NJ) was used as template to PCR-amplify the *Gfp* gene sequence minus the first codon in a 50 µl PCR reaction using 1 unit of *Pfu* in 1x *Pfu* buffer + $MgSO_4$. The sequences of primers used to amplify *Gfp* are shown in table 1. In regards to the amplified *Sik1* product, the two stop codons were removed from the *Sik1* cDNA 3' UTR (untranslated region) and replaced by functional glycine codons with PCR amplification using the same forward primer as for the wild-type *Sik1* but a different *Sik1* reverse cloning primer (see table 1). Fifty ng of *pCR8/GW/TOPO* x *Sik1* were used as template in a 50 µl PCR reaction with otherwise the same reaction components and concentrations as described for amplifying the *Gfp* insert. The PCR cycling conditions were set for 30 sec denaturating at 94^{o}C, 30 sec annealing at 61^{o}C and 5 min extension at 70^{o}C for 20 cycles.

The two PCR products (*Sik1* and *Gfp*) were purified from agarose gel fragments and ligated with 2.5 units of T4 DNA ligase (Invitrogen Corp.) in a 50 µl reaction overnight at room temperature. The product of this ligation was again

PCR-amplified using the forward *Sik1* primer and the reverse *gfp* primer. In this PCR reaction, a mixture of *Taq* and *Pfu* was used in a 10:1 ratio as previously described. This fusion product was again purified from an agarose gel fragment and cloned into the *pCR8/GW/TOPO* entry vector. From this step on, the *Sik1-fl-gfp* expressing adenoviral construct was generated as described previously for the *Sik1*-fl and *Torc2*-fl adenoviral constructs.

Primer	**Sequence (5'-3')**
1. *Sik1* forward cloning primers	CATGGTGATCATGTCGGAGT
2. *Sik1* reverse cloning primers	TTGCTTGGAAGAGTCCATCC
3. *Torc2* forward cloning primer	GATAAGATGGCGACGTCAGG
4. *Torc2* reverse cloning primer	GATAGCAGTAAGGTCCCCTCA
5. *Sik1*-S577A sense primer	GGGCGGAGAGCGGCGGATACGTCTC
6. *Sik1*-S577A anti-sense primer	GAGACGTATCCGCCGCTCTCCGCCC
7. *Torc2*-S171A sense primer	GCACTTAACAGGACAGCCTCTGACTCTGC
8. *Torc2*-S171A anti-sense primer	GCAGAGTCAGAGGCTGTCCTGTTAAGTGC
9. *Gfp* forward cloning primers	GTGAGCAAGGGCGAGGAG
10. *Gfp* reverse cloning primers	GGGAGGTGTGGGAGGTTTT
11. *Sik1* reverse cloning primers #2	GGTGTGGCAGAGTCCCCCTCCCTGTACCAGG

Table 1: Primers used to generate the *Sik1* and *Torc2* overexpression adenoviral constructs. Primer sequences used to amplify the wild-type *Sik1* (1 and 2), *Torc2* (3 and 4) and *Gfp* (9 and 10). The primers used to mutate Ser into an Ala on SIK1 (5 and 6) and TORC2 (7 and 8) are also shown. One of the reverse cloning primers for *Sik1* (11) was used to remove the stop codons of *Sik1*.

2.5 Generating the adenoviral constructs expressing short-hairpins

Small-interfering RNA (siRNA) targets were selected by submitting the full-length rat *Sik1* or *Torc2* cDNAs to the online short-hairpin RNA (shRNA) design utility of Invitrogen Corp. The construction of the adenoviral construct

expressing the shRNA is according to the manufacturer's procedure (Invitrogen Corp.). The siRNA target-sequences for *Sik1* and *Torc2* knockdown are shown in table 2. To knockdown *Sik1*, *Sik1*-sh2 was used in most experiments and *Sik1*-sh5 in selected experiments, and *Torc2*-sh was used to knockdown *Torc2*.

The procedure used to generate the adenoviral constructs expressing the shRNAs was identical to the generation of the overexpression constructs, substituting the appropriate insert and different vectors. To generate the double stranded insert, the single stranded sense oligonucleotide (ordered from Sigma-Aldrich Co.) was annealed to the complementary anti-sense oligonucleotide. The insert was ligated with a T4 ligase into the *pENTR/U6* entry vector from which it was recombined into the *pAd/BLOCK-it-DEST* destination vector. In all other respects, the steps taken to generate the *Sik1*-sh and *Torc2*-sh adenoviral constructs were the same as described for the *Sik1*-fl and *Torc2*-fl adenoviral constructs.

Short-hairpins	**Target sequence (5'-3')**	**Target location**
Sik1-sh2	GGATACGTCTCTCACTCAAGG	1726bp-1747bp
Sik1-sh5	GGGACTGAACAAGATCAAAGG	1802bp-1823bp
Torc2-sh	GCTGCGACTGGCTTATACAAG	168bp-188bp

Table 2: shRNA target locations. The sequences and locations (base-pairs (bp) starting from the ATG start-site) within the *Sik1* and *Torc2* mRNAs that are targeted by the shRNAs.

2.6 Adenoviral transduction of pinealocytes

Titered viral stocks were used to transduce DNAs encoding different contructs of interest into pinealocytes. To control for viral transduction, a *LacZ*

expressing adenovirus was used. Viral stocks were combined with the pinealocyte medium at a multiplicity of infection of approximately 200 viral particles per cell in a total volume of 600 µl. Following an incubation period of ~23 h, the medium was replaced with fresh pineal medium. After a total of 40 h of incubation, the virally transduced pinealocytes were treated with drugs as indicated.

2.7 Reverse-transcription (RT)-PCR

A) RNA extraction and cDNA preparation

To isolate total RNA, 600 µl Trizol reagent (Invitrogen Corp.) was added directly to 150 µl of pinealocyte suspension and incubated for 5 min at room temperature, 120 µl of chloroform (Fisher Scientific, Whitby, Ontario) was then added, shaken vigorously for 15 sec, and held at room temperature for 3 min before centrifuging at 12000 x g for 15 min at 4^{o}C. Next, the aqueous phase (300 µl) was transferred to a new tube and the RNA was precipitated by adding 480 µl of isopropranol. To visualize the RNA pellet better, 3 µl of glycogen (5 µg/µl) was also added. The samples were vortexed for 30 sec, incubated at room temperature for 10 min and centrifuged at 12000 x g for 10 min at 4^{o}C. The pellet was washed by replacing the supernatant with 800 µl of 75 % ethanol followed by centrifugation at 12000 x g for 5 min at room temperature. The ethanol was removed and the pellet was air dried to the point when the white pellet began to turn transparent. The RNA in the pellet was dissolved in 27 µl RNase free water followed by 10 min incubation in a water bath at 60^{o}C.

cDNA was synthesized using the Omniscript reverse-transcriptase kit (Quiagen Inc., Valencia, CA) with random primers. To the dissolved RNA, 4.8 µl of a reaction mixture containing: 1.2 µl 10 x Reaction Buffer, 1.2 µl dNTPs, 1.2 µl random Primers (200 µM), 6 units RNase-OUT (Invitrogen Corp.), and 2.4 units of Omniscript Reverse Transcriptase was added. The reaction was carried out by incubating for 1 h in a 37^{o}C water bath and was terminated by placing the sample in a 93^{o}C water bath for 4 min.

B) PCR

The procedure for the PCR reaction set up has been described before (Price et al., 2004b). Three µl of diluted cDNA sample (diluted to 1:5 with water) was used as template in a 30 µl PCR reaction in regular 1 x PCR buffer containing 1 µM of forward and reverse primers. Specific PCR cycling conditions varied depending on the primer sets that were used and are shown in table 3. Initial denaturing and final extension segments were both 5 min in duration. Primer sequences were designed as described previously and shown in table 4. In some experiments RT-PCR was used to measure *Gapdh*, *Aa-nat*, *mitogen-activated protein kinase phosphatase-1 (Mkp-1)*, *type 2 diodothyronine deiodinase (Dio2)*, *inducible cAMP early repressor (Icer)*, *c-fos* and *Sik1*. All reactions included a water blank as negative control. The PCR products were separated by electrophoresis through a 1.5 % ethidium bromide-stained agarose gel. For semi-quantitative analysis, the PCR products were visualized with a

Kodak 2000R imaging station (Eastman Kodak Co., Rochester, NY) and band densitometry was performed with Kodak 1-D software.

cDNA	Denaturation	Annealing	Extension	Cycle #
Gapdh	1 min at 95 °C	1 min at 63 °C	1 min at 72 °C	22
Aa-nat	30 sec at 95 °C	15 sec at 63 °C	30 sec at 72 °C	24
Mkp-1	1 min at 95 °C	1 min at 63 °C	1 min at 72 °C	24
Icer	1 min at 95 °C	1 min at 63 °C	1 min at 72 °C	26
Dio2	1 min at 95 °C	1 min at 63 °C	1 min at 72 °C	26
c-fos	1 min at 95 °C	1 min at 63 °C	1 min at 72 °C	24
Sik1	30 sec at 95 °C	15 sec at 63 °C	30 sec at 72 °C	24

Table 3: RT-PCR cycling conditions. PCR cycling conditions used to amplify the cDNAs of *Gapdh*, *Aa-nat*, *Mkp-1*, *Icer*, *Dio2*, *c-fos* and *Sik1*, before analysis on ethidium bromide-stained agarose gel.

Some experiments were run with real-time PCR using a StepOne Real-time PCR system (Applied Biosystems, CA). SYBR-Green FAST reagent-mixture was used in a 10 µl PCR reaction containing 300 nM of forward and reverse primers (see table 4.). The PCR cycling conditions were set up as follows: denaturing for 3 sec at 95°C, annealing and extension for 30 sec at 60°C for 40 cycles with initial denaturation for 20 sec at 95°C. The relative amount of PCR product was determined with StepOne Software v.2.0.1. (Applied Biosystems, CA) and expressed as fold differences relative to an internal control that consisted of a fixed amount of pooled cDNA. The relative quantity was then normalized for sample loading based on the amount of *Gapdh.*

Primer	Sequence (5'-3')
Gapdh forward	TGATGACATCAAGAAGGTGG
Gapdh reverse	TTTCTTACTCCTTGGAGGCC
Aa-nat forward	GGTTCACTTTGGGACAAGGA
Aa-nat reverse	GTGGCACCGTAAGGAACATT
Mkp-1 forward	CTGCTTTGATCAACGTCTCG
Mkp-1 reverse	AAGCTGAAGTTGGGGGAGAT
Icer forward	TGGCTGTAACTGGAGATGAAACT
Icer reverse	AGCAGCTTCCCTGTTTTTCA
Dio2 forward	GACTCGGTCATTCTGCTCAAG
Dio2 reverse	AGGCTGGCAGTTGCCTAGTA
c-fos forward	TCACCCTGCCTCTTCTCAAT
c-fos reverse	AGGTAGTGCAGCTGGGAGTG
Sik1 forward	GTCCCTCGGAAGGAACTAGC
Sik1 reverse	CTCGCGTTTTTCCTTAGCTG
Torc2 forward	CAGAAGGTCCCAACAGCAG
Torc2 reverse	GGGGGCTATATGGGTATGG

Table 4: Primer sequences for RT-PCR and real-time PCR. The primer sequences used to amplify the cDNAs of *Gapdh*, *Aa-nat*, *Mkp-1*, *Icer*, *Dio2*, *c-fos*, *Sik1* and *Torc2* for regular PCR and for real-time PCR.

2.8 Western blotting

A) Sample preparation

For experiments analysed by Western blot, pinealocytes were collected by centrifugation (2 min, 6000 g), washed with DMEM to remove serum proteins and homogenized in 1 x sample buffer containing 20 mM Tris-HCL, 2 mM EDTA, 0.5 mM EGTA, 2 mM phenylmethylsulfonylfluoride, 1 µg/ml each of aprotinin, leupeptin, and pepstatin (Sigma-Aldrich Co.), 1 mM sodium vanadate, 1 mM sodium fluoride (pH 7.5). In some experiments samples were run on a

PhosTag gel following an established procedure (Kinoshita et al., 2009). In this case, the cells were washed with 25 mM HEPES buffered saline instead of DMEM and were dissolved in 1 x sample buffer containing all the above described ingredients without EDTA. Samples for normal or PhosTag gels were boiled for 8 min and cooled to room temperature before electrophoresis as described before (Ho and Chik, 2000; Laemmli, 1970; Man et al., 2004).

For the cytoplasmic and nuclear fractionation, a commercial kit from Biovison (Mountain View, CA) was used. After the cells were washed and the supernatant aspirated, the cell pellet was resuspended in 30 µl of cytoplasmic extraction buffer (CEB) containing 0.55 % of CEB-B according to manufacturer instruction (Biovision). The mixture was incubated for 3 min in an ice-water bath and the nuclear fraction was pelleted at 1200 g for 1 min. The cytoplasmic fraction was transferred into a new ice-cold tube and 15 µl of 3 x sample buffer was added. The pellet consisting of the nuclear fraction was resuspended in 1 x sample buffer containing the same ingredients as mentioned above. Samples were then boiled for 8 min and cooled to room temperature prior to electrophoresis.

In some experiments, cell homogenates were also treated with calf-intestinal phosphatases (CIP; 1 unit/10 µl lysate; New England Biolabs Ltd). The cells were pelleted at 2500 x g for 2 min and the supernatant was removed. Then, the cell pellet was resuspended in a mixture containing, 1 x NEBuffer 3 (100 mM NaCl, 50 mM Tris-HCl, 10 mM $MgCl_2$, 1 mM DTT (pH 7.9); New England Biolabs Ltd), 0.25 mM EGTA, 27 µg/ml Leupeptin, Aprotinin, 1 x Protease Inhibitor Cocktail (Sigma-Aldrich Co.). The cells were lysed with three

freeze/thaw cycles using dry ice and an ice-cold water bath. The CIP was added to the lysed cell homogenate and this mixture was incubated for 20 min in a 37^{o}C water bath. The phosphatase reaction was stopped by adding 2 x sample buffer and boiling the samples for 8 min prior to electrophoresis.

B) Sodium dodecyl sulfate polyacrylamide gel electrophoresis (SDS-PAGE)

The SDS-PAGE gel was set up as previously described (Laemmli, 1970; Man et al., 2004) in a Mini-PROTEAN II gel system (Biorad Labroratories, Inc., Herculas, CA). The concentration of polyacrylamide in the gel depended on the size of the proteins of interest in a particular experiment. In general, most samples were run on a 9 % or 12 % running gel. Samples were run at 170 V for 1 h with electrophoresis buffer (25 mM Tris, 190 mM glycine, and 3.5 mM SDS).

For PhosTag gels, the running gel also contained 10 µM of PhosTag-acrylamide (Wako Chemical, Richmond, VA) and 20 µM $MnCl_2$ (Kinoshita et al., 2009). The concentration of polyacrylamide in the gel was 9 % for all PhosTag gels. Samples were run at 80 V through the stacking gel and at 140 V through the running gel for a total of 2 h.

C) Immunoblotting

The immunoblotting was also described (Laemmli, 1970; Man et al., 2004). The gel was equilibrated in transfer buffer (25 mM Tris, 190 mM glycine, and 20 % methanol) for 20 min following completion of electrophoresis. Protein was transferred onto polyvinylidene difluoride (PVDF) membranes, in a mini

vertical gel system (E-C Apparatus Corporation, St. Petersburg, Fl) for 1.5 h at 50 V in transfer buffer.

In case of PhosTag gels, the gels were first soaked in transfer buffer containing 8 mM EDTA for 15 min to remove the $MnCl_2$ (Kinoshita et al., 2009), washed for another 10 min in transfer buffer containing 0.05 % SDS prior to blotting. The transfer was extended to 2.5 h at 100 V in transfer buffer containing 0.05 % SDS.

Next, the PVDF membrane was blocked for 1 h in 5 % skim milk dissolved in a Tris-buffered solution (TBS; 20 mM Tris-HCL, 0.5 M NaCl) containing 0.05 % Tween-20 (TTBS). The membrane was incubated with the desired primary antibody in 5 % skim milk/TTBS overnight at 4^{o}C with gentle rocking. Primary antibodies were prepared with the following dilutions in 5 % skim milk/TTBS: GAPDH (1:2500000), AA-NAT (1:8000), TORC2 (1:20000) and pCREB (1:4000). Next, the membranes were washed on an orbital shaker four times for 15 min with TTBS and incubated for 1 h in the appropriate secondary antibody linked to a horse-radish peroxidase diluted 1:2500 in TTBS containing 5 % skim milk powder. Again, the membrane was washed four times with TTBS for 15 min on an orbital shaker before the membrane was finally washed for at least 5 min in TBS.

D) Visualization and quantification

The desired protein was visualized by incubating the membrane in Immobilion Western Chemiluminesent HRP Substrate solution (Millipore Corp.,

Billerca, MA) and exposing the membrane to an X-ray film (Fuji Film Co, Mississauga, Ontario). For semi-quantitative analysis the films were scanned and the band intensity was measured with densitometry using Kodak 1-D software (Eastman Kodak Co.).

2.9 AA-NAT assay

The enzymatic activity of AA-NAT was measured by radioenzymatic assay as described previously (Man et al., 2004). To the cell pellet, which was stored on dry ice until prior to the assay, 60 µl of reaction mixture was added containing 0.1 M phosphate buffer (pH 6.8), 30 nmol [^{3}H] acetyl coenzyme A (specific activity, 1 mCi/mmol) and 1 µmol tryptamine hydrochloride. After addition of the reaction mixture, the cell pellet was homogenized with brief sonication. Until all the cell pellets were homogenized the enzymatic reaction was inhibited by placing the samples in an ice-water bath. The reaction was carried out for 1 h in a 37^{o}C water bath under gentle shaking. To terminate the reaction 1 ml of methylene chloride was added. This was followed by 10 min of orbital shaking to extract the hydrophobic [^{3}H] acetyl-tryptamine from the aqueous reaction mixture. Samples were centrifuged for 1 min at 6000 g and the aqueous phase was removed. The organic phase containing the [^{3}H] acetyl-tryptamine was washed three times with 250 µl of 0.1 M phosphate buffer (pH 6.8) before the remaining organic phase was transferred into scintillation vials. Once the organic phase was air dried, scintillation counting was used to measure

the amount of radioactive acetylated product. The AA-NAT activity was expressed as a percentage of the NE response obtained.

2.10 Results and Statistical analysis

All values obtained were presented as the mean ± SEM from at least three independent experiments. Densitometric values obtained from RT-PCR and Western blot analysis were presented as percentages normalized to the value obtained for either the maximal optical density (OD) or the NE response OD value as indicated. Each value obtained from real-time PCR and radioenzymatic assays was normalized as indicated. Statistical analysis involved either a paired *t* test or ANOVA with the Newman-Keuls test. Statistical significance was set at $p<0.05$.

Chapter 3

Results

With the onset of darkness, NE stimulation results in a 150-fold induction of the CREB-target gene *Aa-nat* in the rat pineal gland (Roseboom et al., 1996; Roseboom and Klein, 1995). Although PKA-mediated phosphorylation of CREB at the Ser133 residue located in KID is considered a key event to activate CREB-target gene transcription (Gonzalez and Montminy, 1989), the bZIP domain of CREB may also play an important role in modulating CREB activity (Carlezon et al., 2005; Mayr and Montminy, 2001). The bZIP domain is considered to be important for dimerization and promoter binding of CREB (Schumacher et al., 2000) and can serve as a binding site for transcriptional coactivators (Conkright et al., 2003). These coactivators may provide additional mechanisms that regulate the activity of CREB. For example, SIK1 can repress CREB activity by phosphorylating the coactivator of CREB, TORC2, which in turn is exported from the nucleus (Katoh et al., 2004b; Takemori et al., 2007).

The mechanism of regulation and function of the SIK1/TORC2 pathway is unknown in the rat pineal gland. This was investigated with the following objectives:

1. **Regulation of *Sik1* transcription (*section 3.1*)**
2. **Function of SIK1 (*section 3.2*)**
3. **Regulation of TORC2 (*section 3.3*)**
4. **Function of TORC2 (*section 3.4*)**
5. **The role of SIK1 in regulating TORC2 (*section 3.5*)**

3.1 The regulation of *Sik1* transcription in the rat pineal gland

The *Sik1* mRNA has been shown to be expressed in various tissue types, but the regulation of *Sik1* expression appears to be tissue-dependent and has been reported to be induced by elevation of intracellular cAMP or Ca^{2+} (Feldman et al., 2000; Lin et al., 2001). This prompted the study on the regulation of *Sik1* transcription in the rat pineal gland.

A) Sik1 is induced at night in the rat pineal gland

To determine whether there is a diurnal difference in *Sik1* transcription, the pineal glands of animals housed under controlled environmental lighting conditions (14 h of light every 24 hours) were dissected at different time-points during the 24 h lighting regime. The mRNAs were extracted from the dissected glands and measured by real-time PCR. Two hours after the onset of darkness, *Sik1* mRNA levels were induced (Fig. 1A). The induction of *Sik1* was followed by a gradual decline, but elevated *Sik1* mRNA levels (40 % of the peak levels) could still be measured 8 h after the onset of darkness (Fig. 1A). Two hours after the onset of light, *Sik1* mRNA levels declined close to baseline levels (Fig. 1A). The time profile of induced *Sik1* was also compared to the time profile of induced *Aa-nat*. *Aa-nat* mRNA levels were induced at night, peaked 5 h after onset of darkness followed by a gradual decline as previously described (Fig. 1A) (Price et al., 2004b). The induction of *Sik1* preceded the induction of *Aa-nat*. When the rats were housed under constant darkness, the diurnal variation of *Sik1* mRNA persisted (Fig. 1B). This suggests that the induction of *Sik1* is driven by the

endogenous circadian clock. Altogether, these results indicate that the nocturnal induction of *Sik1* is a natural event that takes place in the rat pineal gland during night.

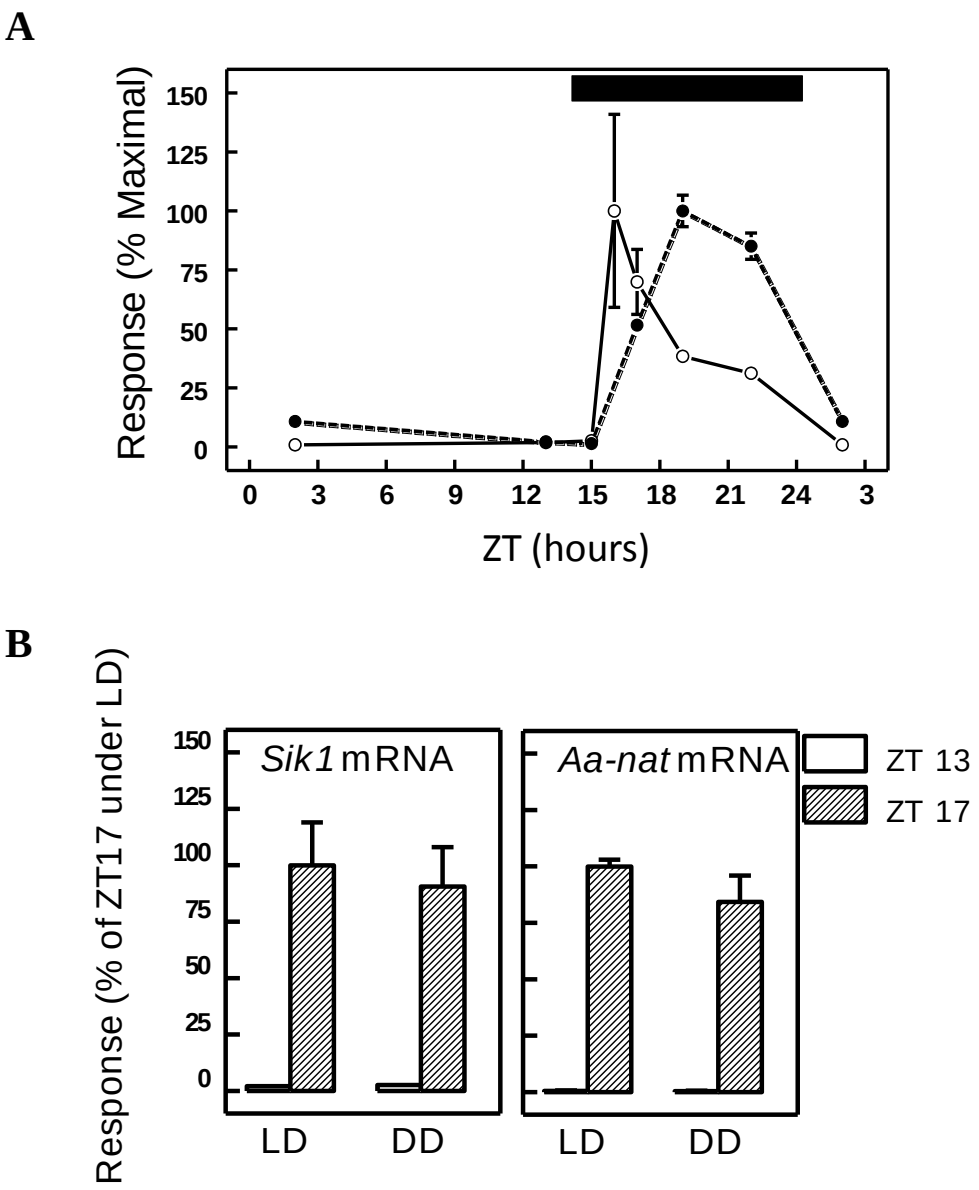

Figure 1: Day/night variation of *Sik1* and *Aa-nat* mRNA levels in the rat pineal gland. Pineal glands were collected and prepared for real-time PCR (see *Materials and Methods*). mRNA levels of *Sik1* and *Aa-nat* were normalized to *Gapdh* values. **A**, Animals were housed under controlled environmental lighting condition with 14 h of light and 10 h of darkness (indicated by dark bar; 14:10 LD) every 24 h before glands were collected at different time-points. The mean values of *Sik1* (solid line) and *Aa-nat* (dotted line) mRNA levels were expressed as percentages of the maximal response. **B**, Pineal glands were also collected from rats housed under constant darkness (DD) and the *Sik1* and *Aa-nat* mRNA levels were compared with those obtained from animals housed under the 14:10 LD lighting regime. The mean values obtained were expressed as a percentage of the mean at ZT 17 under LD. Each value represents the mean ± SEM of three independent experiments. ZT, Zeitgeber time (Kanyo et al., 2009).

B) NE treatment induced Sik1 in rat pinealocytes

To investigate whether *Sik1* was induced by NE-mediated signalling pathways in the rat pineal gland, cultured rat pinealocytes were prepared. Cells were treated with NE (3 μM) for varying time periods and mRNA levels were determined with RT-PCR. mRNA levels of *Gapdh*, a housekeeping gene, was also measured to control for mRNA extraction consistencies between different samples (Fig. 2A). *Sik1* was induced 1 h after NE treatment (80 % of peak levels), peaked at 2 h after treatment and was followed by a gradual decline (Fig. 2). The NE-stimulated time profile of *Sik1* expression was compared to the time profile of *Aa-nat*. *Aa-nat* mRNA levels peaked 4 h after NE treatment and were maintained 6 h after treatment (Fig. 2). The effect of NE on *Aa-nat* was similar to the results described previously (Price et al., 2004b), which served as a control in this experiment. Consistent with the results obtained in the whole animal study, *Sik1* induction preceded the induction of *Aa-nat* and was still elevated (50 % of the peak levels) 6 h after NE treatment. Because *Sik1* was reported to behave like an immediate early gene (Feldman et al., 2000), the time profile of *Sik1* was also compared to the time profile of an established immediate early gene, *c-fos* (Sheng and Greenberg, 1990). The induction of *c-fos* preceded the induction of *Sik1* and was less sustained than that of *Sik1* (Fig. 2). The results above indicate that *Sik1* transcription is adrenergically induced and precedes the induction of *Aa-nat*.

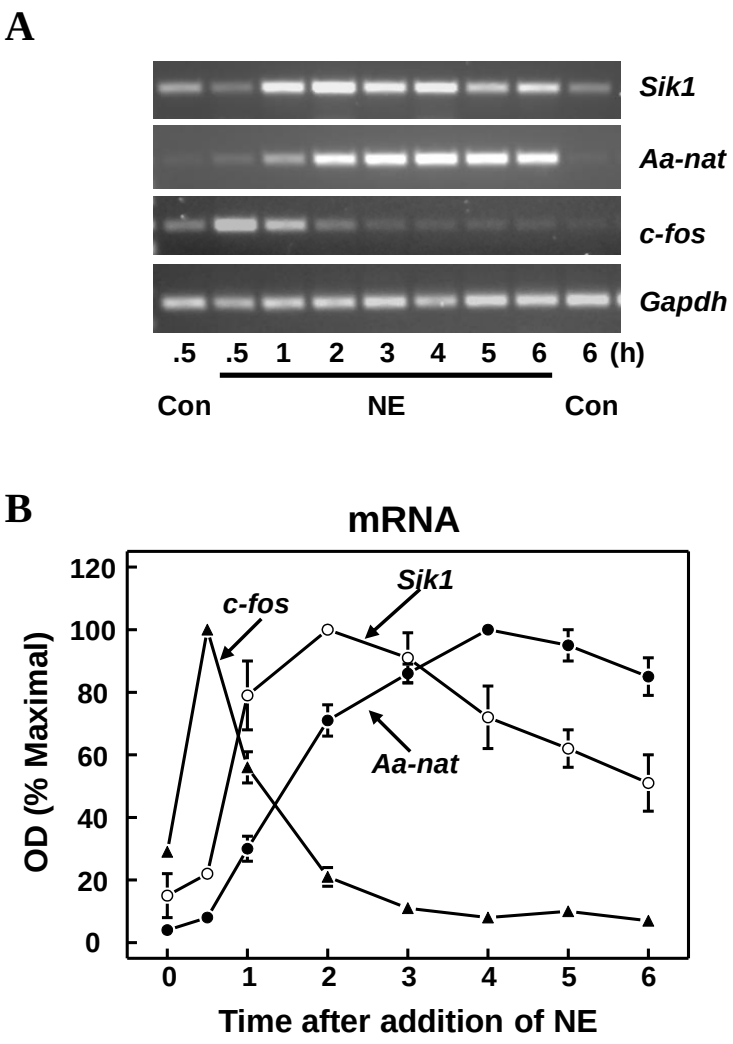

Figure 2: Time-course study on NE-stimulated *Sik1*, *Aa-nat* and *c-fos* expression. Pinealocytes (1.0 x 10^5 cells/150 µl) were treated with NE (3 µM) for different time periods as indicated and prepared for RT-PCR (see *Materials and Methods*). **A**, Representative ethidium bromide-stained agarose gels showing *Sik1*, *Aa-nat*, *c-fos* and *Gapdh* mRNA levels. **B**, Corresponding time profile of the densitometric measurements presented as percentages of the maximum NE-stimulated response. Each value represents the mean ± SEM of three independent experiments (Kanyo et al., 2009).

C) Receptor characterization of adrenergically-induced Sik1 expression

To characterize the adrenergic receptors involved in the NE-stimulated induction of *Sik1*, a series of selective adrenergic receptor agonists and antagonists were used at concentrations that can selectively activate or block, respectively, α_1 or β-adrenergic receptors (Ho and Chik, 2000; Price et al., 2004a). NE-stimulated *Aa-nat* expression was included as control for β-adrenergic receptor activation (Baler et al., 1997; Roseboom et al., 1996; Roseboom and Klein, 1995). Cultured rat pinealocytes were treated for 2 h before mRNA levels were determined with RT-PCR.

Selective activation of the β-adrenergic receptor with 3 μM isoproterenol (a β-adrenergic receptor agonist; in the presence of 3 μM of α_1-adrenergic receptor antagonist, prazosin) induced *Sik1* to the same level as that obtained with NE treatment (3 μM) (Fig. 3A). Selective activation α_1-adrenergic receptor with 3 μM phenylephrine (an α_1-adrenergic agonist; in the presence of 3 μM of a β-adrenergic antagonist, propranolol) also caused an increase in *Sik1* mRNA levels, but to a smaller extent (Fig. 3A). Simultaneous activation of α_1- and β-adrenergic receptors by treatment with isoproterenol plus phenylephrine, or NE, did not cause further elevation of *Sik1* mRNA levels compared to selective β-adrenergic receptor activation (Fig. 3A). In comparison, *Aa-nat* expression was induced only when β-adrenergic receptor was activated (Fig. 3A). The dominant role of β-adrenergic receptor stimulation was also demonstrated by the blockade of NE-stimulated *Sik1* expression by propranolol (3 μM) whereas prazosin (3 μM) only had a smaller inhibitory effect (Fig. 3B). Blockade of the α_1-adrenergic receptor

only had a minor impact on the NE-stimulated *Aa-nat* expression whereas blocking the β-adrenergic receptor inhibited the NE-stimulated *Aa-nat* expression (Fig. 3B). These results suggest that *Sik1* is primarily induced through the β-adrenergic receptor but activation of the α_1-adrenergic receptor can also cause a small elevation in *Sik1* mRNA level.

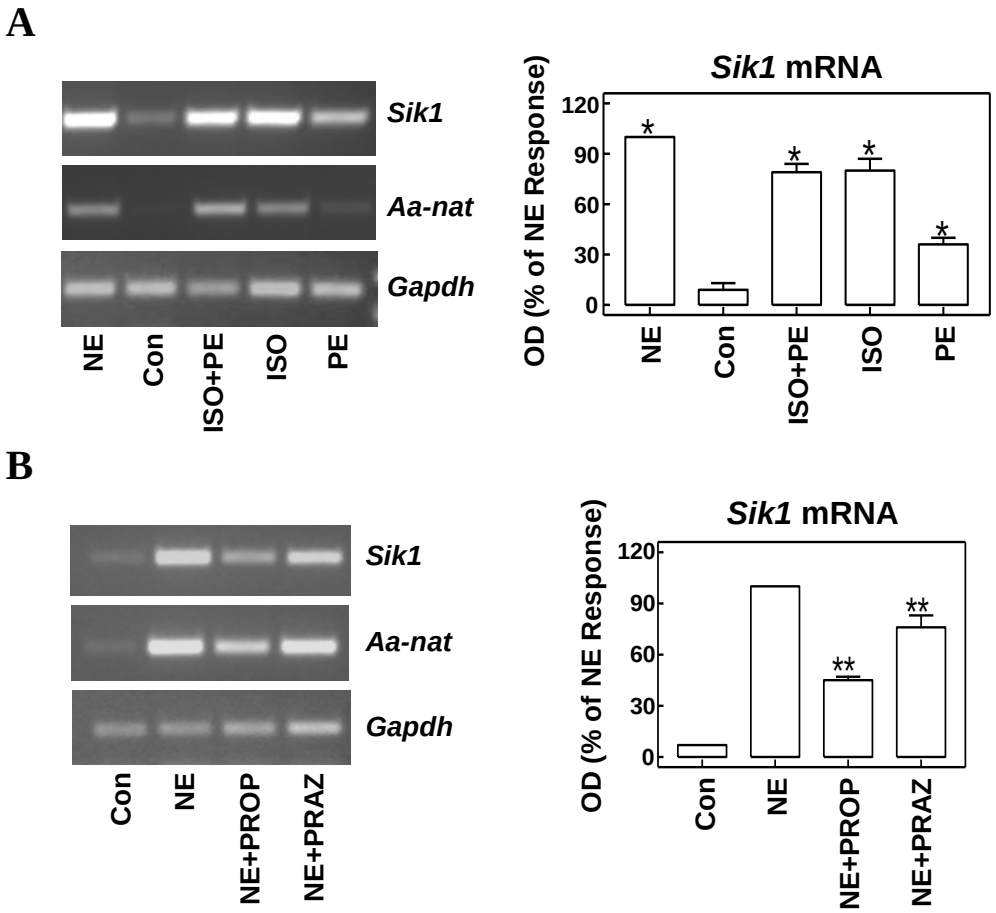

Figure 3: Receptor characterization of NE-stimulated *Sik1* transcription. Pinealocytes (1.0 x 10^5 cells/150 µl) were treated for 2 h as described below and prepared for RT-PCR (see *Materials and Methods*). **A**, Cells were treated with NE (3 µM), isoproterenol (ISO; 3 µM in presence of 3 µM prazosin (PRAZ)), phenylephrine (PE; 3 µM in presence of 3 µM propranolol (PROP)) or ISO plus PE. **B**, Cells were treated with NE (3 µM) alone or in the presence of 3 µM PROP or 3 µM PRAZ. *Left panel*, Representative ethidium bromide-stained gels showing *Sik1*, *Aa-nat* and *Gapdh* mRNA levels. *Right panels*, Histograms of corresponding densitometric measurements normalized to the NE-stimulated response value within the same experiment and presented as percentages. Each value represents the mean ± SEM of three independent experiments. *, Indicates significantly different ($p<0.05$) compared to control (Con; basal condition). **, Indicates significantly different ($p<0.05$) compared to NE (Kanyo et al., 2009).

D) Post-receptor signalling mechanisms involved in Sik1 induction

To determine the relative contributions of different signalling pathways downstream of the α_1- and β-adrenergic receptors (reviewed in Chik and Ho, 1989) in the NE-stimulated *Sik1* induction, a series of pharmacological agents were used. Activation of the β-adrenergic receptor causes intracellular elevations of cAMP and cGMP, which could be mimicked with 0.5 mM of dBcAMP (Chik et al., 2007a; Roseboom and Klein, 1995), a membrane permeable cAMP analogue, and 0.5 mM of dBcGMP (Ho et al., 1999), a membrane permeable cGMP analogue. α_1-adrenergic receptor activation causes intracellular Ca^{2+} elevation, which was achieved by depolarizing the cells with KCl (30 mM) or treatment with ionomycin (1 μM; a Ca^{2+}-ionophore) (Sugden et al., 1987). Intracellular Ca^{2+} elevation activates PKC and the calmodulin-dependent pathway (Ho et al., 1988b; Ho et al., 1991). To selectively investigate the role of PKC in *Sik1* induction, this kinase was activated with 0.1 μM of PMA (Ho et al., 1988b). *Aa-nat* is induced by intracellular elevations of cAMP (Roseboom et al., 1996) and was included as a control.

Cells were treated for 2 h with the above described pharmacological agents and mRNA levels were determined with RT-PCR. Treatment with dBcAMP induced *Sik1* and *Aa-nat* expression (Fig. 4A). In comparison, treatment with ionomycin also caused a small elevation of *Sik1* mRNA, but had no effect on *Aa-nat* expression (Fig. 4). Treatments with other pharmacological agents such as dBcGMP and PMA, did not have any effect on *Sik1* or *Aa-nat* mRNA levels (Fig. 4). To confirm that elevation of intracellular Ca^{2+} can induce

Sik1 mRNA, cells were depolarized with KCl. The increase of *Sik1* mRNA mediated by KCl was blocked by nifedipine (10 μM), a specific voltage-gated L-type Ca^{2+} channel blocker, while having no effect on the NE-stimulated response of *Sik1* and *Aa-nat* (Fig. 4B). These results indicate that *Sik1* transcription is primarily activated by the cAMP-pathway and to a lesser extent by intracellular Ca^{2+} elevation.

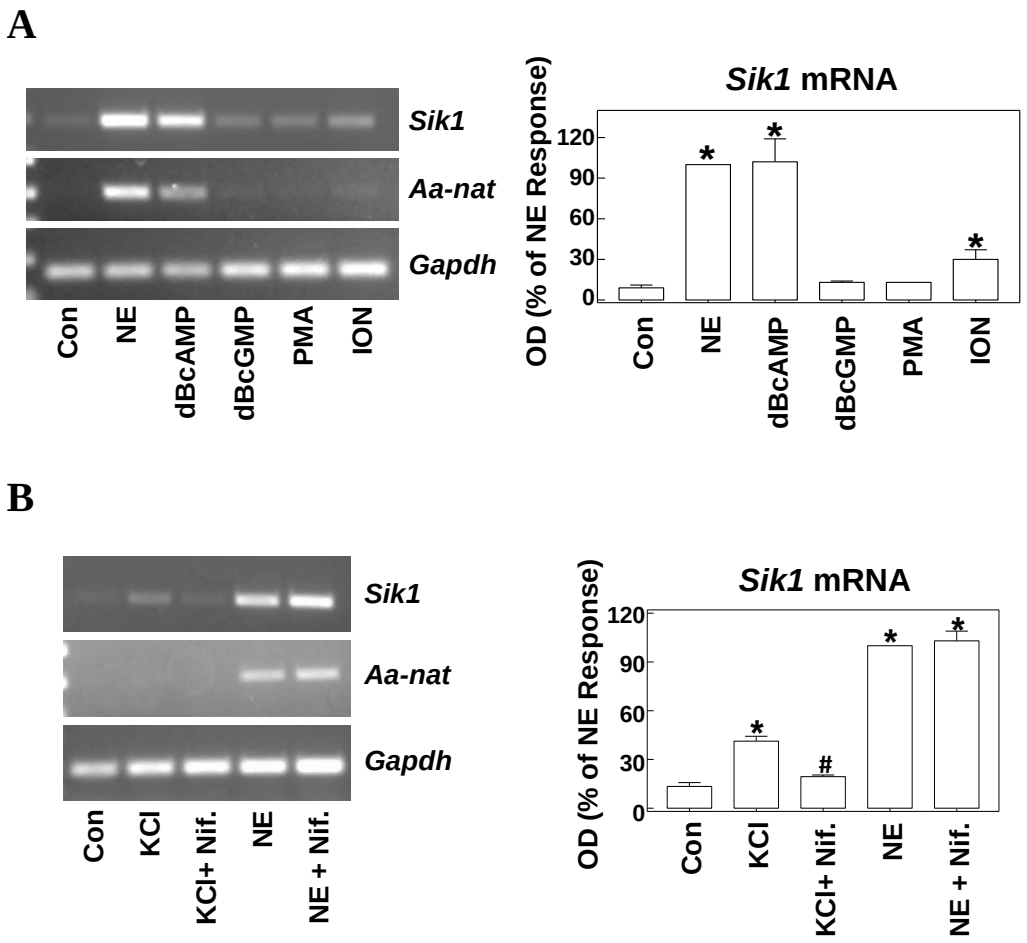

Figure 4: Post-receptor signalling mechanisms involved in *Sik1* induction. Pinealocytes (1.0 x 10^5 cells/150 µl) were treated for 2 h and prepared for RT-PCR (see *Materials and Methods*). **A**, Cells were treated with either NE (3 µM), dBcAMP (0.5 mM), dBcGMP (0.5 mM), PMA (10^{-7} M) or ionomycin (ION; 10^{-6} M). **B**, Cells were treated with either NE (3 µM) or KCl (30 mM) in the presence or absence of nifedipine (Nif.; 10 µM). *Left panel*, Representative ethidium bromide-stained gels show *Sik1*, *Aa-nat* and *Gapdh* mRNA levels. *Right panel*, Histograms of corresponding densitometric measurements normalized to the NE-stimulated response value within the same experiment and presented as percentages. Each value is presented as the mean ± SEM of three independent experiments. *, Indicates significantly different ($p<0.05$) from control (Con). #, Indicates significantly different ($p<0.05$) from KCl (Kanyo et al., 2009).

E) Effect of cyclohexamide treatment on Sik1 transcription

Sik1 was reported to behave like an immediate early gene (Feldman et al., 2000; Okamoto et al., 2004). To investigate whether *Sik1* transcription behaves like the transcription of an immediate early gene in rat pinealocytes, the effect of a protein synthesis inhibitor, cyclohexamide (Glauser et al., 2007), on *Sik1* expression was compared to that of *c-fos*, an established immediate early gene (Sheng and Greenberg, 1990). Pinealocytes were treated with NE (3 µM) for 2 h in the presence or absence of cyclohexamide (30 µg/ml) and *Sik1, c-fos* and *Aa-nat* expression were determined with RT-PCR. The effect of cyclohexamide on *Sik1* expression was similar to that on *c-fos*. Cyclohexamide increased the expression of both *c-fos* and *Sik1* in the presence and absence of NE, but had no effect on the NE-induced expression of *Aa-nat* (Fig. 5), which is not an immediate early gene. The results suggest that *Sik1* also behaves like an immediate early gene in the rat pineal gland and negative feedback signals repressing *Sik1* require synthesis of new proteins.

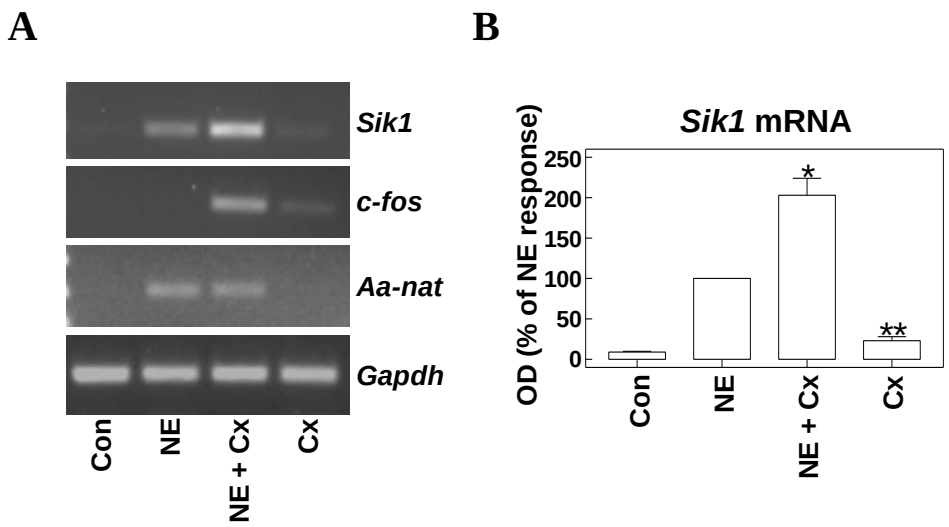

Figure 5: Effect of cyclohexamide on *Sik1* transcription. Pinealocytes (1.0 x 10^5 cells/150 µl) were treated with NE (3 µM) for 2 h in the presence or absence of cyclohexamide (Cx; 30 µg/ml) and prepared for RT-PCR (see *Materials and Methods*). **A**, Representative ethidium bromide-stained gels showing *Sik1*, *c-fos*, *Aa-nat* and *Gapdh* mRNA levels. **B**, Histogram of corresponding densitometric measurements normalized to the NE-stimulated response value within the same experiment and presented as percentages. Each value represents the mean ± SEM of three independent experiments. *, Indicates significantly different ($p<0.05$) from treatment with NE. **, Indicates significantly different ($p<0.05$) from the control (Con) (Kanyo et al., 2009).

F) Summary on the regulation of NE-induced Sik1 transcription.

The results in this section demonstrate that *Sik1* is induced at night by NE acting primarily through the β-adrenergic receptor/cAMP pathway with a minor contribution from the α_1-adrenergic receptor/Ca^{2+} pathway. The induction of *Sik1* precedes the induction of *Aa-nat* and remains elevated throughout the night in the whole animal, and for at least 6 h in cultured rat pinealocytes after NE stimulation.

3.2 The SIK1 effect on the induced AA-NAT expression

The results in the previous section suggest that SIK1 is expressed in the rat pineal gland and that its expression is under adrenergic control. SIK1 has been shown to repress CREB-target gene expression (Doi et al., 2002; Katoh et al., 2004b) and the expression of NE-induced *Aa-nat* in the rat pineal gland is driven by CREB (Bailey et al., 2009; Roseboom and Klein, 1995). Therefore, SIK1 may regulate the expression of *Aa-nat* and was investigated.

A) Effect of Sik1-sh2 and Sik1-fl on Sik1 mRNA levels

To manipulate the *Sik1* mRNA levels, cultured rat pinealocytes were transfected with recombinant adenoviral constructs expressing either a short-hairpin targeting the mRNA of *Sik1* (*Sik1*-sh2) or the full-length *Sik1* transcript (*Sik1*-fl). An adenoviral construct expressing *LacZ* was used to control for the transfection. Transfected cells were treated with NE (3 μM) and mRNA levels of *Sik1* and *Gapdh* were determined with RT-PCR. *Sik1* expression was induced 4 h

after NE treatment in the presence of the *LacZ* virus (Fig. 6). Transient transfection with *Sik1*-sh2 abolished this NE-stimulated increase in the *Sik1* mRNA level. As anticipated, transient transfection of pinealocytes with *Sik1*-fl caused a huge increase in *Sik1* mRNA level (Fig. 6). More importantly, this *Sik1*-fl-mediated increase in *Sik1* mRNA level could be reversed by cotransfection with *Sik1*-sh2 indicating that these transfection protocols could be used in combination to determine the recovery of function during our investigation on the functional aspect of SIK1 in the pineal. None of the viral treatments altered the *Gapdh* level, an established house keeping gene, the expression of which was used to control for mRNA extraction and cDNA synthesis between different samples (Fig. 6).

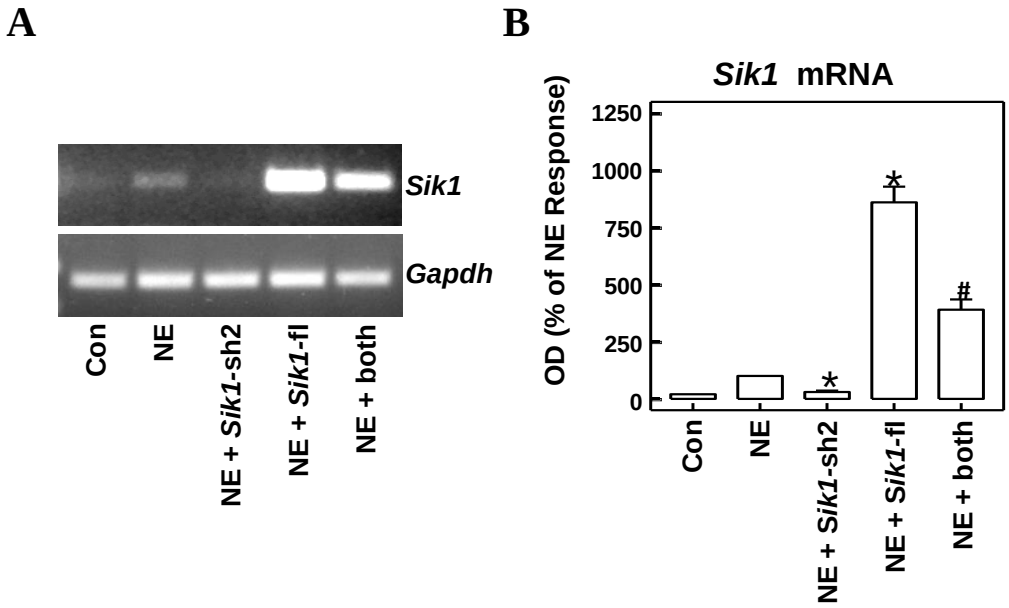

Figure 6: Effect of *Sik1*-sh2 and/or *Sik1*-fl on *Sik1* mRNA levels in cultured rat pinealocytes. Pinealocytes (1.0 x 10^5 cells/0.6 ml) were transiently transfected with recombinant adenoviral constructs expressing *Sik1*-sh2 and/or *Sik1*-fl, treated with NE (3 μM) for 4 h and prepared for RT-PCR (see *Materials and Methods*). **A**, Representative ethidium bromide-stained gels show *Sik1* and *Gapdh* mRNA levels. **B**, Histogram of corresponding densitometric measurements normalized to the NE-stimulated response value within the same experiment and presented as percentages. Each value represents the mean ± SEM of three independent experiments. *, Indicates significantly different ($p<0.05$) from treatment with NE. #, Indicates significantly different ($p<0.05$) from treatment with *Sik1*-fl (Kanyo et al., 2009).

B) Effect of Sik1 mRNA manipulation on NE-stimulated Aa-nat expression

To investigate the effect of SIK1 on adrenergically induced *Aa-nat*, the effects of *Sik1*-sh2 and *Sik1*-fl on NE-stimulated *Aa-nat* expression were determined. Transfected cells were treated for varying time periods with NE (3 μM) and the mRNA levels were measured with real-time PCR. Knockdown of endogenous *Sik1* with *Sik1*-sh2 enhanced NE-stimulated *Aa-nat* expression 4 h after NE treatment, but not after 2 h (Fig. 7). This enhancement of NE-stimulated *Aa-nat* caused by *Sik1*-sh2 persisted up to 32 h after NE treatment (Fig. 7). In contrast, overexpressing *Sik1* with *Sik1*-fl suppressed the NE-stimulated *Aa-nat* at all time-points tested (Fig. 7). Treatment with *Sik1*-fl could counteract the *Sik1*-sh2-mediated enhancement of NE-stimulated *Aa-nat* expression, indicating the specificity of *Sik1*-sh2 actions on *Aa-nat* (Fig. 7). These results suggest that SIK1 represses NE-stimulated *Aa-nat* transcription.

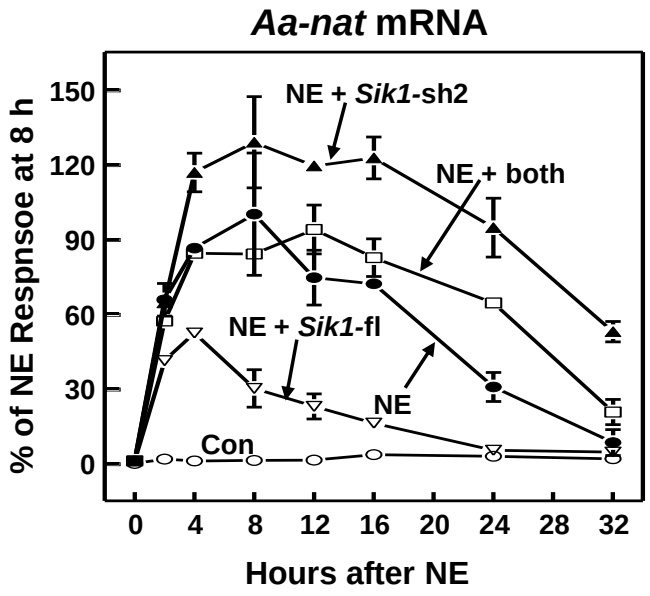

Figure 7: Time-course effects of *Sik1*-sh2 and/or *Sik1*-fl on NE-stimulated *Aa-nat* expression. Pinealocytes (1.0 x 10^5 cells/0.6 ml) were transiently transfected with recombinant adenoviral constructs expressing *Sik1*-sh2 and/or *Sik1*-fl, treated with NE (3 μM) for varying time periods as indicated and prepared for real-time PCR (see *Materials and Methods*). NE-stimulated *Aa-nat* mRNA levels were presented as percentages of the mean NE-stimulated response at 8 h. Each value represents the mean ± SEM of three independent experiments (Kanyo et al., 2009).

To determine whether the changes caused by *Sik1* knockdown or overexpression seen on the *Aa-nat* mRNA can be translated to the protein level, the effects of treatment with *Sik1*-sh2 and/or *Sik1*-fl were also tested on the NE-stimulated AA-NAT protein and enzymatic activity. Immunoblots demonstrated that *Sik1* knockdown enhanced NE-stimulated AA-NAT protein levels 8, 12 and 16 h after NE treatment, but not after 4 h (Fig. 8A). Similar to the results observed with *Aa-nat* mRNA levels, treatments with *Sik1*-fl suppressed the NE-stimulated AA-NAT protein levels at all the time-points tested (Fig. 8A). The *Sik1*-sh2-mediated enhancement could be counteracted with simultaneous *Sik1*-fl treatment (Fig. 8, A and B). Consistent with the results obtained on the AA-NAT protein, treatment with *Sik1*-sh2 caused an enhancement of the NE-stimulated AA-NAT activity 8 h after NE treatment while having no effect 4 h after treatment (Fig. 8C). The effect of *Sik1*-sh2 on AA-NAT activity persisted up to 32 h after NE treatment (Fig. 8C). In contrast, treatment with *Sik1*-fl suppressed the NE-stimulated enzymatic activity of AA-NAT at all time-points measured. The enhancing effect of *Sik1*-sh2 on the enzymatic activity of AA-NAT could be counteracted with simultaneous *Sik1*-fl treatment. Overall, the results obtained on the AA-NAT protein and enzymatic activity were similar to those obtained on the *Aa-nat* mRNA. This suggests that the effect of SIK1 on the NE-induced *Aa-nat* transcription is translated to the AA-NAT protein and enzymatic activity. Together the results show that SIK1 can repress NE-stimulated *Aa-nat* in the rat pineal gland.

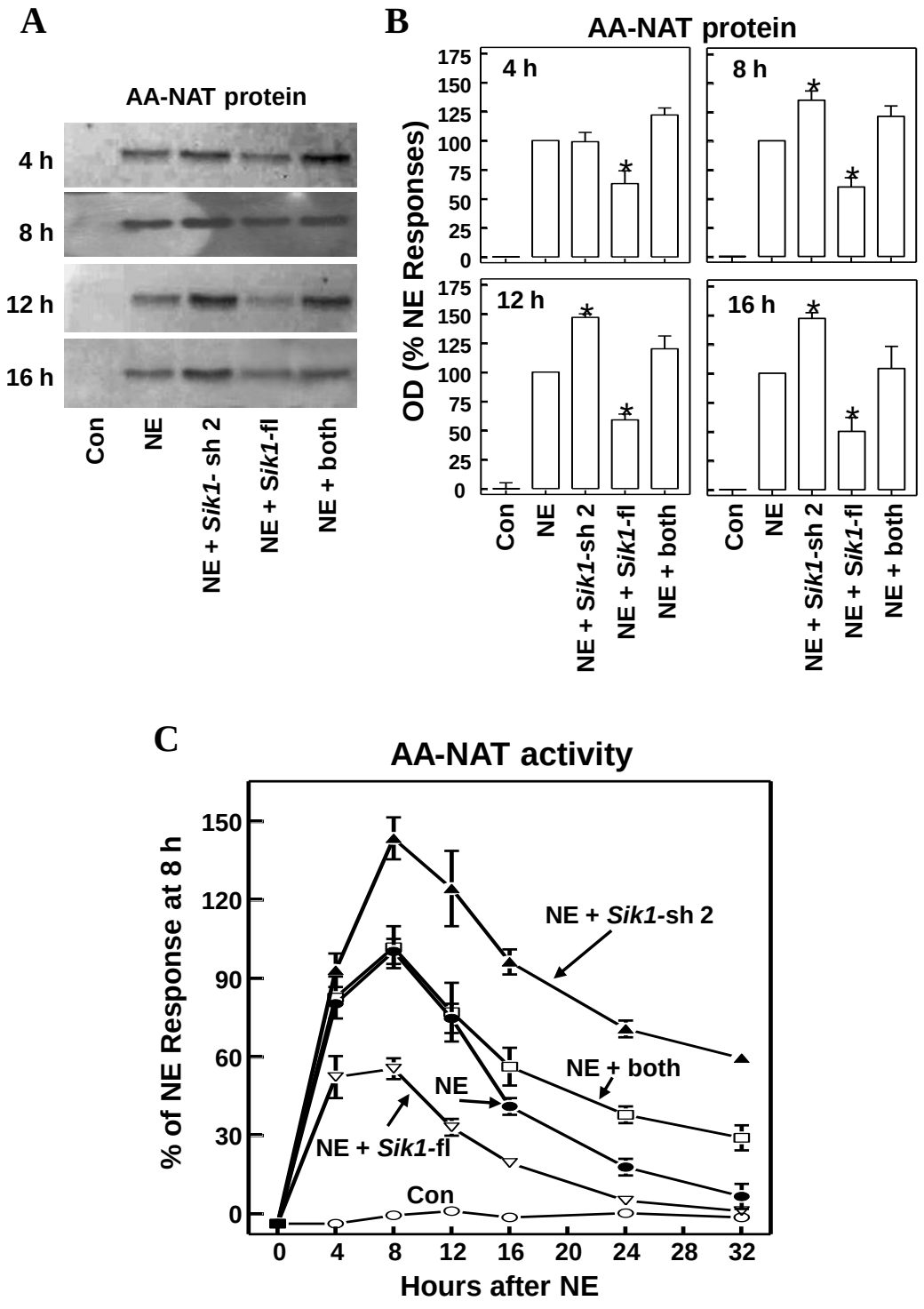

Figure 8: Effect of *Sik1*-sh2 and/or *Sik1*-fl on NE-stimulated AA-NAT protein and enzymatic activity (see next page for figure legend).

Figure 8: Effect of *Sik1*-sh2 and/or *Sik1*-fl on NE-stimulated AA-NAT protein and enzymatic activity. Pinealocytes (1.0×10^5 cells/0.6 ml) were transfected with adenoviral constructs expressing *Sik1*-sh2 and/or *Sik1*-fl, treated with NE (3 μM) for varying time periods as indicated and prepared for Western blot analysis or radioenzymatic assay (see *Materials and Methods*). **A**, Representative immunoblots from three independent experiments probed against AA-NAT. **B**, The corresponding densitometric measurements for A normalized to the NE-stimulated response value within the same experiment and presented as percentages. *, Indicates significantly different ($p<0.05$) from treatment with NE. **C**, AA-NAT activity normalized to the percentage of the mean NE response at 8 h. Each value represents mean ± SEM of three independent experiments (Kanyo et al., 2009).

C) Effect of Sik1-sh2 and Sik1-fl on the expression of other CREB-driven genes

The results suggesting SIK1 can repress induced *Aa-nat* raised the possibility that this kinase can also regulate the expression of other CREB-driven genes in the rat pineal gland. To investigate the effect of SIK1 on other CREB-driven genes, cultured pinealocytes were transfected with *Sik1*-sh2 and/or *Sik1*-fl and treated with NE (3 μM) for 2, 4 or 12 h. The mRNA levels of *Aa-nat* and three other CREB-driven genes previously investigated in rat pinealocytes were determined with RT-PCR. The three selected inducible genes were *Mkp-1* (Price et al., 2004a), *Dio2* (Chik et al., 2007b) and *Icer* (Ho et al., 2007b). Overexpressing *Sik1* mRNA resulted in suppression of NE-stimulated *Aa-nat*, *Mkp-1*, *Dio2* and *Icer* after 2, 4 and 12 h of NE treatment (Fig. 9). Similar to the results obtained on *Aa-nat*, *Sik1*-sh2 enhanced the NE-stimulated expression of *Mkp-1*, *Icer* and *Dio2* 4 and 12 h after NE treatment, but had no effect 2 h after treatment (Fig. 9). The results suggest that SIK1 can repress other CREB-target genes in the rat pineal gland.

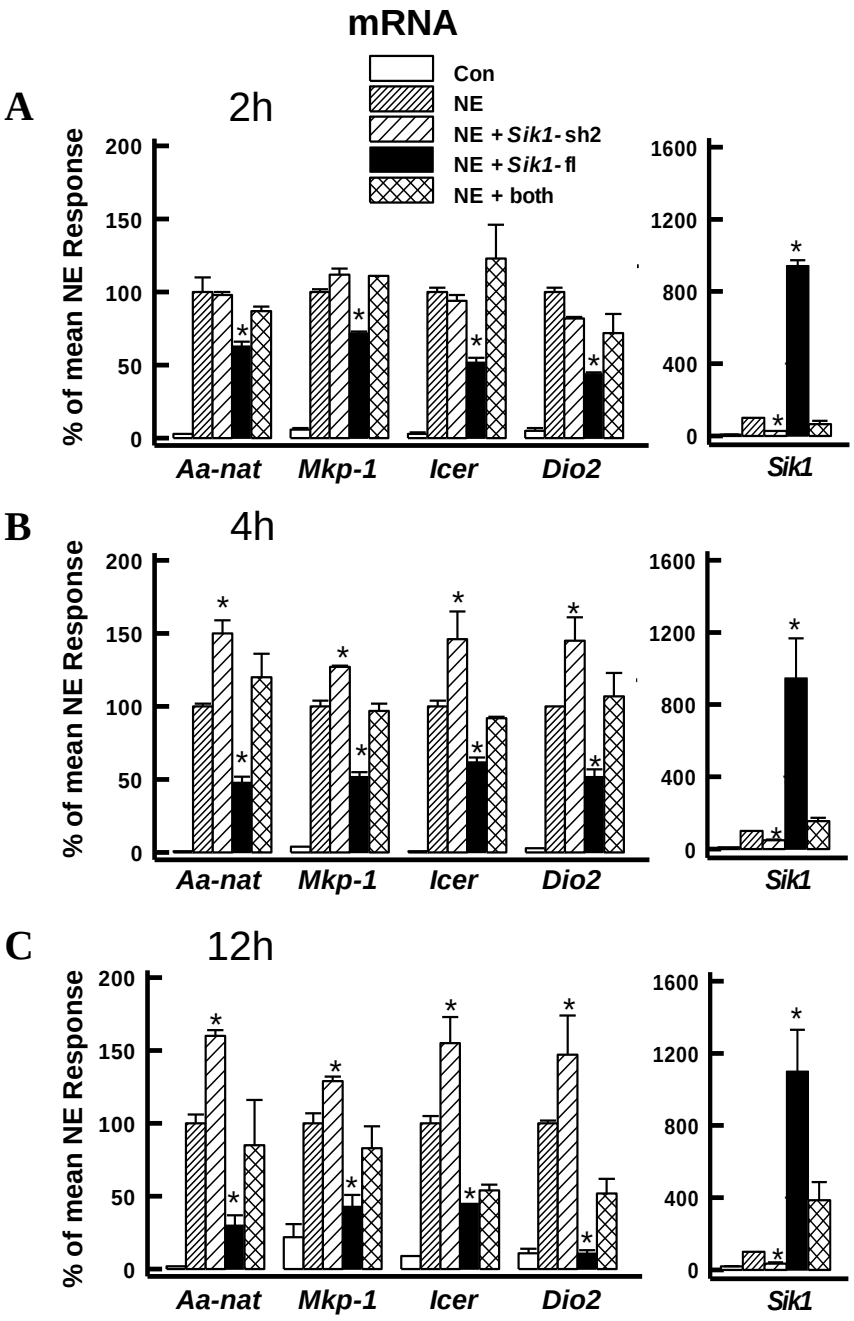

Figure 9: Effect of *Sik1*-sh2 and *Sik1*-fl on CREB-driven gene transcription. Pinealocytes (1.0 x 10^5 cells/0.6 ml) were transiently transfected with adenoviral constructs expressing *Sik1*-sh2 and/or *Sik1*-fl and treated with NE (3 µM) for 2 h (**A**), 4 h (**B**) or 12 h (**C**). mRNA levels of *Aa-nat*, *Mkp-1*, *Dio2*, *Icer* and *Sik1* were prepared for RT-PCR (see *Materials and Methods*) and densitometric measurements were presented as percentages of the mean NE-stimulated response. Each value represents the mean ± SEM of three independent experiments. *, Indicates significantly different ($p<0.05$) from NE (Kanyo et al., 2009).

D) Effect of Sik1-sh5 on adrenergically induced genes

A second adenoviral construct, *Sik1*-sh5, targeting a different sequence of the *Sik1* mRNA (1802-1823 bp from the start-site) was also investigated based on its effectiveness in knocking down the endogenous *Sik1* mRNA (Fig. 10A). To confirm that the enhancing effect of the *Sik1*-sh2 on the NE-stimulated *Aa-nat, Mkp-1, Icer* and *Dio2* expression was because of the reduction of endogenous *Sik1* mRNA levels, cultured rat pinealocytes were transfected with *Sik1*-sh5 and treated with NE (3 μM) for 16 h. The effect of *Sik1*-sh5 treatment on NE-stimulated expression of *Aa-nat, Mkp-1, Icer* and *Dio2* was measured with RT-PCR. Similar to the results obtained with *Sik1*-sh2, treatment with *Sik1*-sh5 construct enhanced the NE-stimulated expression of *Aa-nat, Mkp-1, Icer* and *Dio2* in rat pinealocytes 16 h after treatment (Fig. 10B). This result further supports the idea that endogenous SIK1 represses NE-stimulated *Aa-nat*.

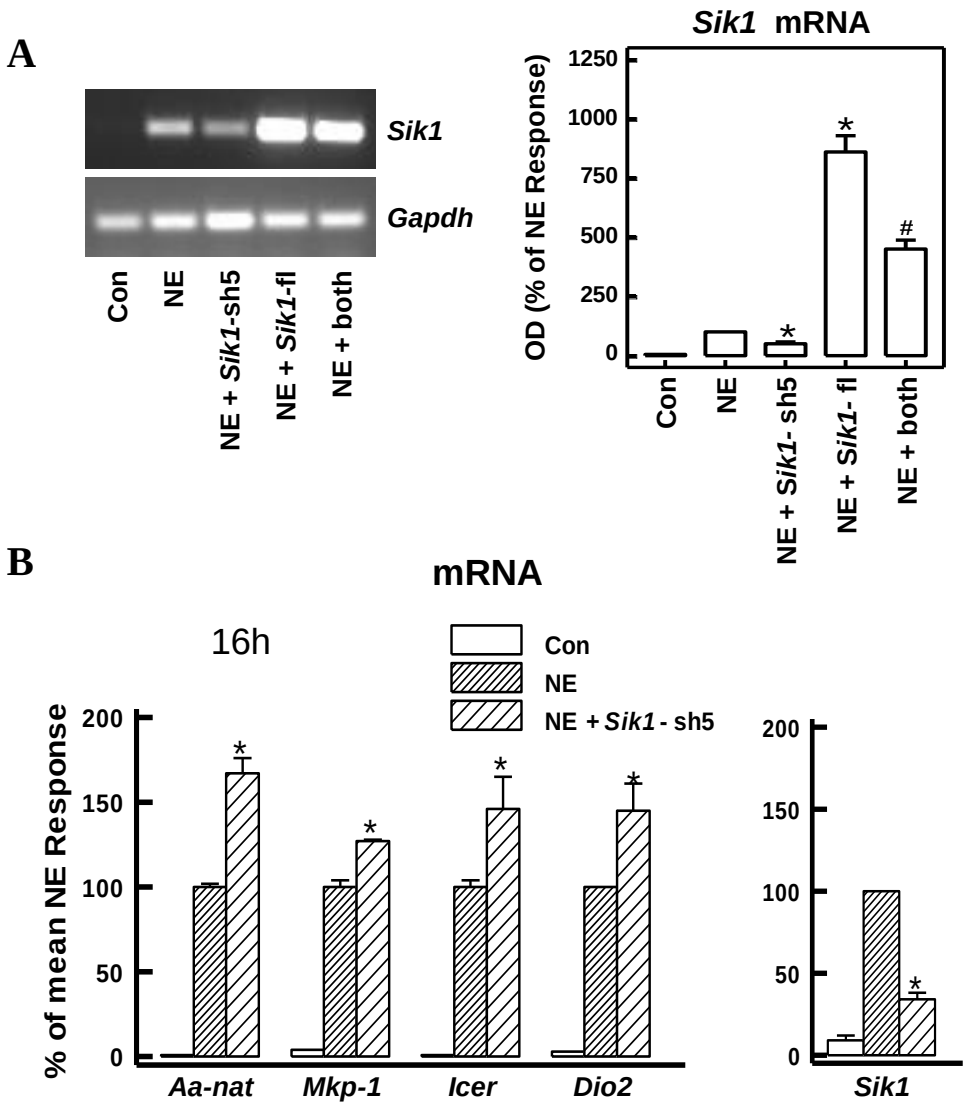

Figure 10: Effect of *Sik1*-sh5 on NE-stimulated gene transcription. Pinealocytes (1.0 x 10^5 cells/0.6 ml) were transfected with an adenoviral construct expressing *Sik1*-sh5, treated with NE (3 µM) for 16 h and prepared for RT-PCR (see *Materials and Methods*). **A**, Representative ethidium bromide-stained gel showing *Sik1* and *Gapdh* mRNA levels (*left panel*). Corresponding histogram of densitometric measurements normalized to the NE response value within the same experiment and presented as percentages (*right panel*). **B**, Histograms of densitometric measurements of *Aa-nat*, *Dio2*, *Icer* and *Mkp-1* mRNA levels were presented as percentages of the mean NE response. Each value represents the mean ± SEM of three independent experiments. *, Indicates significantly different ($p<0.05$) from treatment with NE. #, Indicates significantly different ($p<0.05$) from treatment with *Sik1*-fl (Kanyo et al., 2009).

E) Expression and effect of Sik1-fl-gfp on NE-stimulated AA-NAT protein

Because no suitable SIK1 antibody was commercially available, a fusion construct of *Sik1*-fl was used to demonstrate that the *Sik1*-fl could lead to an increase in SIK1 protein level and repressed NE-stimulated *Aa-nat* expression. The *Sik1* full-length gene was fused to a *Gfp* gene to generate the *Sik1-fl-gfp* adenoviral construct. Cultured rat pinealocytes were transfected with either a control virus expressing *Gfp* or varying amounts of the *Sik1-fl-gfp* adenoviral construct. Transfected cells were treated with NE (3 μM) for 6 h and the corresponding immunoblots were probed with an antibody targeting the GFP protein. Immunoblots showed the GFP protein (migrated close to the 32 kDa marker; expressed by the control virus) and the SIK1-fl-GFP fusion protein (migrated just below the 119 kDa marker) (Fig. 11). The increased intensity of the SIK1-fl-GFP band corresponded to the increasing amounts of *Sik1-fl-gfp* added and correlated with an increased suppression of the NE-stimulated AA-NAT protein levels (Fig. 11). These results confirm that transfection with adenoviral construct expressing *Sik1*-fl will lead to increased SIK1 protein and that SIK1 represses AA-NAT expression.

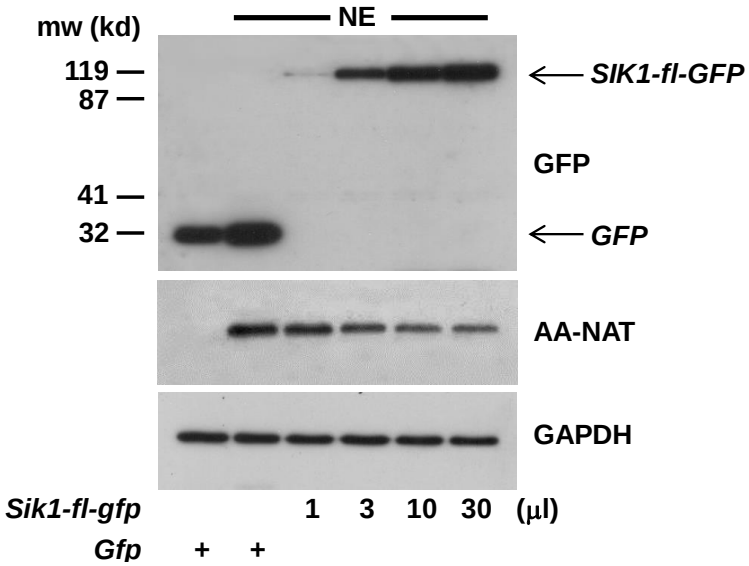

Figure 11: Effect of *Sik1-fl-gfp* on NE-stimulated AA-NAT. Pinealocytes (1.0 x 10^5 cells/ 0.6 ml) were transfected with adenoviral constructs expressing either *Gfp* (control virus) or different doses of *Sik1-fl-gfp*. Cells were then treated with NE (3 µM) for 6 h and prepared for Western blot analysis (see *Materials and Methods*). Figure shows representative immunoblots of three independent experiments probed with antibodies targeting GFP, AA-NAT and GAPDH. Arrows point out the GFP protein (around the 32 kDa marker) and the SIK1-fl-GFP fusion product (around the 119 kDa marker) (Kanyo et al., 2009).

F) Effect of the Sik1-S577A mutant on NE-stimulated Aa-nat transcription

SIK1 can be phosphorylated by PKA at the Ser577-site (Takemori et al., 2002). To investigate the role of this phosphorylation site on the effect of SIK1 in repressing NE-stimulated gene expression in the rat pineal gland, a recombinant adenoviral construct expressing a phosphorylation-defective *Sik1* (*Sik1*-S577A) mutant was generated via site-directed mutagenesis. Cultured rat pinealocytes were transfected with adenoviral constructs expressing either the wild-type (*Sik1*-fl) or the mutated form of *Sik1* (*Sik1*-S577A). Cells were treated with NE (3 μM) for 4 h and *Sik1* mRNA levels were determined with real-time PCR. Treatments with *Sik1*-fl or *Sik1*-S577A increased *Sik1* mRNA levels and caused a reduction in the NE-stimulated expressions of *Aa-nat*, *Mkp-1*, *Icer* and *Dio2* (Fig. 12). Compared with *Sik1*-fl, similar levels of *Sik1*-S577A overexpression were more potent in repressing the expression of the 4 NE-stimulated genes investigated (Fig. 12). These results suggest that the Ser577-site on SIK1 can have an inhibitory role on SIK1 function.

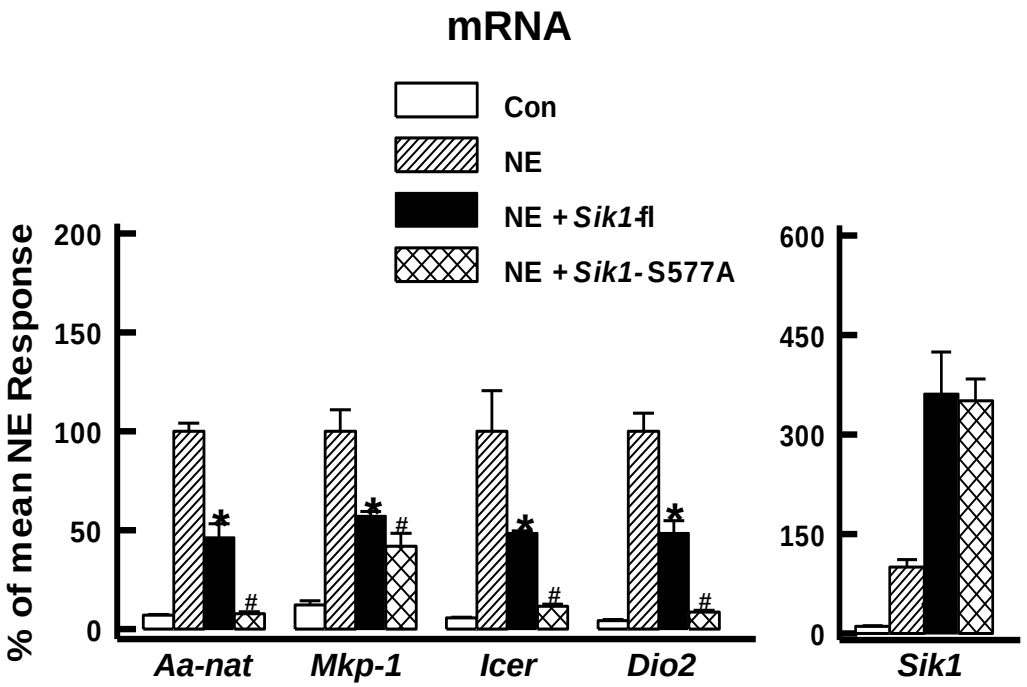

Figure 12: Effect of overexpressing *Sik1*-fl vs mutated *Sik1*-S577A on NE-stimulated gene transcription in rat pinealocytes. Pinealocytes (1.0×10^5 cells/0.6 ml) were transfected with adenoviral constructs expressing *Sik1*-fl or *Sik1*-S577A, treated with NE (3 µM) for 4 h and prepared for real-time PCR (see *Materials and Methods*). *Aa-nat, Mkp-1, Icer, Dio2* and *Sik1* mRNA levels were measured and presented as percentages of the mean NE response. Each value represents the mean ± SEM of three independent experiments. *, Indicates significantly different ($p<0.05$) from treatment with NE. #, Indicates significantly different ($p<0.05$) from treatment with *Sik1*-fl.

G) Summary on the effect of SIK1 on NE-stimulated Aa-nat expression

The results in this section indicate that SIK1 can repress NE-stimulated *Aa-nat* expression. Although overexpressing *Sik1* inhibited NE-stimulated *Aa-nat* at all time-points measured, knockdown of the endogenous *Sik1* enhanced NE-stimulated *Aa-nat* mRNA only after 4 h of stimulation and protein levels 8 h. The effects of manipulating *Sik1* expression levels on other CREB-driven genes were similar to that of *Aa-nat*.

3.3 The regulation of TORC2 in the rat pineal gland

Next, the mechanism by which SIK1 could repress the NE-stimulated *Aa-nat* expression was investigated. SIK1 has been demonstrated to phosphorylate and cause the nuclear export of the CREB-coactivator, TORC2 (Katoh et al., 2004b; Takemori et al., 2007) and may represent the mechanism through which SIK1 mediates its repressor effect. Since SIK1 can repress NE-stimulated *Aa-nat* transcription, this raises the possibility that TORC2 may also function as a coactivator in the rat pineal gland. However, the regulation of TORC2 in the rat pineal gland is unknown.

A) Diurnal regulation of the TORC2 protein in the rat pineal gland

To determine whether TORC2 is regulated by the day/night cycle in the rat pineal gland, *Torc2* mRNA and protein levels were determined from freshly dissected glands collected at selected time-points in animals housed under controlled environmental lighting conditions (14 h of light every 24 hours). Real-

time PCR analysis revealed that relative to the nocturnal induction of *Aa-nat*, *Torc2* mRNA levels did not differ between day and night (Fig. 13A). As for the TORC2 protein, immunoblots revealed two TORC2 bands around the 75 kDa marker (Fig. 13B). During daytime, the slower migrating band (upper band) was more dominant whereas during nighttime the lower band was more prominent (Fig. 13B). One hour after onset of darkness, the intensity of the upper band declined while the intensity of the faster migrating band (lower band) of TORC2 increased (Fig 13B). In contrast, one hour after onset of light, the intensity of the lower band of TORC2 declined while the upper band became more dominant (Fig. 13B). The shift of the TORC2 bands with the onset of darkness occurred before the phosphorylation of CREB and the appearance of the AA-NAT protein. These results indicate that the *Torc2* mRNA has no diurnal rhythm, but there is a day/night variation in the band pattern of the TORC2 protein migration on the Western blot.

A

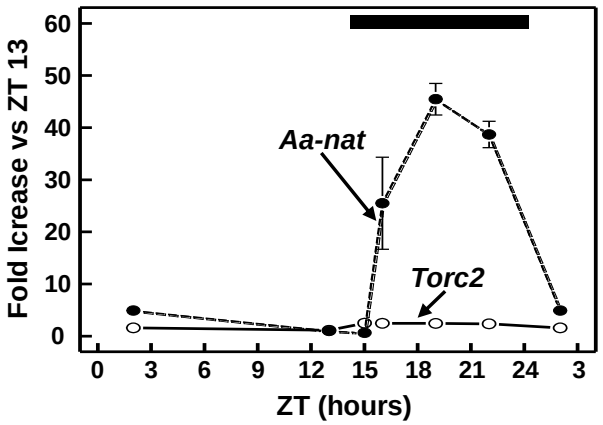

B

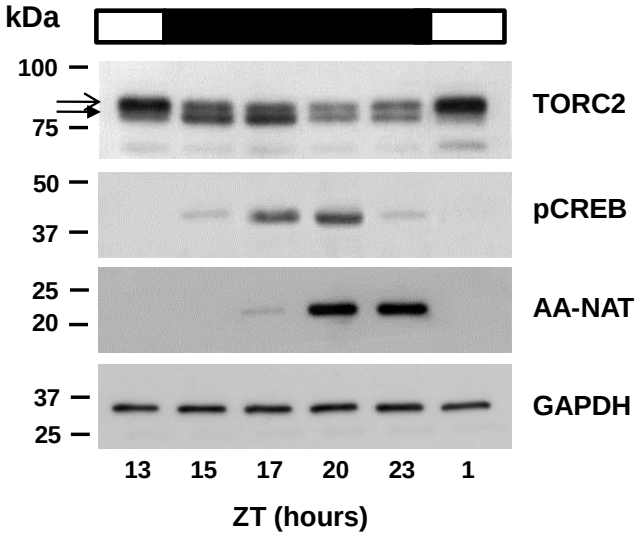

Figure 13: Day/night variation in *Torc2* mRNA and protein levels in the rat pineal gland. Animals were housed under controlled environmental lighting conditions (night is indicated by a dark bar; 14:10 LD). Rat pineal glands were collected at different time-points as indicated and prepared for real-time PCR or Western blot analysis (see *Material and Methods*). **A**, *Aa-nat* and *Torc2* mRNA levels were normalized to *Gapdh* levels. Mean values ± SEM from three independent experiments are expressed as fold increase over the mean value obtained one hour before onset of darkness. **B**, Representative immunoblots from three independent experiments probed for TORC2, pCREB and AA-NAT. GAPDH was included to demonstrate loading consistency. The two arrows show upper and lower TORC2 bands. ZT, Zeitgeber time (Kanyo et al., 2011).

B) The lower TORC2 band is adrenergically induced

To investigate the signalling pathways involved in the regulation of TORC2, the effects of NE on the *Torc2* mRNA and protein levels were determined. Cultured rat pinealocytes were prepared and treated with NE (3 µM) for varying duration. The TORC2 protein was analyzed with Western blot analysis and the *Torc2* and *Aa-nat* mRNA levels were determined by real-time PCR. In comparison to NE-stimulated *Aa-nat* mRNA levels, which peaked 4 h after treatment, *Torc2* mRNA levels did not change after the addition of NE (Fig. 14A). Analysing the TORC2 protein on immunoblots revealed that the slower migrating upper band of TORC2 decreased in intensity 30 min after NE treatment while the intensity of the faster migrating lower band was increased (Fig. 14, B and C). The level of the lower TORC2 band peaked 30 min after NE treatment and gradually declined over 8 h after NE treatment (Fig. 14, B and C). The increase in the lower TORC2 band intensity paralleled the appearance of pCREB and preceded that of AA-NAT (Fig. 14B). The NE-stimulated shift of the TORC2 band obtained with cultured rat pinealocytes was similar to that obtained after the onset of darkness in the pineal gland with the whole animal study.

To determine the NE dose-response relationship on the induced shift in the TORC2 protein, cultured rat pinealocytes were treated for 15 min with varying concentrations of NE. A small increase in intensity of the lower TORC2 band was already obtained with 3 nM of NE and reached the maximum intensity with 300 nM of NE (Fig. 14, D and E). The NE dose-dependent increase of the lower band correlated with the decrease in the intensity of the upper band of TORC2

(Fig. 14D). This suggests that the induced shift in the TORC2 band is very sensitive to NE stimulation. Altogether, the results indicate that the nighttime induced shift of the TORC2 band is due to stimulation by NE. This shift is as rapid and as sensitive to NE stimulation as the phosphorylation of CREB.

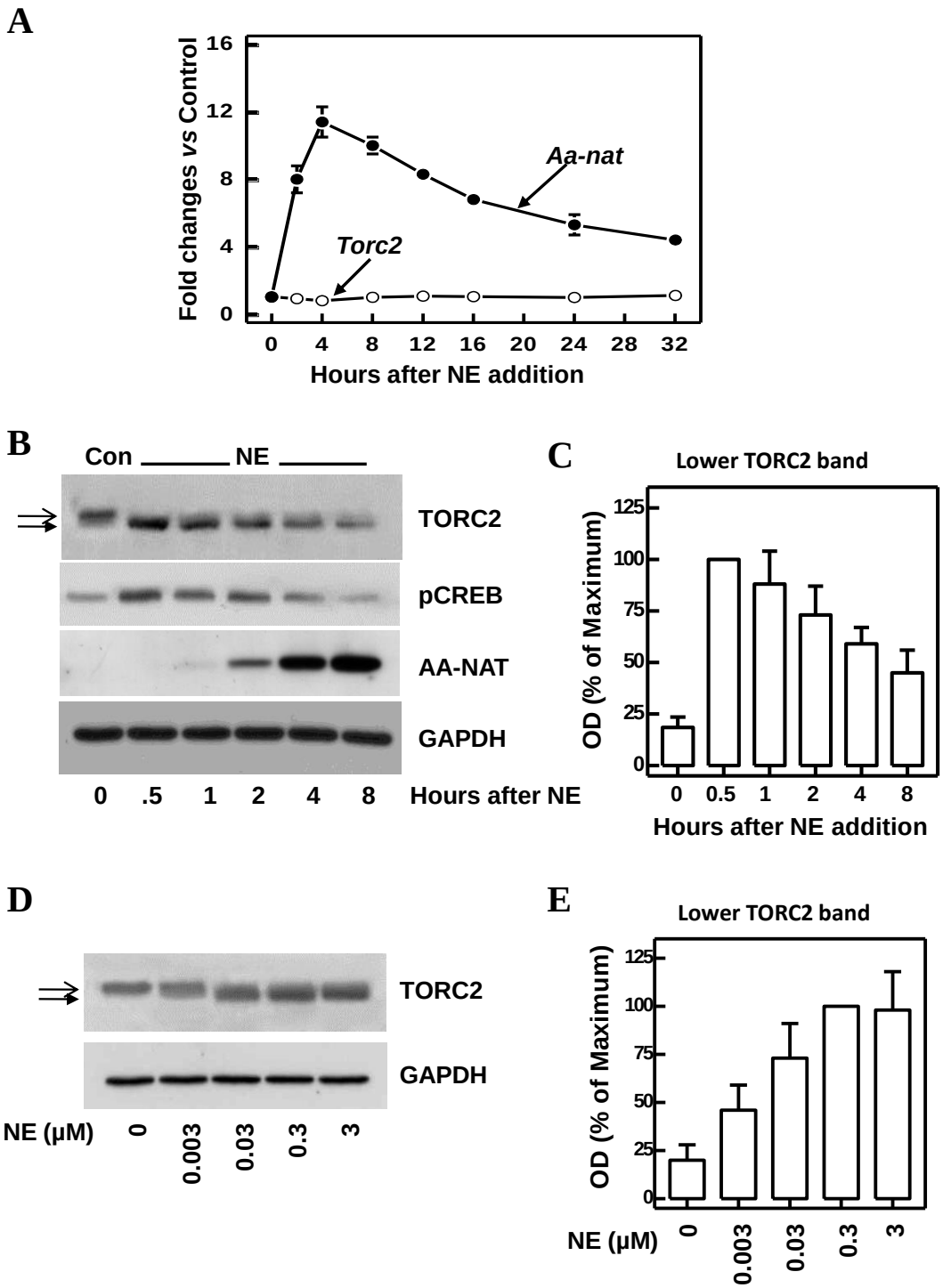

Figure 14: Effect of NE on TORC2 (see next page for figure legend).

Figure 14: Effect of NE on TORC2. Pinealocytes (1.0 x 10^5 cells/300 µl) were treated by either varying the duration (**A**-**C**) or the concentration (**D** and **E**) of NE and prepared for either real-time PCR or Western blot analysis (see *Materials and Methods*). **A**, The time profile of *Aa-nat* and *Torc2* mRNA levels, normalized to *Gapdh* mRNA levels and presented as a fold change against the control. **B,** Representative immunoblots probed for TORC2, pCREB, AA-NAT and GAPDH. The two arrows show upper and lower TORC2 bands. **C**, Histogram of densitometric measurements of the lower TORC2 band from B presented as percentages of the maximal NE-stimulated response within the same experiment. **D**, Representative immunoblots probed for TORC2 and GAPDH. **E**, Histogram of densitometric measurements of the lower TORC2 band from D. Each value represents the mean ± SEM of three independent experiments (Kanyo et al., 2011).

C) NE stimulation causes dephosphorylation of TORC2

The identities of the upper and lower TORC2 bands obtained on the immunoblots were also determined. Earlier studies have shown that TORC2 can be phosphorylated (Screaton et al., 2004; Takemori et al., 2007) and phosphorylated TORC2 may migrate differently than dephosphorylated TORC2 on the SDS gel. To test this possibility, cultured rat pinealocytes were stimulated with NE (3 μM) for 15 min and cell lysates were treated with calf intestinal alkaline phosphatase (CIP) before SDS-PAGE and monitored on immunoblots. The results showed that treatment with CIP caused the lower band of TORC2 to be more dominant under basal conditions while having no additional effect on the NE-stimulated lower band (Fig. 15A). CIP treatment also abolished the NE-stimulated pCREB, which serves as a positive control for dephosphorylation. The result indicates that the lower band induced by NE is the dephosphorylated form of TORC2.

To investigate the time-course effects of NE stimulation on the TORC2 phosphorylation status, cells were treated for varying duration with NE and samples were separated on a PhosTag gel. The addition of PhosTag to the SDS-polyacrylamide gel can retard the migration of phosphorylated proteins (Kinoshita et al., 2009). Figure 15B shows that in comparison to untreated control samples the NE-stimulated shift of the TORC2 band was more dramatic on the PhosTag gel than previously observed on a normal gel (Fig 14B). This effect of NE was observable within 15 min and was maintained 8 h after the treatment (Fig. 15B). pCREB which was also induced by NE was monitored to control for the drug

treatment (Fig. 15B). The results demonstrate that NE stimulation induces rapid TORC2 dephosphorylation and this effect is sustained for at least 8 h.

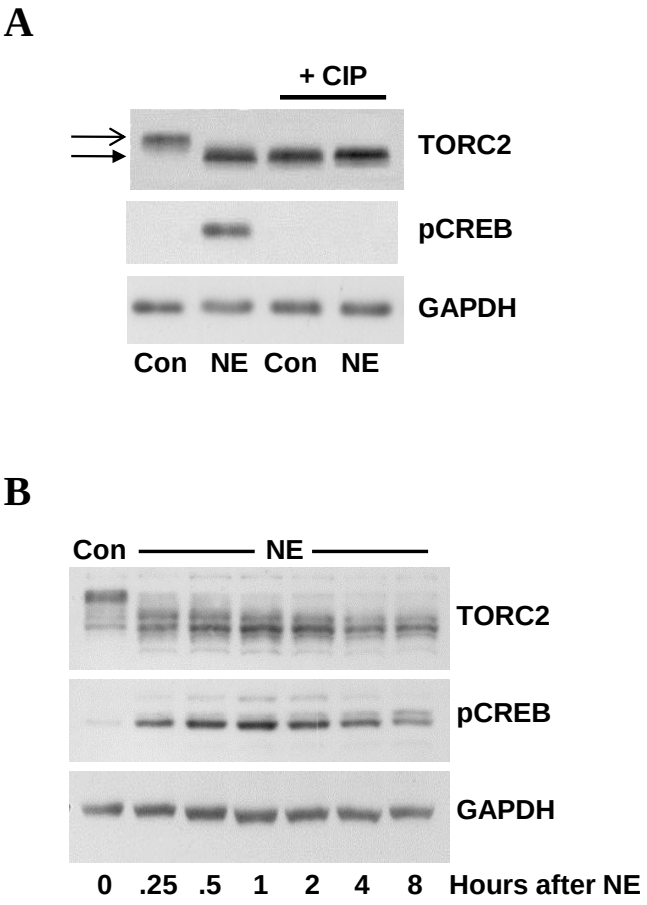

Figure 15: NE stimulates dephosphorylation of TORC2. Pinealocytes (1.0 x 10^5 cells/300 µl) were treated with NE (3 µM) and prepared for Western blot analysis (see *Materials and Methods*). **A**, Cells were stimulated for 15 min and harvested cell lysates were treated with calf intestinal alkaline phosphatase (CIP). The two arrows show upper and lower TORC2 bands (Kanyo et al., 2011). **B**, Cells were stimulated for varying time periods and samples were separated on a PhosTag gel. The immunoblots are representatives from three independent experiments and were probed for TORC2, pCREB and GAPDH (McTague et al., 2012).

D) Receptor characterization of the NE-stimulated TORC2 dephosphorylation

The receptor subtypes regulating the NE-stimulated dephosphorylation of TORC2 were then characterized. pCREB was included to control for β-adrenergic receptor stimulation (Fig. 16A) (Roseboom and Klein, 1995). Concentrations of the agonists used were based on the NE dose-response study (Fig. 14D and E). The dose of NE (30 nM) which increased dephosphorylated TORC2 levels to 75 % of maximal was chosen (Fig. 14D and E). Since TORC2 dephosphorylation could be observed with 3 nM of NE stimulation (Fig. 14D and E), to ensure that the receptor was effectively blocked by the antagonist, the concentration of the antagonists used was set at 1 μM.

Selective activation of the β-adrenergic receptor with 30 nM of isoproterenol (in presence of 1 μM of prazosin) increased the intensity of pCREB and the dephosphorylated version of TORC2 (lower band) (Fig. 16A). In comparison, selective activation of the α_1-adrenergic receptor with 30 nM of phenylephrine (in presence of 1 μM of propranolol) caused no change in pCREB levels or in the levels of the phosphorylated TORC2 upper band (the phosphorylated TORC2). Activation of α_1- and β-adrenergic receptors with combined treatment of phenylephrine and isoproterenol, or NE, had the same effect as selective β-adrenergic receptor activation. This suggests that β-adrenergic receptors activation alone is sufficient to mimic the effect of NE. The dominant role of the β-adrenergic receptor was also demonstrated with adrenergic-receptor antagonists. The effect of NE (30 nM) on pCREB and

TORC2 could be blocked by propranolol (1 μM) but not by prazosin (1 μM) (Fig 16A).

Samples from a separate experiment with the identical protocol as described above were separated on a PhosTag gel. The effect of selectively activating or blocking the adrenergic receptors on the TORC2 protein band pattern was compared with that stimulated by NE. Activation of the β-adrenergic receptor yielded the same TORC2 band-pattern obtained after NE treatment (Fig. 16A bottom). In contrast, activation of the α_1-adrenergic receptor had no effect on the TORC2 migration on the PhosTag gel, suggesting that this receptor has no major role in the NE-stimulated TORC2 dephosphorylation (Fig. 16A). These results indicate that the NE-stimulated dephosphorylation of TORC2 is primarily triggered by the activation of the β-adrenergic receptor.

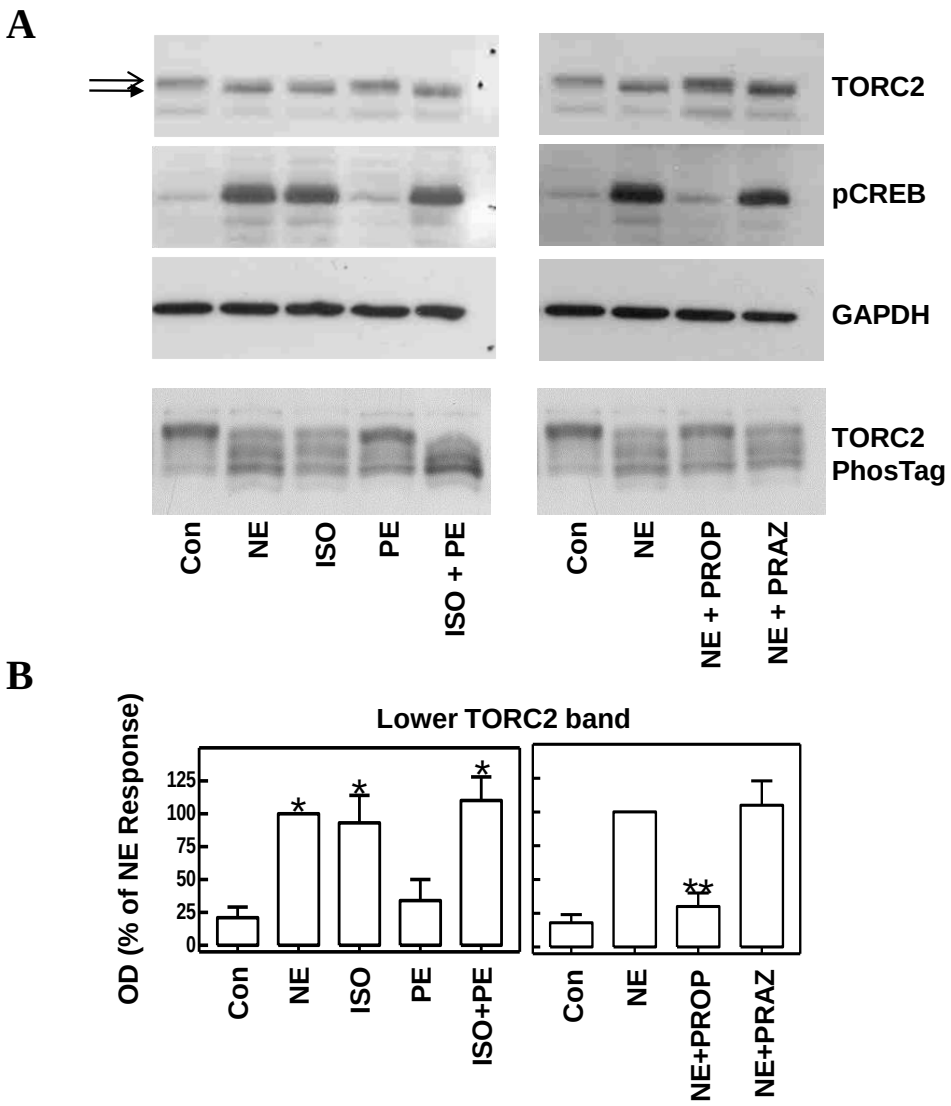

Figure 16: Receptor characterization of NE-stimulated TORC2 dephosphorylation. Pinealocytes (1.0 x 10^5 cells/300 µl) were treated with NE (30 nM), isoproterenol (ISO; 30 nM with 1 µM of prazosin (PRAZ)), phenylephrine (PE; 30 nM with 1 µM of propranolol (PROP)), ISO plus PE, NE (30 nM) in presence of 1 µM PRAZ or PROP. **A**, Representative immunoblots were prepared and probed for TORC2, pCREB and GAPDH (see *Materials and Methods*). The two arrows show upper and lower TORC2 bands. Samples were also separated on a PhosTag gel and immunoblots were probed for TORC2 (TORC2 PhosTag). **B**, Histograms of densitometric measurements of the lower TORC2 bands presented as percentages NE-stimulated response within the same experiment. Each value represents the mean ± SEM of three independent experiments. *, Significantly different from control (Con). **, Significantly different from NE.

E) Post-receptor signalling mechanisms involved in the NE-stimulated dephosphorylation of the TORC2 protein

Following the receptor characterization, the signalling pathways downstream of the α_1- and β-adrenergic receptor were investigated. pCREB is induced through the β-adrenergic receptor/cAMP-pathway (Roseboom and Klein, 1995) and was included as control for NE and dBcAMP treatments. Treatment of cultured rat pinealocytes for 30 min with dBcAMP (0.5 mM) mimicked the effect of NE (3 μM) on TORC2 dephosphorylation and also increased pCREB level (Fig. 17A). Depolarizing the cells with KCl, which elevates intracellular Ca^{2+} through voltage-gated L-type Ca^{2+} channel, had a small effect on TORC2 dephosphorylation. Treatments with other pharmacological agents such as dBcGMP (0.5 mM) and PMA (0.1 μM) had no effect (Fig. 17A). To confirm the small effect of KCl treatment on TORC2, samples were also separated on a PhosTag gel. Treatment with KCl (30 mM) revealed multiple lower TORC2 bands suggesting that elevating intracellular Ca^{2+} treatment can also cause TORC2 dephosphorylation (Fig. 17A). Using the PhosTag gel also revealed similar TORC2 band-patterns between treatments with NE and dBcAMP (Fig. 17A). However, these patterns were different from that obtained with KCl. Treatment with dBcGMP (0.5 mM) and PMA (0.1 μM) had no effect on TORC2. Together, these results suggest that elevation of both intracellular cAMP and Ca^{2+} can cause dephosphorylation of TORC2, but the band-patterns obtained from the PhosTag gel suggest that the NE-mediated dephosphorylation is primarily driven by the cAMP pathway.

The results also show that whereas selective α_1-adrenergic receptors stimulation cannot cause TORC2 dephosphorylation (Fig. 16), depolarizing cells with K^+ is effective (Fig. 17). This suggests that intracellular Ca^{2+} elevation mediated through activation of α_1-adrenergic receptors is different than that mediated by KCl treatment.

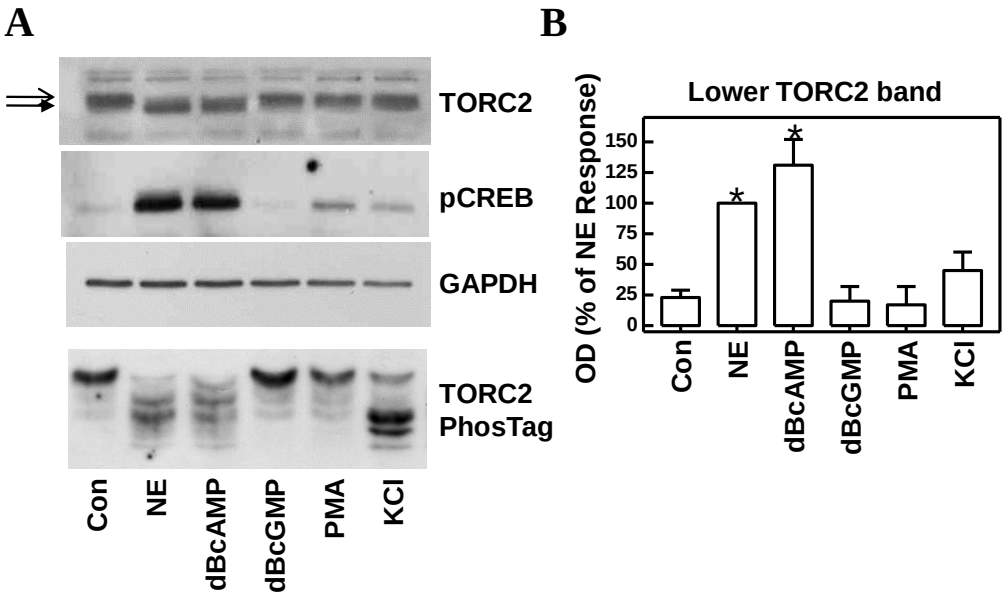

Figure 17: Post-receptor signalling pathways in TORC2 dephosphorylation. Pinealocytes (1.0 x 10^5 cells/300 µl) were treated for 30 min with NE (3 µM), dBcAMP (0.5 mM), dBcGMP (0.5 mM), PMA (10^{-7} M), or KCl (30 mM) and prepared for Western blot analysis (see *Materials and Methods*). **A**, Blots obtained from samples separated on regular and PhosTag gels probed for TORC2, pCREB and GAPDH. **B**, Histogram of densitometric measurements of the lower TORC2 band obtained from samples run on a regular gel and presented as percentages of the NE-stimulated response within the same experiment. Each value represents the mean ± SEM of three independent experiments. *, Significantly different from control (Con). The two arrows show upper and lower TORC2 bands (Kanyo et al., 2011; McTague et al., 2012).

F) NE-stimulated dephosphorylation causes TORC2 nuclear translocation

The phosphorylation status of TORC2 has been suggested to be important in determining the cellular distribution of this coactivator (Screaton et al., 2004; Takemori et al., 2007). Previous results indicate that NE stimulation can cause the dephosphorylation of TORC2 in the rat pineal gland, which prompted us to investigate the effects of NE on the cellular localization of TORC2. Pinealocytes were treated with NE (3 μM) for 30 min and fractionated into cytoplasmic and nuclear fractions prior to Western blot analysis. To monitor the effectiveness of the fractionation, immunoblots were probed for GAPDH (a cytoplasmic protein), histone H3 (a nuclear protein) and pCREB (a nuclear protein with its phosphorylation stimulated by NE treatment). Immunoblots showed that histone H3 was exclusively present in the nuclear fraction and pCREB was elevated in the nuclear fraction after NE treatment (Fig 18A). GAPDH was mostly present in the cytoplasmic fraction with a minor portion present into the nuclear fraction (Fig 18A). Treatment with NE for 15 min caused the nuclear translocation of dephosphorylated TORC2 (lower band) (Fig. 18). The phosphorylated form of TORC2 (upper band) that was detected under basal conditions was exclusively present in the cytoplasmic fraction (Fig. 18A). Together, these results suggest that NE treatment stimulates the dephosphorylation and the nuclear translocation of TORC2.

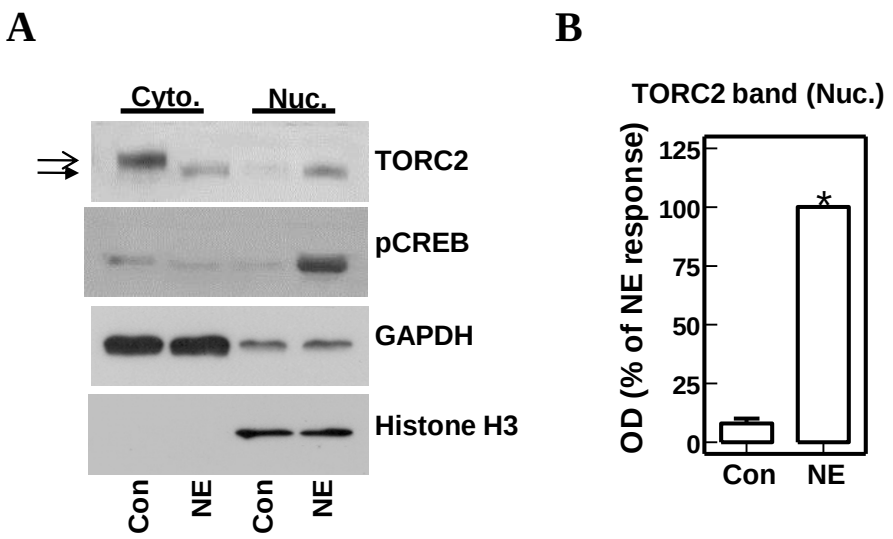

Figure 18: NE-stimulated nuclear translocation of TORC2. Pinealocytes (2.0 x 10^5 cells/300 µl) were treated with NE (3 µM) for 15 min, fractionated into cytoplasmic (Cyto.) and a nuclear fractions (Nuc.) and prepared for Western blot analysis (see *Materials and Methods*). **A**, Representative immunoblots of three independent experiments probed for TORC2, histone H3 (H3), pCREB and GAPDH. The two arrows show upper and lower TORC2 bands. **B**, Histogram of densitometric measurements of the TORC2 bands in the nucleus presented as percentage of NE-stimulated response within the same experiment. Each value represents mean ± SEM from three independent experiments. *, Significantly different from control (Con) (Kanyo et al., 2011).

G) The time profile of NE-stimulated TORC2 nuclear translocation

To determine the time profile of the level of nuclear TORC2 following adrenergic stimulation, pinealocytes were treated with NE (3 μM) for varying durations. The cells were fractionated into nuclear and cytoplasmic fractions and prepared for Western blot analysis. Immunoblots demonstrated increased pCREB levels in all samples treated with NE, which served as a control for drug treatment (Fig. 19). In the nuclear fraction, the TORC2 protein level peaked at 15 min after NE stimulation and was maintained for 2 h. The levels of nuclear TORC2 gradually declined after 2 h but were still above basal levels 8 h after NE stimulation (Fig. 19). In the cytoplasmic fraction, immunoblots showed that TORC2 was dephosphorylated 15 min after NE treatment and gradually declined in intensity similar to the nuclear TORC2 protein (Fig. 19A). Both the dephosphorylation and nuclear translocation preceded the appearance of the AA-NAT protein, which suggests that the dephosphorylated form of TORC2 is present in the nucleus during *Aa-nat* transcription.

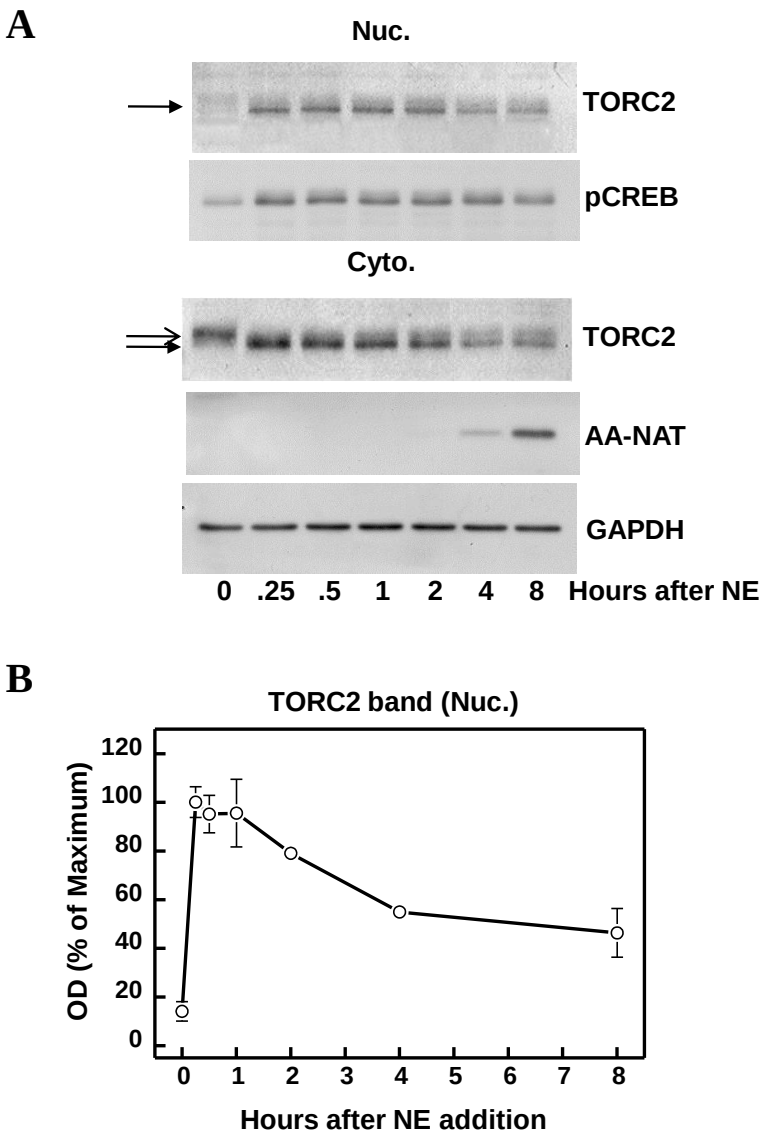

Figure 19: NE-stimulated time profile of nuclear TORC2. Pinealocytes (2.0 x 10^5 cells/300 µl) were treated with NE (3 µM) for varying durations as indicated (0 h is equivalent to basal conditions), fractionated into cytoplasmic (Cyto.) and nuclear fractions (Nuc.) and prepared for Western blot analysis (see *Materials and Methods*). **A**, Representative immunoblots probed for TORC2, pCREB, AA-NAT and GAPDH. Single arrow indicates TORC2 bands. Two arrows indicate the TORC2 protein including the upper and lower bands. **B**, Densitometric measurements of the TORC2 bands in the nucleus presented as percentages of the maximum mean NE response after NE treatment. Each value represents mean ± SEM of three independent experiments.

H) Signalling pathways involved in NE-stimulated TORC2 nuclear translocation

The adrenergic receptors and post-receptor signalling mechanism involved in the NE-stimulated TORC2 nuclear translocation were determined. The drug concentrations used were the same as those used in the study investigating the dephosphorylation of TORC2. The receptor subtypes regulating the NE-stimulated nuclear translocation of TORC2 were characterized. pCREB was measured to control for the β-adrenergic receptor stimulation (Roseboom and Klein, 1995). Selective activation of the β-adrenergic receptor with 30 nM of isoproterenol (in the presence of 1 μM of prazosin) increased pCREB and TORC2 levels in the nuclear fraction (Fig. 20A). In comparison, selective activation of the α_1-adrenergic receptor with 30 nM of phenylephrine (in presence of 1 μM of propranolol) caused no change in the level of pCREB and the TORC2 protein (Fig. 20A). Simultaneous activation of both α_1- and β-adrenergic receptors with combined treatment of isoproterenol plus phenylephrine, or NE, had the same effect as selective β-adrenergic receptor activation (Fig. 20A). The dominant role of the β-adrenergic receptor was also demonstrated with adrenergic-receptor antagonists. The effect of NE (30 nM) on pCREB and TORC2 could be blocked by propranolol (1 μM) but not with prazosin (1 μM) (Fig 20A). Immunoblots showing the cytoplasmic fraction demonstrated that only activation of β-adrenergic receptors caused dephosphorylation of TORC2 which correlated with elevated level of TORC2 in the nucleus (Fig. 20A). This suggests the NE-stimulated TORC2 dephosphorylation and nuclear translocation is mediated through the β-adrenergic receptor.

In addition, the post-receptor signalling pathways involved in the NE-stimulated nuclear translocation of TORC2 were investigated. pCREB was measured to control for NE and dBcAMP treatments. Treatment of cultured rat pinealocytes for 30 min with dBcAMP (0.5 mM) had the same effect as NE (3 μM), which increased both TORC2 and pCREB levels in the nuclear fraction (Fig. 20B). Treatment with other pharmacological agents such as dBcGMP (0.5 mM), PMA (0.1 μM) or elevating intracellular Ca^{2+} levels with KCl (30 mM) caused no nuclear translocation of TORC2 (Fig. 20B). However, immunoblots of the cytoplasmic fraction (Fig. 20B) indicated that both dBcAMP and KCl treatment could cause the dephosphorylation of TORC2. These results suggest that both intracellular cAMP and Ca^{2+} elevations can lead to dephosphorylation of TORC2, but only cAMP can stimulate nuclear translocation.

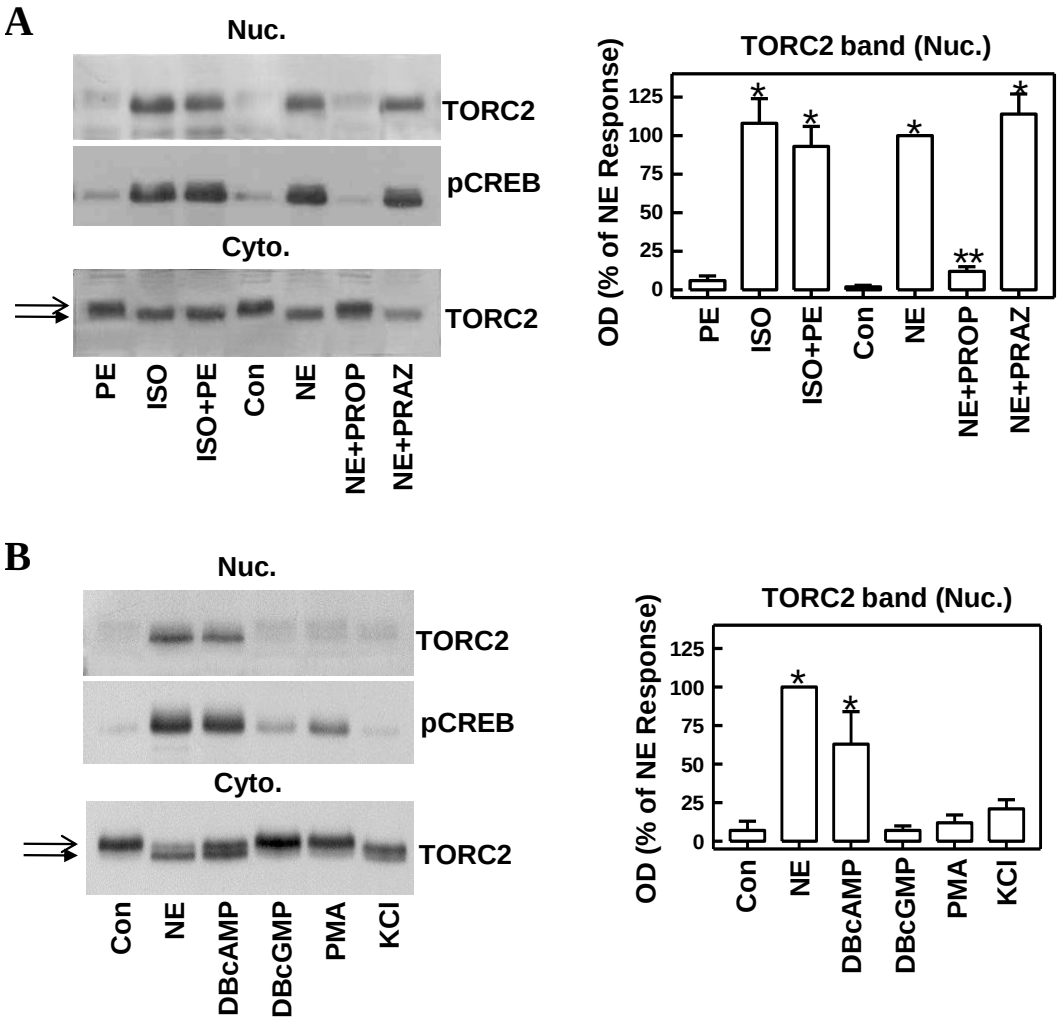

Figure 20: Signalling pathways involved in NE-stimulated TORC2 nuclear translocation. Pinealocytes (1.0 x 10^5 cells/300 µl) were treated for 30 min as described below, fractionated into cytoplasmic (Cyto.) and nuclear (Nuc.) fractions and prepared for Western blot analysis (see *Materials and Methods*). **A**, Cells were treated with NE (30 nM), isoproterenol (ISO; 30 nM with 1 µM of prazosin (PRAZ)), phenylephrine (PE; 30 nM with 1 µM of propranolol (PROP)), ISO plus PE, NE (30 nM) in presence of 1 µM PRAZ or PROP. **B**, Cells were treated with NE (3 µM), dBcAMP (0.5 mM), dBcGMP (0.5 mM), PMA (0.1 µM) or KCl (30 mM). *Left panel*, Representative blots probed for TORC2 and pCREB. The two arrows show upper and lower TORC2 bands. *Right panel*, Histograms of densitometric measurements of the TORC2 bands in the nucleus presented as percentages of the NE-stimulated response within the same experiment. Each value represents mean ± SEM of three independent experiments. *, Significantly different from control (Con). **, Significantly different from NE (Kanyo et al., 2011).

I) Effect of phosphatase inhibitors on NE-stimulated dephosphorylation and nuclear translocation of TORC2

Because NE can induce dephosphorylation and nuclear translocation of TORC2, the effects of established phosphatase inhibitors (Oliver and Shenolikar, 1998) on these NE-stimulated effects were investigated. To study the role of PP1 and PP2A, phosphatase inhibitors tautomycin (IC50: PP1=1 nM; PP2A=10 nM) (MacKintosh and Klumpp, 1990), calyculin A (IC50: PP1=2 nM; PP2A=0.5-1 nM) (Figurov et al., 1993; Murakami et al., 1994) and okadaic acid (IC50: PP1=10-15 nM; PP2A=100 pM) (Haystead et al., 1989; Nomura et al., 1992) were used. The role of PP2B was investigated with cyclosporine A, a specific PP2B inhibitor (IC50=65 nM) (Groblewski et al., 1994).

First, the effect of protein phosphatase inhibitors on the NE-stimulated dephosphorylation of TORC2 was determined. Cultured rat pinealocytes were treated with NE (3 μM) for 15 min in the presence of varying concentrations of the phosphatase inhibitors. Only calyculin A (at 10 nM and 30 nM) and okadaic acid (at 1 μM) could inhibit the NE-stimulated dephosphorylation of TORC2 (Fig. 21). In contrast, tautomycin and cyclosporine A had no effect even at 3 and 10 μM, respectively. These results suggest that PP2A is involved in the NE-stimulated dephosphorylation of TORC2.

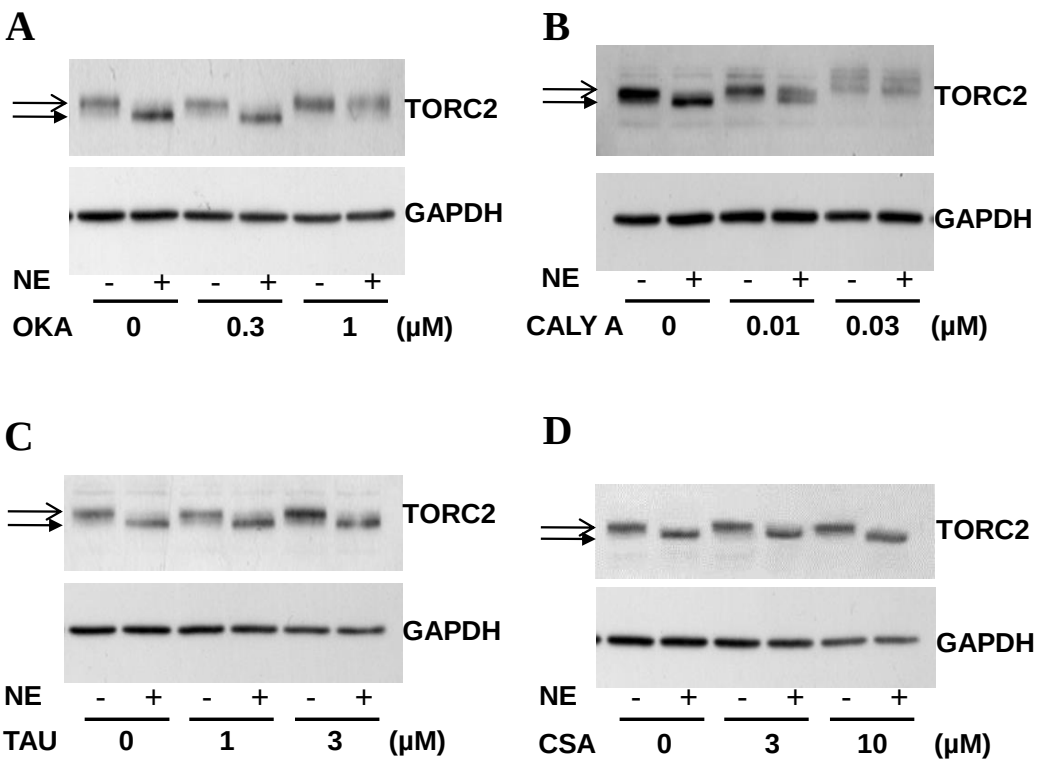

Figure 21: Effects of phosphatase inhibitors on NE-induced TORC2 dephosphorylation. Pinealocytes (1.0 x 10^5 cells/300 µl) were treated 15 min with NE (3 µM) in the presence of varying concentrations of OKA (**A**), CALY A (**B**), TAU (**C**) or CSA (**D**) as indicated and prepared for Western blot analysis (see *Materials and Methods*). Representative immunoblots of three independent experiments were probed for TORC2 and GAPDH. The two arrows show upper and lower TORC2 bands. Inhibitors, when present, were added 15 min before NE (Kanyo et al., 2011).

To investigate the effect of phosphatase inhibitors on the NE-stimulated nuclear translocation of TORC2, cultured pinealocytes were treated with NE (3 μM) for 30 min in the presence of okadaic acid, calyculin A, tautomycin or cyclosporine A. The concentration of phosphatase inhibitors used was established in the study shown in figure 21.

The cells were treated and the nuclear and cytoplasmic fractions were prepared for immunoblot analysis. In the nuclear fraction, immunoblots revealed that only treatments with okadaic acid and calyculin A could inhibit the NE-stimulated nuclear translocation of TORC2 while tautomycin and cyclosporine A had no effect (Fig. 22). Treatments with the phosphatase inhibitors in the absence of NE had no effect on TORC2 nuclear translocation (Fig. 22A). pCREB was induced in all samples that were treated with NE and in samples that have been treated with okadaic acid and calyculin A only. Immunoblots of the cytoplasmic fraction showed that only treatments with okadaic acid and calyculin A, but not tautomycin and cyclosporine A, could abolish the effect of NE-stimulated TORC2 dephosphorylation, as shown in non-fractionated cells earlier (Fig. 21). Overall, the results suggest that the NE-stimulated dephosphorylation and nuclear translocation of TORC2 is mediated by PP2A rather than PP1 or PP2B.

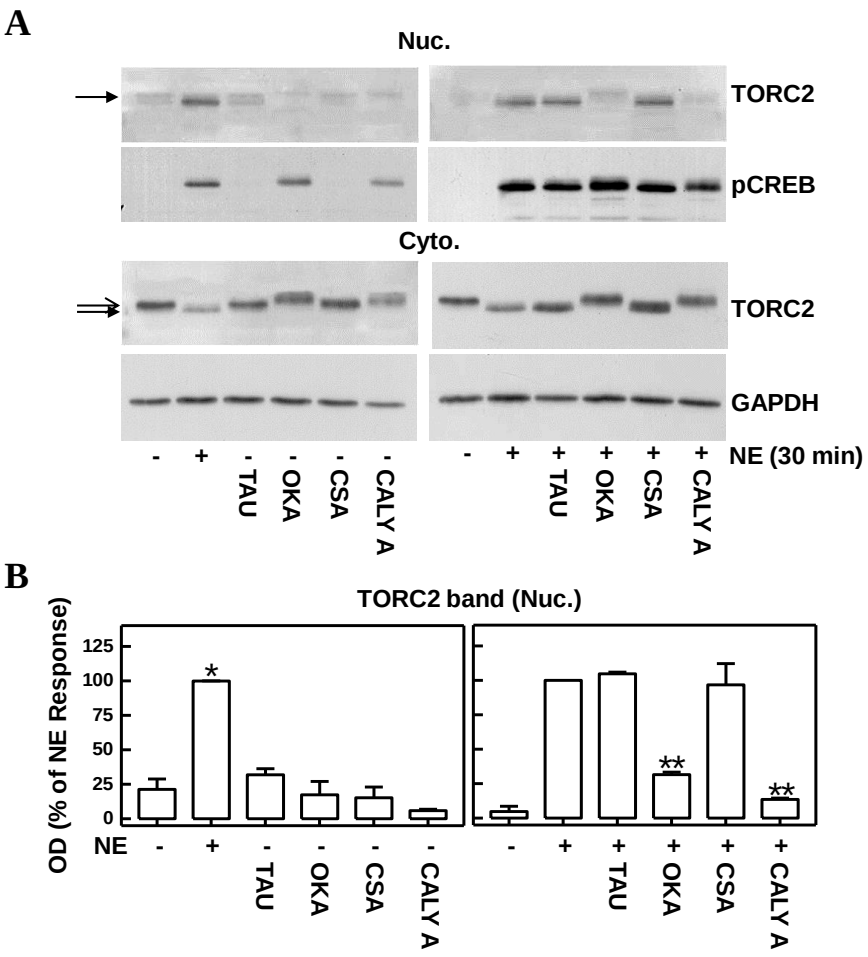

Figure 22: Effects of phosphatase inhibitors on NE-mediated TORC2 nuclear translocation. Pinealocytes (1.0 x 10^5 cells/300 µl) were treated 30 min with NE (3 µM) in presence of CALY A (20 nM), TAU (10 µM), OKA (1 µM) and CSA (10 µM). Cytoplasmic (Cyto.) and the nuclear fractions (Nuc.) were prepared for Western blot analysis (see *Materials and Methods*). **A**, Representative blots were probed for TORC2, pCREB and GAPDH. Arrows show TORC2 bands. **B**, Histograms of densitometric measurements of the TORC2 bands in the nucleus presented as percentages of the NE-stimulated response within the same experiment. Each value represents mean ± SEM of three independent experiments. *, Significantly different from control. **, Significantly different from NE. Inhibitors, when present, were added 15 min before NE.

J) Summary on TORC2 regulation

In this section, immunoblots obtained from whole animal studies show the appearance of a lower TORC2 band with the onset of darkness which is maintained until onset of light. Using cultured rat pinealocytes, immunoblots also show a lower TORC2 band in response to NE stimulation, which is identified as the dephosphorylated form of TORC2, using CIP treatment and PhosTag gel. The dephosphorylation and the nuclear translocation of TORC2 are triggered through the β-adrenergic receptor/cAMP-pathway within the first 15 min of stimulation (Fig. 23). Intracellular Ca^{2+} elevation mediated by KCl treatment can cause TORC2 dephosphorylation, but has no effect on TORC2 nuclear translocation. Studies with phosphatase inhibitors suggest that PP2A is involved in NE-stimulated TORC2 dephosphorylation and the nuclear translocation. The NE-stimulated TORC2 level in the nucleus gradually declines over time, but is still detectable above basal levels 8 h after treatment.

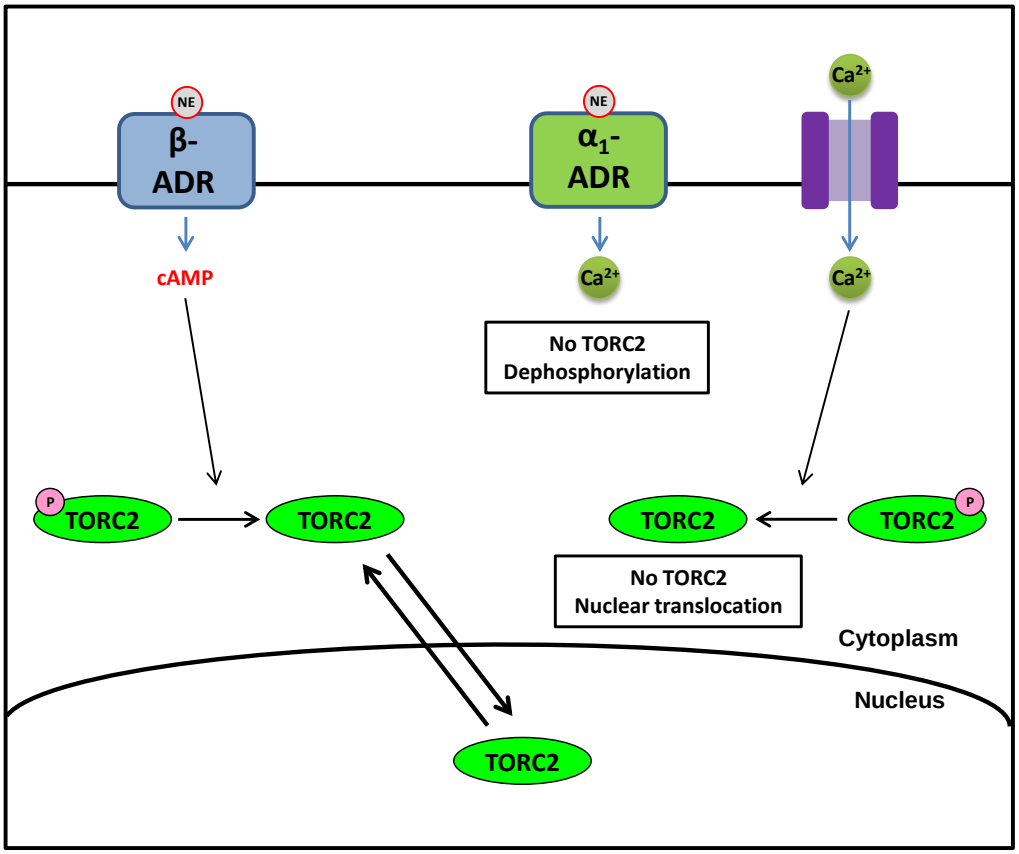

Figure 23: NE-mediated regulation of TORC2 in the rat pinealocyte. Under basal conditions, TORC2 is phosphorylated and sequestered in the cytoplasm. Stimulation of the β-adrenergic receptor (β-ADR) increases intracellular cAMP levels, which causes dephosphorylation and nuclear translocation of TORC2. Stimulation of the α_1-ADR which increases intracellular Ca^{2+} levels has no effect on TORC2 dephosphorylation or nuclear translocation. However, intracellular elevations of Ca^{2+} mediated through voltage-gated L-type Ca^{2+} channel (purple) causes dephosphorylation of TORC2 but no nuclear translocation.

3.4 The effect of TORC2 on the induction of *Aa-nat*

The results in the previous section show that the dephosphorylation and nuclear translocation of TORC2 in rat pinealocytes is stimulated by NE. The nuclear translocation of TORC2 takes place within 15 min of adrenergic stimulation and precedes the induction of *Aa-nat* indicating that the TORC2 protein is present in the nucleus when *Aa-nat* transcription takes place. Whether and how this coactivator affects *Aa-nat* transcription is unknown in the rat pineal gland. This section shows results on the effect of TORC2 on NE-stimulated *Aa-nat* expression. The amount of TORC2 in cultured pinealocytes was manipulated with recombinant adenoviral constructs similarly as described previously (*section 3.3*).

A) Effect of Torc2-sh and Torc2-fl on TORC2 levels

To manipulate TORC2 protein levels inside the cell, cultured rat pinealocytes were transfected with recombinant adenoviral constructs expressing either a short-hairpin targeting the *Torc2* mRNA (*Torc2*-sh) or the full-length *Torc2* transcript (*Torc2*-fl). To control for the viral transfection, cells were transfected with adenoviral constructs expressing *LacZ.* *Torc2*-sh was able to knockdown, whereas *Torc2*-fl could elevate *Torc2* mRNA and protein levels (Fig. 24). Co-treatment with *Torc2*-sh and *Torc2*-fl revealed that *Torc2*-sh was able to counteract the overexpressed *Torc2* mRNA and protein levels by *Torc2*-fl (Fig. 24). Therefore, this method is suitable to manipulate the levels of TORC2 in

cultured rat pinealocytes. None of the adenoviral constructs used altered the GAPDH levels (Fig. 24B), the protein product of a house keeping gene.

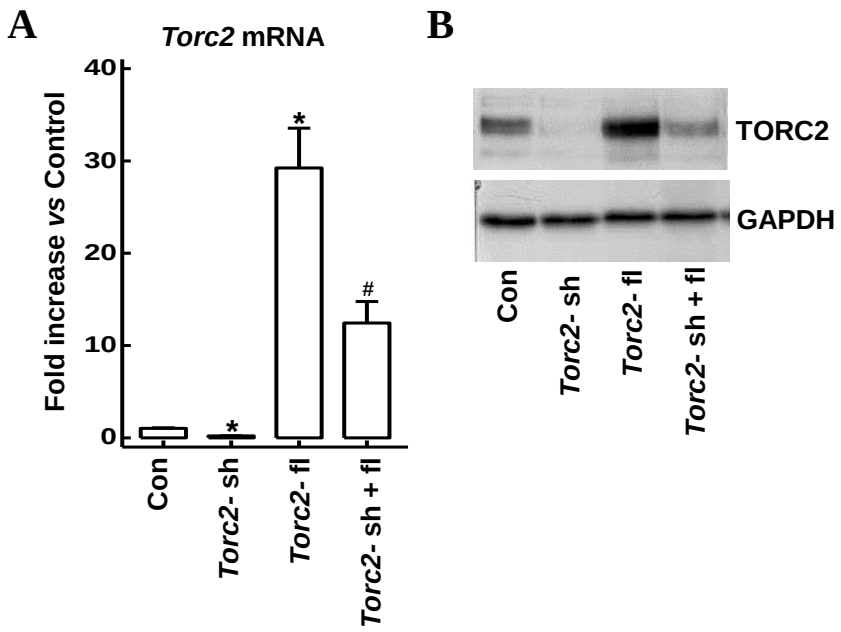

Figure 24: Effect of *Torc2*-sh and *Torc2*-fl on TORC2 levels. Pinealocytes (1.0 x 10^5 cells/0.6 ml) were transfected with adenoviral constructs expressing *Torc2*-sh and/or *Torc2*-fl and prepared to measure the *Torc2* mRNA and the protein (see *Materials and Methods*). **A**, mRNA levels of *Torc2* were presented as fold increase vs control. Each value represents the mean ± SEM of three independent experiments. *, Significantly different from control (Con). #, Significantly different from *Torc2*-fl. **B**, A representative immunoblot of three independent experiments shows TORC2 and GAPDH levels (Kanyo et al., 2011).

B) Effect of manipulating TORC2 levels on NE-stimulated Aa-nat expression

To investigate the effect of TORC2 on NE-stimulated *Aa-nat* expression, *Torc2*-sh and *Torc2*-fl were used to manipulate the levels of TORC2 inside the cell. The time-course effects of *Torc2* knockdown or overexpression on the NE-stimulated *Aa-nat* mRNA levels was determined with real-time PCR. Neither overexpression nor knockdown of *Torc2* had an effect on the *Aa-nat* mRNA levels during the first 4 h of NE stimulation (Fig. 25A). However, treatment with *Torc2*-fl enhanced the *Aa-nat* mRNA levels 8 h after NE stimulation (Fig. 25A). This enhancement persisted for 32 h (Fig. 25A). In comparison, treatment with *Torc2*-sh caused a reduction of NE-induced *Aa-nat* mRNA levels 8 h after NE stimulation (Fig. 25A). This reduction persisted for up to 24 h, but no reduction was observed at 32 h after NE stimulation.

To investigate whether the changes on the *Aa-nat* mRNA levels caused by *Torc2* knockdown and overexpression could be translated to the protein levels, the effects of *Torc2*-sh and *Torc2*-fl were also tested on the NE-stimulated AA-NAT protein level and enzymatic activity. Overexpressing TORC2 enhanced the induced AA-NAT protein levels after 16 h of NE (3 μM) treatment, but knockdown of TORC2 had no effect (Fig. 25B). However, treatment with *Torc2*-sh was effective in reducing the *Torc2*-fl-mediated enhancement of AA-NAT. To determine whether the enhancing effect of TORC2 overexpression was dependent on the duration of NE treatment, immunoblots were prepared from cells that were treated with NE for 6, 18, 32 or 40 h. NE-stimulated AA-NAT was enhanced by treatment with *Torc2*-fl after 18, 32 and 40 h of NE treatment, but not after 6 h

(Fig. 25C). After 32 h of treatment, NE-stimulated pCREB declined to basal levels suggesting that TORC2 enhanced AA-NAT beyond CREB phosphorylation (Fig. 25C). The time-course effect of *Torc2*-fl on the NE-stimulated AA-NAT activity was also determined with radioenzymatic assay. Overexpressing *Torc2* enhanced the enzymatic activity of AA-NAT 12 h after NE treatment and persisted up to 36 h after treatment (Fig. 25D). Overall, the effect of *Torc2*-fl obtained on the mRNA level of *Aa-nat* was reflected also on the protein and the enzymatic activity of AA-NAT. Together, the results suggest that TORC2 can modulate the NE-stimulated *Aa-nat* mRNA and protein level when overexpressed. Knockdown of endogenous *Torc2* has a small effect on the NE-stimulated *Aa-nat* mRNA, an effect not translated to the protein level or enzyme activity.

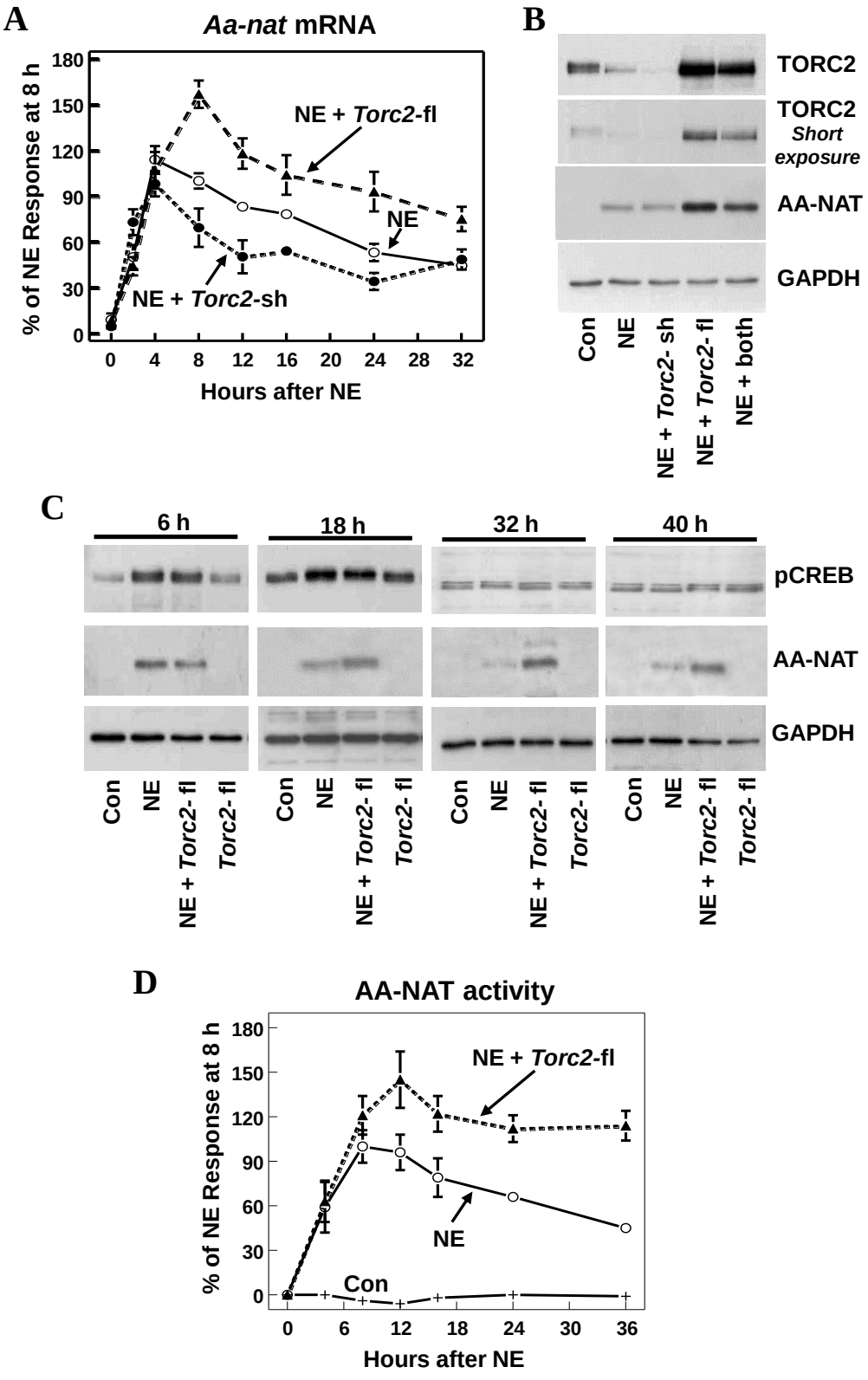

Figure 25: NE-stimulated *Aa-nat* mRNA, protein and enzymatic activity after manipulating TORC2 levels (see figure legend).

Figure 25: NE-stimulated *Aa-nat* mRNA, protein and enzymatic activity after manipulating TORC2 levels. Pinealocytes (1.0×10^5 cells/0.6 ml) were transfected with adenoviral constructs expressing *Torc2*-sh and/or *Torc2*-fl, treated with NE (3 µM) for the time periods indicated above and described below (see *Materials and Methods*). **A**, *Aa-nat* mRNA levels measured with real-time PCR and presented as percentages of NE-stimulated response after 8 h. **B**, Immunoblots showing the effects of *Torc2*-sh and/or *Torc2*-fl on AA-NAT protein levels 16 h after NE treatment. **C**, Immunoblots showing the effects of *Torc2*-fl on AA-NAT after NE treatments for the specific duration indicated. All immunoblots presented in this figure are representatives of three independent experiments probed for TORC2, pCREB, AA-NAT and GAPDH as indicated. **D**, Effects of *Torc2*-fl on NE-stimulated AA-NAT activity measured with radioenzymatic assay. Each value obtained was normalized to the mean NE-stimulated response at 8 h. Values represent the mean ± SEM of three independent experiments (Kanyo et al., 2011).

C) Effect of TORC2 on other CREB-driven genes

To determine whether TORC2 can modulate the transcription of other CREB-driven genes besides *Aa-nat*, the time-course effect of changing *Torc2* levels on the NE-stimulated *Icer*, *Dio2* and *Mkp-1* mRNA levels were investigated with real-time PCR.

Although *Torc2* overexpression did not prevent the decline of *Icer, Dio2* and *Mkp-1* expression after 2 and 4 h of NE stimulation (i.e. induction phase), the mRNA levels were still enhanced at time-points measured after 8 h of NE stimulation (i.e. declining phase; Fig. 26). Overexpressing *Torc2* increased the NE-stimulated mRNA level of *Dio2* after 8 h of stimulation and that of *Icer* and *Mkp-1* after 12 h (Fig. 26). Other differences in the *Torc2*-fl enhancing effect between the three genes were also observed. In the case of *Icer,* the enhancing effect of *Torc2*-fl treatment showed a gradual increase starting at 2 h after NE stimulation and persisted for at least 32 h after stimulation (Fig. 26). In the case of *Dio2* and *Mkp-1*, the same treatment enhanced their mRNA expressions after 12 h of NE stimulation. This enhancement also persisted until at least 32 h after stimulation, but no increase was observed (Fig. 26). Overall, the effect of *Torc2* overexpression on the other CREB-driven genes are similar in that no effect during the induction phase but strong *Torc2*-fl-mediated enhancing effect during the declining phase, as seen previously on *Aa-nat* (Fig. 25A). Some subtle differences in the temporal characteristics of the enhancing effect between different genes were also observed.

Like its effect on *Aa-nat*, knockdown of *Torc2* had no effect on NE-stimulated *Icer*, *Dio2* and *Mkp-1* mRNA levels prior to 4 h of NE stimulation (Fig. 26). The most notable effect of *Torc2*-sh treatment, if any, on the NE-stimulated expression of all the three genes was observed after 4 h of NE stimulation (Fig. 26). Since the NE-stimulated mRNA levels of *Icer*, *Dio2* and *Mkp-1* had declined close to the basal levels after 8 h, any additional *Torc2*-sh-mediated reduction in mRNA levels would be difficult to detect. In the case of *Icer*, no significant effect with *Torc2*-sh treatment was observed (Fig. 26). The most prominent effect by *Torc2* knockdown was observed on *Dio2* expression where noticeable reduction could still be observed 8 h after NE stimulation (Fig. 26). *Torc2*-sh treatment also reduced NE-stimulated *Mkp-1* expression at 8 and 12 h after stimulation, but not at later time-points (Fig. 26). Together, these results suggest that endogenous TORC2 has no noticeable effect on NE-stimulated *Icer*, *Dio2* and *Mkp-1* mRNA levels during the induction phase. If any, an effect is only noticeable during the declining phase, as in the case for *Aa-nat* shown previously (Fig.25A).

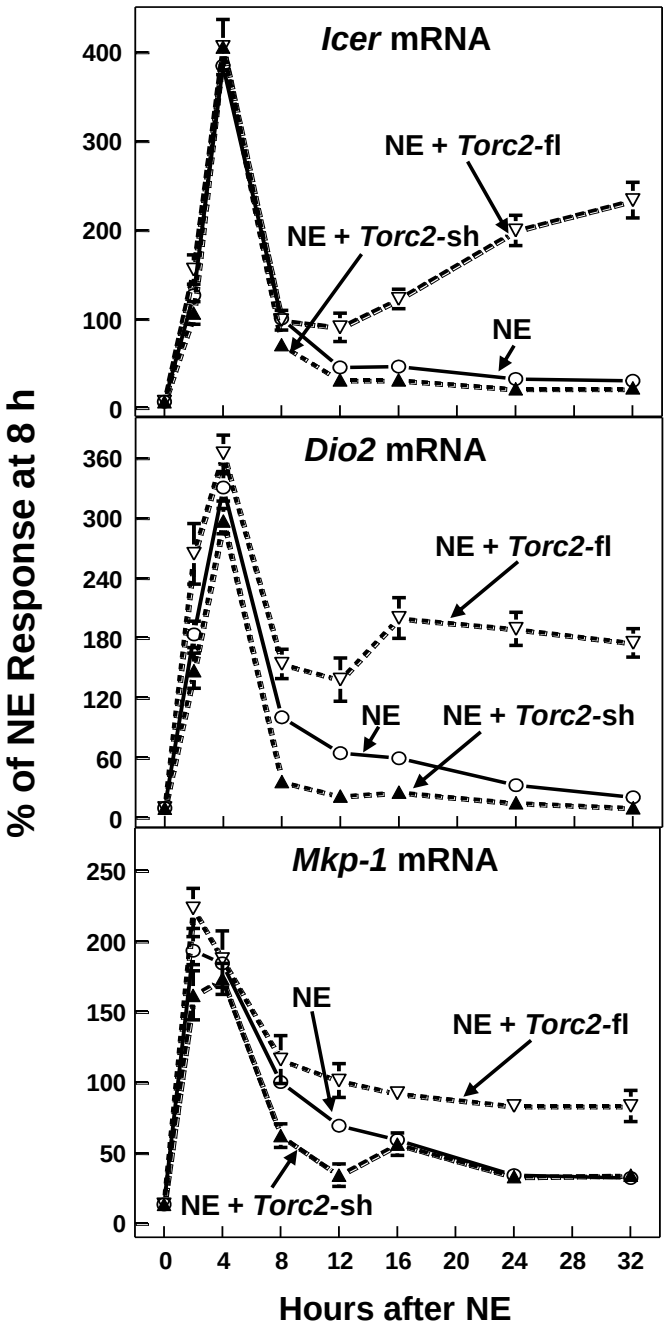

Figure 26: Effect of *Torc2*-sh or *Torc2*-fl on CREB-driven gene transcription. Pinealocytes (1.0 x 10^5 cells/0.6 ml) were transfected with adenoviral constructs expressing either *Torc2*-sh or *Torc2*-fl, treated with NE (3 µM) for varying time periods as indicated and prepared for real-time PCR (see *Materials and Methods*). mRNA levels of *Icer*, *Dio2* and *Mkp-1* were determined and presented as percentages of the mean NE-stimulated response after 8 h. Each value represents the mean ± SEM of three independent experiments.

D) Effect of the Torc2-S171A mutant on NE-stimulated gene transcription

The Ser171 residue on TORC2 was identified as a SIK phosphorylation site (Dentin et al., 2007; Screaton et al., 2004). To investigate the role of the Ser171 phosphorylation on TORC2 function, a Ser171 phosphorylation-defective *Torc2* (*Torc2*-S171A) mutant was generated. The effect of overexpressing the mutant *Torc2*-S171A on NE-stimulated *Aa-nat, Mkp-1*, *Icer* and *Dio2* expressions was compared to that of the wild-type *Torc2*-fl. Transfected cells were treated with NE (3 μM) for 24 h and mRNA levels were determined with real-time PCR. While causing similar elevations on the *Torc2* mRNA levels, the *Torc2*-S171A treatment was found to have a greater enhancement on the NE-stimulated expression of *Aa-nat*, *Mkp-1*, *Icer* and *Dio2* than the *Torc2*-fl treatment (Fig. 27). The results suggest that the Ser171 phosphorylation-defective TORC2 protein is more potent than the wild-type TORC2 in enhancing NE-stimulated gene expression in cultured rat pinealocytes.

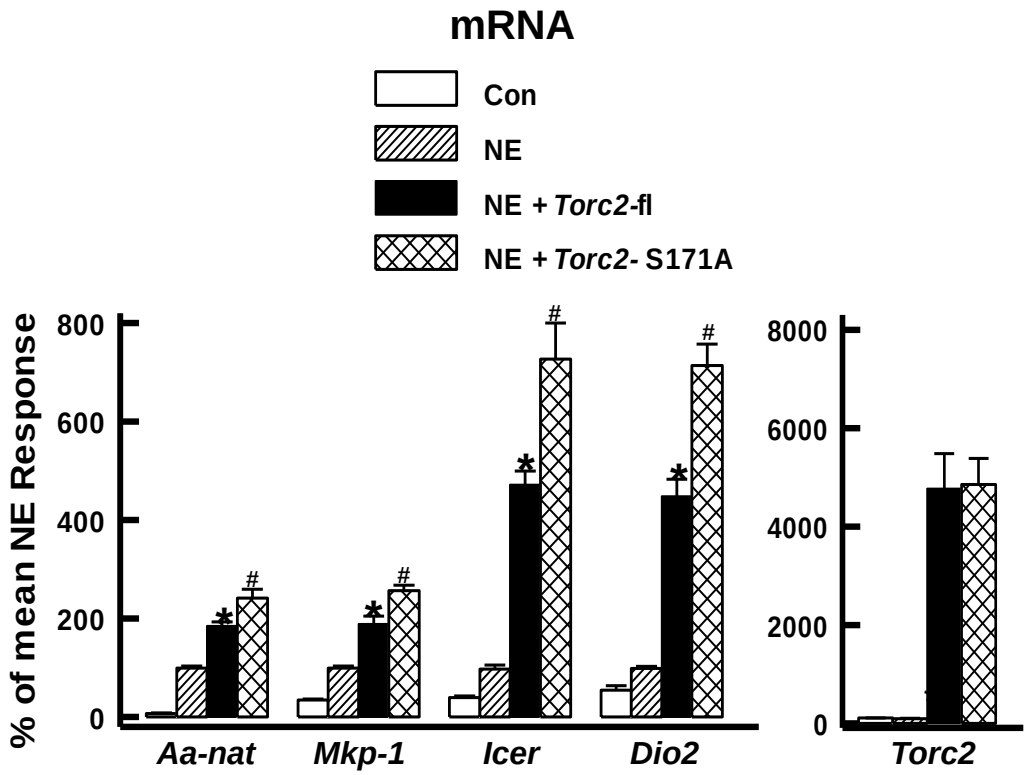

Figure 27: Effect of overexpressing *Torc2*-fl vs mutated *Torc2*-S171A on adrenergically stimulated genes. Pinealocytes (1.0 x 10^5 cells/0.6 ml) were transfected with adenoviral constructs expressing either the wild type *Torc2*-fl or the mutated *Torc2*-S171A, treated 24 h with NE (3 µM) and prepared for real-time PCR (see *Materials and Methods*). *Aa-nat, Dio2, Icer, Mkp-1* and *Torc2* mRNA levels were determined and presented as percentages of the mean NE-stimulated response. Each value is the mean ± SEM from three independent experiments. *****, Indicates significantly different ($p<0.05$) from treatment with NE. #, Indicates significantly different ($p<0.05$) from treatment with *Torc2*-fl.

E) Summary on the effect of TORC2 on NE-stimulated Aa-nat expression

The results presented in this section showed that overexpressed TORC2 can only enhance the NE-stimulated *Aa-nat* mRNA after 8 h and protein expression and enzymatic activity after 12 h of NE treatment. Knockdown of the endogenous TORC2 protein has a modest inhibitory effect on the NE-stimulated *Aa-nat* mRNA expression only after 8 h of NE-treatment. However, this inhibitory effect was not translated to the AA-NAT protein level. Manipulating *Torc2* levels has similar effect on the mRNA level of other CREB-target genes stimulated by NE.

3.5 The effect of SIK1 on TORC2

Phosphorylation of TORC2 by SIK1 has been reported to cause the export of TORC2 from the nucleus (Katoh et al., 2004b; Takemori et al., 2007). Results in *section 3.3* show that NE can regulate the phosphorylation status and cellular distribution of TORC2. Therefore, we determined whether the repressive effect of SIK1 on NE-stimulated *Aa-nat* expression (see *section 3.2*) was mediated by the phosphorylation and the nuclear export of TORC2.

A) Effect of SIK1 on NE-stimulated TORC2 dephosphorylation in whole cells

Here, the effect of manipulating *Sik1* mRNA levels with *Sik1*-sh2 and *Sik1*-fl on the NE-stimulated dephosphorylation of TORC2 was determined. *Sik1*-sh2 and *Sik1*-fl transfected cells were stimulated with NE (3 μM) for 8 h and the effect of the transfection on TORC2 and AA-NAT was investigated in the

whole cell preparation with Western blot analysis. Knockdown of *Sik1* enhanced NE-stimulated AA-NAT levels whereas overexpression of *Sik1* suppressed AA-NAT levels (Fig. 28A), as previously described (Fig. 8 A and B). Under basal conditions, treatment with *Sik1*-sh2 or *Sik1*-fl did not affect the phosphorylation status of TORC2, which remained phosphorylated (Fig. 28A). After NE stimulation, overexpressing *Sik1* increased the intensity of the upper TORC2 band suggesting that SIK1 can phosphorylate TORC2 (Fig. 28A). However, treatment with *Sik1*-sh2 had no observable effect on the phosphorylation status of TORC2 stimulated by NE (Fig. 28A).

The effect of *Sik1* knockdown and overexpression on the NE-stimulated TORC2 dephosphorylation was further investigated using the PhosTag gel. pCREB was also measured to control for NE stimulation. Immunoblots after PhosTag gel separation showed that *Sik1* knockdown had no effect on the TORC2 phosphorylation pattern under basal or NE-stimulated conditions (Fig. 28B). In comparison, overexpressing *Sik1*, while having no effect on the already phosphorylated TORC2 under basal conditions, caused the appearance of the upper phosphorylated TORC2 band in the NE (6 h) stimulated sample similar to that in control (Fig. 28B). This suggests that while overexpressed SIK1 can rephosphorylate TORC2 after NE stimulation, endogenous SIK1 has little effect on the TORC2 phosphorylation status under basal or NE-stimulated conditions.

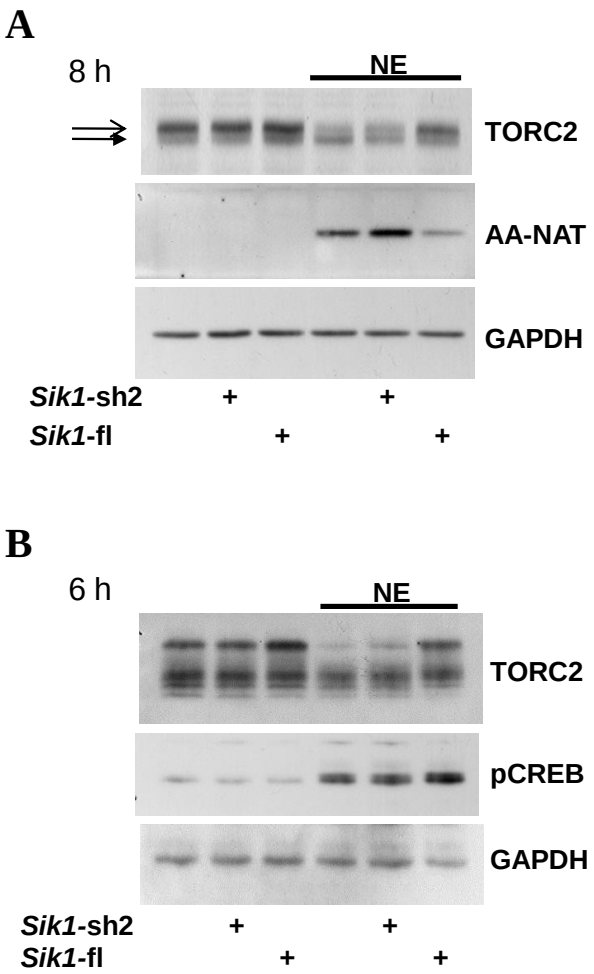

Figure 28: Effect of *Sik1*-sh2 and *Sik1*-fl on TORC2. Pinealocytes (1.0 x 10^5 cells/0.6 ml) were transfected with adenoviral constructs expressing either *Sik1*-sh2 or *Sik1*-fl, treated with NE (3 µM) as indicated and prepared for Western blot analysis (see *Materials and Methods*). Immunoblots are representatives of three independent experiments. **A**, Immunoblots were probed for TORC2 and AA-NAT. ⟶ indicates phosphorylated TORC2 and ⟶ indicates dephosphorylated TORC2. GAPDH was included to demonstrate loading consistency. **B**, Samples were also separated on a PhosTag gel prior Western blot analysis and immunoblots were probed for TORC2, pCREB and GAPDH.

B) Effect of SIK1 on the cellular distribution of TORC2

The effect of SIK1 on the TORC2 cellular distribution was also determined. Cultured rat pinealocytes were treated with *Sik1*-sh2 and *Sik1*-fl adenoviral constructs, stimulated with NE (3 μM) for the duration indicated, separated into nuclear and cytoplasmic fractions and analyzed by immunoblots. The effect of *Sik1* knockdown and overexpression was monitored 0.5, 3 and 8 h after NE stimulation. These time-points were chosen based on the time-course study on the NE-stimulated nuclear translocation of TORC2 (Fig. 19) and reflected the peak, the declining and steady phases of nuclear TORC2 levels after NE stimulation.

Immunoblots obtained from the nuclear fraction showed that knockdown of *Sik1* had no effect on nuclear TORC2 levels under basal conditions (Fig. 29). Treatment with *Sik1*-sh also did not affect nuclear TORC2 levels at 0.5 and 3 h after NE stimulation suggesting that neither the peak nor the declining phases of NE-stimulated nuclear TORC2 levels is regulated by endogenous SIK1 (Fig. 29 A and B). Immunoblots obtained from samples stimulated for 8 h with NE were exposed longer due to low nuclear TORC2 levels, as indicated in the NE time-course study (Fig. 19). The longer exposure resulted in higher background, but also showed that *Sik1* knockdown had no effect on nuclear TORC2 levels 8 h after NE stimulation (Fig. 29C) indicating that endogenous SIK1 also has no effect on the nuclear TORC2 level at the steady phase. Together, these results suggest that endogenous SIK1 does not regulate the cellular distribution of TORC2. In addition, immunoblots also showed that *Sik1* knockdown enhanced

NE-stimulated AA-NAT expression 8 h after stimulation (Fig. 29C), as shown previously (Fig. 8 A and B). Together, these results imply that endogenous SIK1 represses NE-stimulated AA-NAT protein by a mechanism other than regulating the cellular distribution of TORC2.

Overexpressing *Sik1* did not change the nuclear levels of TORC2 under basal conditions or 0.5 h after NE stimulation (Fig. 29A). However, *Sik1*-fl treatment decreased the intensity of the lower dephosphorylated TORC2 band and caused the appearance of an upper phosphorylated TORC2 band at 3 and 8 h after NE stimulation in the nucleus (Fig. 29 B and C). These results imply that, while having no effect on the peak levels of NE-stimulated nuclear TORC2 at 0.5 h, overexpressed SIK1 can cause the phosphorylation of TORC2 in the nucleus during the declining phase at 3 and 8 h after NE stimulation. The effect of *Sik1*-fl treatment on the total NE-stimulated nuclear TORC2 levels was difficult to determine after 3 and 8 h of stimulation due to a shift in the TORC2 band (Fig. 29 B and C).

Immunoblots from the cytoplasmic fraction showed a similar shift as described above in the TORC2 band at 3 and 8 h after NE stimulation when *Sik1* was overexpressed (Fig. 29 B and C). This indicates that exogenous SIK1 can also cause the phosphorylation of TORC2 in the cytoplasm at 3 and 8 h after NE stimulation. In addition, at the same time-points (3 and 8 h NE stimulation), the intensity of the TORC2 band was greatly increased after overexpression of SIK1 (Fig. 29 B and C). The results also showed that *Sik1*-fl treatment while having an effect on the TORC2 levels and the phosphorylation status at 3 and 8 h after NE

stimulation, it had no effect at 0.5 h (Fig. 29A). Treatment with *Sik1*-fl reduced NE-stimulated AA-NAT protein 8 h after stimulation, as previously shown (Fig. 8 A and B).

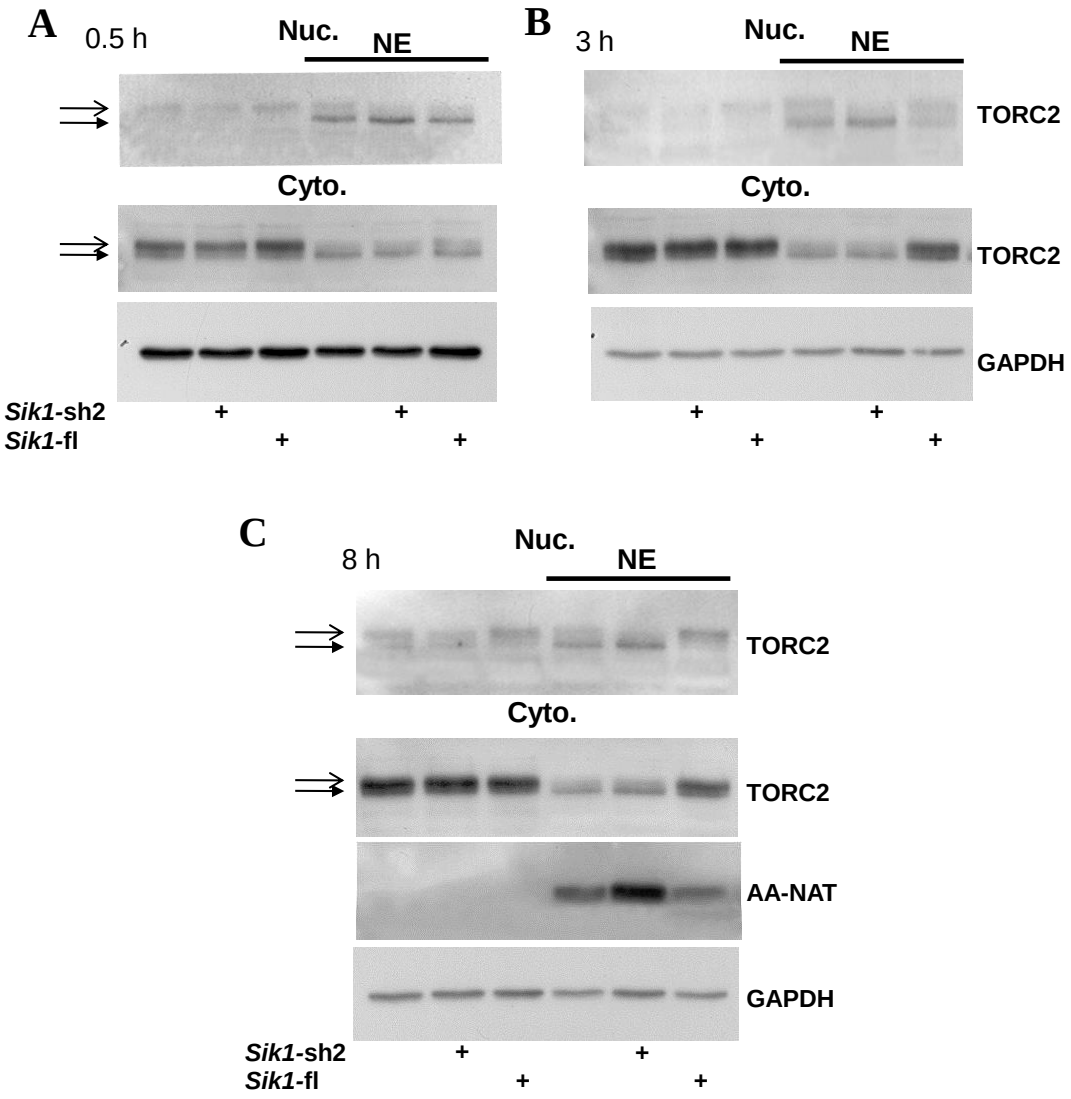

Figure 29: Effect of *Sik1*-sh2 and *Sik1*-fl on NE-stimulated TORC2 nuclear translocation. Pinealocytes (1.0 x 10^5 cells/0.6 ml) were transfected with adenoviral constructs expressing *Sik1*-sh2 or *Sik1*-fl, treated for 0.5 h (**A**), 3 h (**B**) or 8 h (**C**) with NE (3 μM) as indicated, fractionated (into nuclear (Nuc.)- and cytoplasmic (Cyto.)-fractions) and prepared for Western blot analysis (see *Material and Methods*). Immunoblots were probed for TORC2, AA-NAT and GAPDH as indicated. ⟶ indicates phosphorylated TORC2 and ⟶ indicates dephosphorylated TORC2. For **C**, the nuclear TORC2 protein levels were relative low. And the blot was overexposed to show the TORC2 band, hence the high background. Immunoblots are representatives of at least three independent experiments.

C) Summary on the effect of SIK1 on TORC2

Although overexpressed SIK1 can phosphorylate TORC2 after NE stimulation, endogenous SIK1 has little effect on the phosphorylation status and cellular distribution of TORC2. Since *Sik1* knockdown can enhance NE-stimulated AA-NAT without changing nuclear TORC2 levels, endogenous SIK1 may repress NE-stimulated AA-NAT by a mechanism not involving the nuclear export of TORC2. Moreover, overexpressing *Sik1* has no effect on the dephosphorylated TORC2 at 0.5 h after NE stimulation, suggesting that the exogenous SIK1 can be inhibited at this early time-point.

Chapter 4

Discussion

In the rat pineal gland, the synthesis of melatonin is under adrenergic control through the rhythm-generating enzyme, AA-NAT (reviewed by Klein 1985). This enzyme is induced at night in response to NE stimulation from the sympathetic neurons through activation of the β-adrenergic → protein kinase A (PKA) pathway (reviewed in Klein DC, 1985; Maronde and Stehle, 2007). At the transcriptional level, the adrenergic-stimulated induction of AA-NAT is mediated by PKA through phosphorylation of CREB (Roseboom and Klein, 1995). Phosphorylated CREB binds to CREs in the promoter region of cAMP-regulated genes and causes activation of transcription (Baler et al., 1997). This activation results in a 150-fold increase in the mRNA level of *Aa-nat*, and in turn an increase in melatonin production (Roseboom et al., 1996).

Two domains of importance to the transcriptional activity of CREB are the KID which interacts with the KIX domain of the coactivator CBP/p300 (Chrivia et al., 1993; Radhakrishnan et al., 1997), and the bZIP domain which promotes dimerization and promoter binding (Schumacher et al., 2000). Phosphorylation of Ser-133 in the KID is generally accepted as a key event in the regulation of CREB-mediated transcription (Gonzalez and Montminy, 1989). However, it has been reported in other tissues that the bZIP domain of CREB may provide an additional control mechanism that regulates the CREB-mediated transcription. These mechanisms include the Ser133-independent activation by TORC, which binds directly to the bZIP domain of CREB (Conkright et al., 2003), and the related repression by SIK, which induces the export of TORC from the nucleus through phosphorylation (Katoh et al., 2004b; Koo et al., 2005). The focus of this

thesis is to investigate the importance of the SIK1/TORC2 pathway in regulating AA-NAT synthesis in the rat pineal gland.

4.1 SIK1: An inducible kinase repressing *Aa-nat* transcription

Because of the importance of the transcriptional activity of CREB in the regulation of *Aa-nat* induction, its potential repression by SIK1 through the bZIP domain prompted the investigation of SIK1 as a possible repressor in the rhythmic expression of *Aa-nat* in the rat pineal gland. As shown in the result section, the expression of *Sik1* is under adrenergic control in the rat pineal gland. Moreover, the induction of *Sik1* in response to NE stimulation is rapid, and this induction is enhanced by treatment with cycloheximide in a manner like *c-fos*, an established immediate early gene (Sheng and Greenberg, 1990).

In rat pinealocytes, our results indicate that the *Sik1* expression is stimulated by NE, as in a recent report using pineal organ culture (Bailey et al., 2009) and the NE-induced *Sik1* response precedes that of *Aa-nat*. Investigations into the receptors involved indicate that β-adrenergic receptors are primarily involved in the NE induction of *Sik1* and the contribution from α_1-adrenergic receptors is relatively minor. This is based on the observation that selective activation of β-adrenergic receptors alone causes a similar level of *Sik1* induction as that produced by NE, whereas selective activation of α_1-adrenergic receptors results in a modest induction of *Sik1*. Moreover, propranolol, the β-adrenergic antagonist, is more effective than prazosin, the α_1-adrenergic antagonist, in blocking the NE induction of *Sik1*.

At the second messenger level, the results indicate that only dBcAMP and, to a lesser extent, intracellular Ca^{2+}-elevating agents can stimulate *Sik1* induction. These findings are consistent with the results from the receptor characterization studies above. Moreover, it has been established that the synthesis of cAMP is regulated through the β-adrenergic receptors, whereas elevation of intracellular Ca^{2+} concentration is controlled by the α_1-adrenergic receptors in rat pinealocytes (Klein, 1985; Sugden et al., 1987; Vanecek et al., 1985)). In support of these observations, previous studies in PC12 cells and in mouse Y1 adrenocortical tumor cell lines also indicate the involvement of cAMP and intracellular Ca^{2+} in the induction of *Sik1* (Feldman et al., 2000; Lin et al., 2001).

Together, these results indicate that, although NE can activate multiple signalling pathways in the pinealocyte, the *Sik1* induction by NE in this tissue is primarily regulated through the cAMP signalling pathway. Because it has been established that NE stimulation can increase both cAMP and intracellular Ca^{2+} levels (Klein, 1985; Sugden et al., 1987; Vanecek et al., 1985), the physiological significance of the modest induction of *Sik1* by elevating intracellular Ca^{2+} alone is not clear. However, it may account for the suppressive effect of elevating intracellular Ca^{2+} on the induction of AA-NAT activity in an earlier report (Ho et al., 1992).

In parallel to the cell culture studies, there is a 50-fold increase in the *Sik1* mRNA level within 2 h after the onset of darkness. This rapid increase in *Sik1* transcription between 1 and 2 h after onset of darkness (ZT15 and ZT16) was overlooked in the earlier study (Bailey et al., 2009) on the rat pineal transcriptome

that identified *Sik1* as one of the numerous genes activated at night and induced by cAMP. In addition, the nighttime induction of *Sik1* also persists under constant darkness. This finding suggests that the induction of *Sik1*, besides being a naturally occurring circadian event in the rat pineal gland, is driven by the nightly release of NE from the sympathetic nerve under the control of the endogenous clock. Moreover, the rapid increase in the induction of *Sik1* during the early phase of the dark period is consistent with its role as a modulator of transcription of other nocturnally induced genes.

By using adenoviral transfection to modulate the expression of *Sik1*, the NE induction of *Aa-nat* mRNA and protein levels as well as enzyme activity is reduced in pinealocytes over-expressing *Sik1*, suggesting that SIK1 can function as a repressor for the expression of *Aa-nat*. This is further supported by the result of the *Sik1* knockdown experiment. Knockdown of the NE-stimulated *Sik1* induction leads to an enhancing effect on the NE-induced *Aa-nat* expression. Together, these results indicate that the induction of *Sik1* during the early phase of NE stimulation probably feeds back negatively on the *Aa-nat* gene transcription and shapes the temporal profile of its induction.

As for the impact of *Sik1* expression on the temporal profile of NE-stimulated *Aa-nat* expression, changes in *Sik1* levels can modulate the maximal NE-stimulated *Aa-nat* mRNA level as assessed in a time-course study. However, changes in *Sik1* levels appear to have no effect on the rate of decline of *Aa-nat* mRNA levels as estimated from the slope of decline in the time-course study. Therefore, the primary impact of SIK1 on the NE-stimulated *Aa-nat* response is

likely a modulating effect on the maximal level of its induction. The prolonged (up to 32 h) enhancing effect of *Sik1*-sh treatment on the NE induction of *Aa-nat* transcription observed may simply reflect the higher peak mRNA level of *Aa-nat* attained during the initial NE stimulation and its slow degradation. These secondary changes may account for the modulating effect of SIK1 on the duration of the stimulated *Aa-nat* response.

It should be noted that the inhibitory effect of SIK1 on *Aa-nat* expression appears delayed in spite of the rapid induction of *Sik1* by NE. Treatment with *Sik1*-sh only amplifies *Aa-nat* mRNA after 2 h of NE treatment and AA-NAT protein and enzyme activity after 4 h of NE treatment. This suggests that either a significant amount of SIK1 needs to be present to repress the induction of *Aa-nat* expression by NE, or SIK1 is inactive during the early phase of *Aa-nat* induction. One possible explanation is that SIK1 protein may be exported from the nucleus following PKA-mediated phosphorylation of Ser577 during the early period of NE stimulation as demonstrated in mouse adrenocortical tumor cells (Takemori et al., 2002). In support of this explanation is the observation that overexpression of pinealocytes transfected with the phosphorylation defective *SIK1*-S577A construct results in a more potent repressive effect on NE-stimulated *Aa-nat* expression.

The above results support SIK1 playing a repressor role on the NE-induced *Aa-nat* expression and that this repression by SIK1 can in turn impacted on the duration of the *Aa-nat* response. However, the mechanism through which SIK1 exerts its effect on the NE-stimulated *Aa-nat* expression is not known.

Other studies indicate that SIK1 may exert its action by phosphorylating TORC, a CREB-specific coactivator. When TORC is in its dephosphorylated state, it binds to the bZIP domain of CREB and activates CREB in a Ser133 phosphorylation-independent manner (Conkright et al., 2003; Screaton et al., 2004). However, phosphorylation of TORC by SIK1 will lead to the export of TORC from the nucleus, resulting in the reduction of CREB-targeted transcription activity (Katoh et al., 2004b; Koo et al., 2005). Studies that addressed the mechanism whereby TORC2/SIK1 can impact on the adrenergic induction of *Aa-nat* expression were examined as described in the result section and will be discussed in *section 4.3*.

Given that SIK1 mediates its effect through CREB (Doi et al., 2002), one would expect other CREB-target genes will respond similarly to manipulation of SIK1 levels. Besides *Aa-nat*, other CREB-target genes characterized previously in the rat pineal gland, including *Mkp-1*, *Icer* and *Dio2*, behave similarly to changes in SIK1 levels. Overexpressing *Sik1* suppresses the three NE-stimulated genes tested, and abolishing the NE-stimulated increase in *Sik1* by *Sik1*-sh2 or *Sik1*-sh5 enhances the NE-stimulated *Mkp-1*, *Icer* and *Dio2* transcription after 4 h of NE stimulation.

In other cell types such as the skeletal myocytes, SIK1 can function as a class II HDAC kinase that triggers the cytoplasmic export of HDAC, resulting in the activation of myocyte enhancer factor 2-dependent transcription (Berdeaux et al., 2007). However, it is unlikely that SIK1 represses induced CREB-target genes by acting as a HDAC kinase in the rat pineal gland. Although we have not investigated whether SIK1 can phosphorylate HDAC in rat pinealocytes, the

effect of inhibition of HDAC on NE-stimulated gene transcription in rat pinealocytes is gene specific (Ho et al., 2007a). Whereas inhibiting HDAC suppresses the NE-stimulated *Aa-nat* and *Dio2* transcription, it has little effect on the transcription of *Icer* and *Mkp-1*, and enhances the transcription of *c-fos.* Moreover, the effect of HDAC inhibition on the NE-stimulated expression of *Aa-nat*, *Dio2*, *Icer* and *Mkp-1* is different from that of SIK1. While HDAC inhibition likely has an impact on the amplitude of induced *Aa-nat* expression, SIK1 likely affects the duration of stimulated *Aa-nat* transcription.

Besides *Sik-1*, earlier studies have shown that the NE/cAMP/PKA signalling pathway also causes the synthesis of other inhibitory transcription factors, ICER (Stehle et al., 1993) and Fra-2 (Baler and Klein, 1995). ICER, by competing with pCREB for the CRE site, can inhibit *Aa-nat* transcription (Foulkes et al., 1997; Maronde et al., 1999). Although significant elevation of ICER protein can be detected in the pineal gland at night, the physiological impact of this increase on *Aa-nat* transcription is not clear. This is based on the observations that in CREM mutant mice (whereby ICER and CREM are inactivated), the *Aa-nat* rhythm is largely normal except for a minor effect on the amplitude of its expression (Foulkes et al., 1996). Moreover, in cultured pineal cells, transient knockdown of the adrenergic-stimulated ICER synthesis through *Icer*-sh has no effect on the induction of *Aa-nat* (Ho et al., 2007b). This differs from the result observed with either *Sik1*-sh2 or *Sik1*-sh5 whereby transient knockdown of the adrenergic-stimulated SIK1 synthesis has an enhancing effect on the mRNA levels of induced *Aa-nat* and other CREB-target genes.

Another potential repressor in the rat pineal gland is Fra-2. Fra-2, which is also induced in the pineal at night and following NE stimulation of rat pinealocytes (Baler and Klein, 1995) may inhibit *Aa-nat* transcription by interacting with the AP-1 site on the *Aa-nat* gene (Baler et al., 1997). In whole animals with pineal-specific transgenic knockdown of Fra-2 has no effect on the *Aa-nat* rhythm after onset of darkness (Smith et al., 2001). Moreover, knockdown of Fra-2 by transiently expressed *Fra*-sh in pinealocytes also has no effect on *Aa-nat* transcription after NE stimulation (Ho et al., 2007b), which again differs from the enhancing effect on the mRNA levels of induced *Aa-nat* and other CREB-target genes observed here. However, it is of interest to note that in animals with pineal-specific transgenic knockdown of Fra-2 as well as knockdown of Fra-2 by transiently expressed *Fra*-sh in pinealocytes, the induced *Dio2* transcription is increased (Chik et al., 2007b). Therefore, it will be of interest to further investigate the difference in the transcriptional control between *Aa-nat* and *Dio2* in future studies.

The above results indicate that whereas there is an early induction of *Sik1* by NE in the rat pineal gland, the repressor effect of SIK1 on *Aa-nat* expression appears to be delayed, suggesting that SIK1 protein either needs to be present in a significant amount to exert its effect or its repressive function is temporary inhibited during initial NE stimulation. Studies on other transcription repressors, such as ICER or Fra-2, on their role in limiting the duration of *Aa-nat* transcription have yielded negative results. Findings from our SIK1 studies allow the working model for pineal adrenergic-regulated gene expression to include an

important transcription repressor role for SIK1. Whereas adrenergic-regulated gene expression is up-regulated through a cAMP mechanism, to shape the time profile, cAMP also induces the synthesis of SIK1 which functions as a repressor for gene transcription by influencing the transcriptional activity of CREB genes (Fig. 1). The mechanism by which SIK1 exerts its effect on NE-stimulated *Aa-nat* transcription could be through the CREB-specific coactivator TORC2.

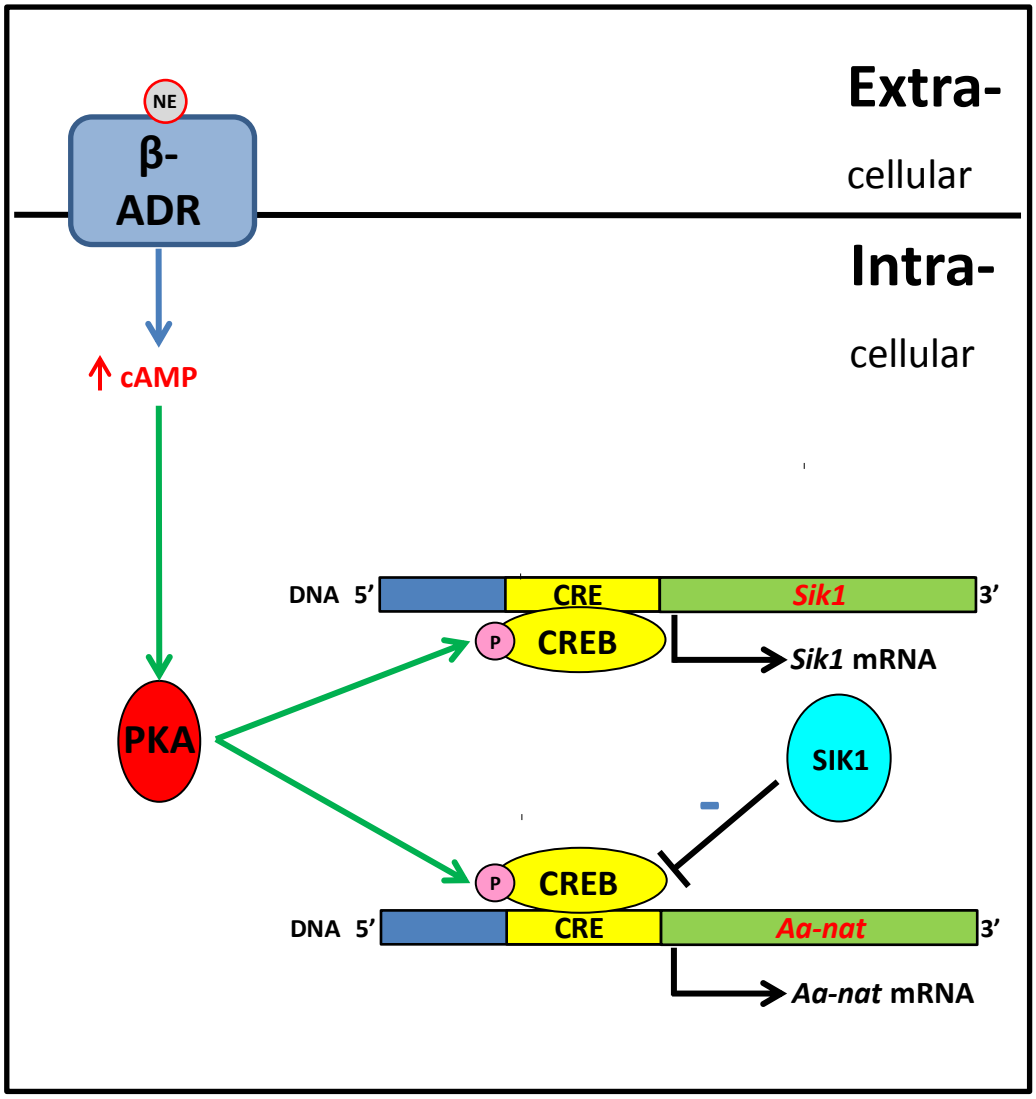

Figure 1: Regulation and function of the Salt-inducible kinase 1 (SIK1) in the rat pineal gland. NE stimulates β-adrenergic receptor (ADR), which leads to an intracellular elevation of cAMP. cAMP in turn activates protein kinase A (PKA). PKA phosphorylates the cAMP-response-element binding protein (CREB) that in turn activates the transcription of *Sik1* and *Aa-nat*. The quantity of the protein product of *Sik1* increases and represses *Aa-nat* transcription.

4.2 The CREB-coactivator TORC2 in the rat pineal gland

As reviewed in the Introduction, the two domains of importance to the transcriptional activity of CREB are KID, which interacts with the KIX domain of the coactivator CREB-binding protein/p300, and bZIP, which promotes dimerization and promoter binding. Phosphorylation of Ser133 in the KID is generally accepted as a key event in the regulation of CREB-mediated transcription (Gonzalez and Montminy, 1989). However, the bZIP domain of CREB can provide an additional control mechanism that regulates CREB-mediated transcription (Doi et al., 2002). One such mechanism is the up-regulation of CREB activity through binding of the CREB-specific coactivator, TORC, to the bZIP domain of CREB (Conkright et al., 2003).

TORC has been identified as a family of proteins that functions as transcriptional coactivator for CREB (Conkright et al., 2003; Iourgenko et al., 2003). Under basal conditions, TORC is reported to be phosphorylated by SIK and sequestered in the cytoplasm via phosphorylation-dependent association with 14-3-3 proteins (Screaton et al., 2004). In the case of the rat pinealocyte, the basal mRNA level of SIK1 is low, and its transcription is increased by NE stimulation, suggesting that the activity of SIK1 may also be low under basal conditions. This in turn can influence the cellular distribution of TORC in the pinealocyte.

Although all three members of the TORC family, TORC1, TORC2, and TORC3, can be phosphorylated by SIK and subjected to SIK1-dependent nuclear export, only TORC2 is ubiquitously expressed (Altarejos et al., 2008; Katoh et al.,

2006; Koo et al., 2005; Song et al., 2010; Wu et al., 2006). To address the potential role of TORC in regulating rhythmic gene expression in the rat pineal gland, the regulation of TORC2 and the characterization of the cellular distribution of TORC2 under basal and NE-stimulated conditions have been investigated.

Studies using cultured pinealocytes indicate that the expression of *Torc2* is not under adrenergic regulation. However, the state of phosphorylation and the intracellular distribution of TORC2 protein are tightly regulated by NE. Moreover, studies in which TORC2 level is manipulated provide support that TORC2 can function as a transcriptional coactivator of CREB-target gene expression including that of *Aa-nat*.

The time-course study reveals that there is no nocturnal induction of the *Torc2* gene in the rat pineal gland. However, the onset of darkness causes the appearance of a faster migrating TORC2 protein band when analyzed by immunoblot. This faster migrating band is maintained throughout darkness, but rapidly declines with the onset of light. Since the postganglionic nerve fibres projected from the SCG innervate the pineal gland and release NE at night (Klein et al., 1983; Moore and Klein, 1974), these findings raise the possibility that the appearance of the faster migrating TORC2 band during darkness is due to the nocturnal NE stimulation of the rat pineal gland. This is confirmed by the parallel observation of the faster migrating TORC2 band in NE-stimulated cultured pinealocytes.

Changes in migration of proteins on the SDS gel can be due to post-translational modifications such as phosphorylation. The identity of the TORC2 bands is identified with CIP treatments, which demonstrates that the faster migrating TORC2 band is the dephosphorylated form of TORC2. This implies that under basal conditions, most of the TORC2 protein is phosphorylated and that NE stimulation causes rapid dephosphorylation of TORC2 in the rat pineal gland.

Previous reports have shown that TORC2 can be phosphorylated at multiple sites (Jansson et al., 2008; Koo et al., 2005; Uebi et al., 2010), resulting in different levels of TORC2 phosphorylation. To better delineate the effect of NE on the phosphorylation status of TORC2, protein samples collected from the time-course experiment were also separated on the PhosTag gel. With no difference in the band pattern of TORC2 between 15 min and 8 h after NE stimulation, this result suggests that once NE stimulates the dephosphorylation of TORC2, there is no major change in its phosphorylation status as long as NE stimulation continues.

Investigations into the receptors involved indicate that β-adrenergic receptors are primarily involved in the NE-induced dephosphorylation of TORC2. This is based on the observations that selective activation of β-adrenergic receptors causes a similar effect as that produced by NE, whereas selective activation of α_1-adrenergic receptors is without any effect. Moreover, propranolol, the β-adrenergic antagonist, is more effective than prazosin, the α_1-adrenergic antagonist, in blocking the NE effect on TORC2.

At the second messenger level, our results show that both dBcAMP and elevating intracellular Ca^{2+} concentration through depolarization of K^+ can cause rapid dephosphorylation of TORC2. Since selective activation of α_1-adrenergic receptors has no effect on the phosphorylation status of TORC2, our results suggest that the NE-stimulated TORC2 dephosphorylation is mediated primarily through the β-adrenergic/cAMP pathway. This is further supported by the observation that the banding pattern of TORC2 observed after dBcAMP treatment is similar to that of NE stimulation but different from that of treatment with KCl.

Whereas elevation of intracellular Ca^{2+} concentration by a depolarizing concentration of K^+ can cause TORC2 dephosphorylation, intracellular Ca^{2+} elevation mediated by activation of α_1-adrenergic receptors has no effect. One possible explanation is the difference in magnitude of the concentration of intracellular Ca^{2+} attained through the two mechanisms that elevate intracellular Ca^{2+}. In contrast to the known effect of PP2B on dephosphorylation of TORC2 with activation of voltage-gated L-type Ca^{2+} channels (Screaton et al., 2004), it is possible that the intracellular Ca^{2+} elevation mediated through α_1-adrenergic receptors in the rat pineal gland is not sufficient to activate PP2B.

By comparing the potencies of different phosphatase inhibitors in blocking the NE-stimulated TORC2 dephosphorylation, PP2A is identified as the phosphatase most likely involved in the rapid dephosphorylation of TORC2. Although both calyculin A and okadaic acid are effective in blocking the NE-stimulated dephosphorylation of TORC2, inhibiting PP1 with tautomycin or PP2B with cyclosporine A is without effect. The observation that cyclosporine A has no

effect on the NE-stimulated dephosphorylation of TORC2 is in agreement with the finding that α_1-adrenergic stimulation also has no effect on TORC2 dephosphorylation. Together our results support the involvement of cAMP in causing the dephosphorylation of TORC2 protein via PP2A.

Although PP2A appears to be activated by intracellular cAMP elevation, the activating mechanism may not be dependent on the simultaneous cAMP-dependent increase in PKA activity. This is suggested by findings in NRK-52E cell lines which show that an established PKA inhibitor, H89, has no effect on the cAMP-stimulated PP2A activity (Feschenko et al., 2002). In addition, earlier reports have shown that A-kinase anchoring protein (AKAP) can interact with PP2A and the cAMP-sensitive regulatory subunit of PKA (reviewed in Tasken and Aandahl, 2004). Therefore, it is tempting to speculate that cAMP may stimulate PP2A-mediated TORC2 dephosphorylation with the involvement of the regulatory subunit of PKA rather than through phosphorylation of PKA.

In a previous study, TORC2 is reported to be dephosphorylated by the synergistic actions of cAMP and Ca^{2+} (Screaton et al., 2004). Whereas Ca^{2+} activates PP2B, cAMP is thought to inhibit SIK from phosphorylating TORC2. In agreement with the previous study, our results show that treatment with either dBcAMP or KCl treatment can cause TORC2 dephosphorylation in rat pinealocytes. However, there is a major difference. Although NE stimulation elevates intracellular cAMP and Ca^{2+} levels, NE-stimulated dephosphorylation of TORC2 is mediated through a cAMP- rather than a Ca^{2+}-dependent mechanism. This can be explained by our finding that the main phosphatase targeting TORC2

after NE stimulation is PP2A, rather than the Ca^{2+}-dependent PP2B. Therefore, the Ca^{2+} pathway is not necessary in the NE-stimulated dephosphorylation of TORC2 in the rat pineal gland.

Previous investigations using hepatocytes (Koo et al., 2005), beta cells of pancreatic islets (Jansson et al., 2008) and COS-7 cells (Uebi et al., 2010) have identified three Ser residues on TORC2 that can be phosphorylated: Ser171, Ser275 and Ser307. The specific Ser residue(s) dephosphorylated after elevation of either intracellular cAMP or Ca^{2+} remains to be determined in rat pinealocytes. However, based on the banding patterns observed by using the PhosTag gel, it is probable that the Ser residue(s) on TORC2 that are dephosphorylated after intracellular elevation of cAMP differ from that after elevation of intracellular Ca^{2+}.

Fractionating the pinealocyte into cytosolic and nuclear fractions reveals that dephosphorylation of TORC2 leads to nuclear translocation of the protein. Although only the dephosphorylated TORC2 is found in the nucleus, both the phosphorylated and native forms of TORC2 are present in the cytosolic fraction after NE stimulation, indicating that although dephosphorylation is required for nuclear localization, it may not be the only rate-limiting step in determining the quantity of nuclear TORC2 level. The correlation between the NE-stimulated decline of total TORC2 protein level in whole cells and the NE-stimulated decline of nuclear TORC2 in the time-course study suggests that the quantity of nuclear TORC2 may also be controlled by regulating the total TORC2 protein level.

By selectively activating β- or α_1-adrenergic receptors, we show that nuclear translocation of TORC2 is mediated through the β-adrenergic receptors. Selective activation of β-adrenergic receptors causes similar elevation in nuclear TORC2 level as that produced by NE, whereas selective activation of α_1-adrenergic receptors has no effect. Moreover, propranolol, the β-adrenergic antagonist, is more effective than prazosin, the α_1-adrenergic antagonist, in blocking the NE-stimulated accumulation of nuclear TORC2.

At the second messenger level, our results indicate that only treatment with dBcAMP can cause the nuclear translocation of TORC2. This finding is consistent with the results from the receptor characterization studies. Together, these findings suggest that the nuclear translocation of TORC2 is mediated through the β-adrenoreceptor/cAMP pathway.

Our results suggest that dephosphorylation of TORC2 by PP2A causes the nuclear translocation of this coactivator. This is based on experiments comparing the potencies of phosphatase inhibitors in blocking the NE-stimulated TORC2 nuclear translocation, as described previously. Among the phosphatase inhibitors, only okadaic acid and calyculin A (PP2A inhibitors), which inhibit the NE-stimulated dephosphorylation of TORC2, can block its nuclear translocation. In comparison, treatment with either tautomycin (a PP1 inhibitor) or cyclosporine A (a PP2B inhibitor) has no effect on the NE-stimulated nuclear translocation of TORC2.

Interestingly, intracellular Ca^{2+} elevation mediated by voltage-gated L-type Ca^{2+} channels can cause dephosphorylation of TORC2, but not its nuclear

translocation. Hence, not all stimulated dephosphorylation of TORC2 can lead to nuclear translocation. Therefore, the phosphorylation status may not accurately reflect the activation status of TORC2. This raises the issue whether TORC2 can function as a Ca^{2+}- and cAMP-coincident detector in all cell types. Since reports from earlier studies have shown that TORC2 can be phosphorylated at multiple sites (Jansson et al., 2008; Koo et al., 2005; Uebi et al., 2010), one possibility is that only dephosphorylation of specific Ser residues on TORC2 allow this coactivator to enter the nucleus. However, which of the three Ser residues on TORC2 (Ser171, Ser275 or Ser307) is important for nuclear translocation remains to be determined in the rat pineal gland. Nevertheless, our finding highlights the importance of investigating the specific phosphorylation sites on TORC2, especially the ones that are coupled to nuclear translocation, hence allowing TORC2 to function as a coactivator.

The time profile of NE-stimulated TORC2 nuclear translocation indicates that TORC2 is present in the nucleus when *Aa-nat* transcription is active. Within 15 min of NE stimulation, there is an increase in nuclear TORC2 level which precedes the NE induction of *Aa-nat*. The NE-stimulated nuclear TORC2 starts to decline after 2 h but remains detectable after 4 h of NE stimulation. Since it is accepted that *Aa-nat* is a CREB-target gene (Roseboom and Klein, 1995) and TORC2 is a CREB-specific coactivator (Conkright et al., 2003), these findings raise the possibility that TORC2 may have a role in controlling the activation and duration of *Aa-nat* transcription.

By using adenoviral transfection to overexpress *Torc2*, our results suggest that TORC2 can function as a coactivator in the rat pineal gland and modulate the duration of NE-induced *Aa-nat* transcription. Overexpressing TORC2 increases the level of dephosphorylated TORC2 after NE stimulation. In terms of its impact on the temporal profile of NE-stimulated *Aa-nat* mRNA levels, overexpressing TORC2 does not have an effect on *Aa-nat* mRNA and AA-NAT protein during the first 4 and 6 h of NE stimulation, respectively. This delayed effect suggests that in spite of the rapid translocation, the contribution by TORC2 to the transcription of *Aa-nat* is minimal during the initial NE stimulation.

In contrast, the major impact of increasing TORC2 expression is to prolong the duration of the sustained increase in NE-stimulated *Aa-nat* mRNA level, hence resulting in a higher peak *Aa-nat* response occurring at a later time-point. In addition, overexpressing TORC2 does not appear to have an effect on the rate of decline of *Aa-nat* mRNA level (as estimated from the slope of decline in the time-course studies). Together, these results suggest that the effect of overexpressing TORC2 on the sustained induction of *Aa-nat* may simply reflect the higher amplitude of *Aa-nat* mRNA level attained during the initial NE stimulation.

Another consideration is the stability of the *Aa-nat* message as demonstrated by a lack of decline of the peak NE-stimulated *Aa-nat* mRNA level after inhibiting gene transcription with actinomycin for 1 h (Chik et al., 2007b). The slow degradation of the *Aa-nat* mRNA likely contributes to the prolonged

duration of *Aa-nat* transcriptional activity and elevated level of AA-NAT protein up to 40 h after NE stimulation in pinealocytes overexpressing TORC2.

Also in support of an effect of TORC2 on *Aa-nat* transcription is the finding of *Torc2* knockdown being effective in reducing the NE induction of *Aa-nat* mRNA. However, this reduction is only modest and has no impact on the NE-stimulated AA-NAT protein level. Although this discrepancy can be related to an insufficient knockdown of the TORC2 protein, this is unlikely because the transfection protocol is able to reduce the *Torc2* mRNA by more than 80% and the protein to undetectable level.

Another possibility is the existence of redundancy in the coactivator system. It is possible that simultaneous knockdown of both TORC1 and TORC2 is needed to have an impact on the protein level of AA-NAT in the rat pineal gland. Indeed, TORC1, which appears to be important in neuronal tissues, has also been shown to regulate CREB-target gene expression (Li et al., 2009). Moreover, both TORC1 and TORC2 are similar in structure and can interact with the bZIP domain of dimerized CREB as tetramers (Conkright et al., 2003). Therfore, TORC1 may be interchangeable with TORC2 and perhaps TORC1 and TORC2 can assemble as heterotetramers. If the function of endogenous TORC2 is compensated by TORC1, it can account for the modest effect of *Torc2* knockdown on the NE-stimulated *Aa-nat* mRNA level.

The exact mechanism whereby TORC2 can affect the duration of CREB-driven gene expression is not clear. TORC2 has been shown to interact with TAF130 (a component of the GTF, TFIID) (Conkright et al., 2003), implying that

TORC2 can function as a CREB coactivator by helping the assembly of the PIC. In rat pinealocytes, our results suggest that TORC2 by itself is not important during the activation of *Aa-nat* transcription. Neither overexpression nor knockdown of *Torc2* has an effect on NE-stimulated *Aa-nat* mRNA levels during the first 8 h of NE stimulation. Since the general role of GTFs is to assemble the PIC, which is required during the activation of gene transcription (reviewed in Lee and Young, 2000), it is unlikely that TORC2 has a major role in modulating *Aa-nat* transcription by promoting the recruitment of GTFs.

TORC2 has also been shown to enhance CREB activity by increasing cooperative interactions between CBP and phosphorylated CREB (Ravnskjaer et al., 2007), leading to increased stability of PIC and prolongs the duration of gene transcription. Stabilizing the PIC appears to be the more likely mechanism through which TORC2 enhances *Aa-nat* transcription in the rat pineal gland since time-course studies show that the main impact of overexpressing TORC2 is to increase the duration of its transcription. However, if endogenous TORC2 can be compensated by TORC1, the effect of *Torc2* knockdown on the PIC stability may not be reflected on the NE-stimulated *Aa-nat* mRNA level.

Since TORC2 has been found to function through the bZIP domain of CREB (Conkright et al., 2003), the NE-stimulated expressions of other CREB-target genes such *Dio2, Icer* and *Mkp-1* are expected to respond to changes in TORC2 levels in a manner similar to that of *Aa-nat*. Indeed, overexpressing *Torc2,* only enhances the mRNA levels of *Icer, Dio2* and *Mkp-1* after 8 h but not at 2 and 4 h of NE stimulation. This suggests that exogenous TORC2 can

modulate the duration of NE-stimulated *Icer*, *Dio2* and *Mkp-1* transcription, as in the case for *Aa-nat*. Knockdown of *Torc2* also has no noticeable effect on the NE-stimulated *Icer*, *Dio2* and *Mkp-1* mRNA levels during the induction phase and only a modest effect is noted during the declining phase at 8 h after NE stimulation. Compared with other cell types (Dentin et al., 2007; Koo et al., 2005), the role of endogenous TORC2 in the regulation of CREB-driven genes in the rat pinealocyte may not be as critical.

The expression of other TORC isoforms may govern the importance of TORC2 in regulating CREB-driven genes in a specific cell type. For example, in hepatocytes, there is a much higher expression of TORC2 than TORC1 protein (Koo et al., 2005) and a loss of TORC2 may not be easily compensated by TORC1 as in other tissues where the expression of TORC1 protein is much higher. In rat pinealocytes, *Torc2* knockdown only has a modest effect on CREB-target gene expression 8 h after stimulation, suggesting a potential compensatory effect of TORC1, as discussed previously. This further highlights the necessity of investigating the role of other TORC isoforms in the same cell type.

Overall, our results show that in the rat pinealocyte, TORC2 dephosphorylation through the β-adrenoreceptor/cAMP/PP2A-pathway leads to nuclear translocation of TORC2 (Fig. 2). Endogenous TORC2 only has a modest role in modulating the duration of NE-stimulated *Aa-nat* transcription, a finding that differs from the important role of TORC2 in regulating CREB-target gene expression in other cell types (Dentin et al., 2007; Koo et al., 2005).

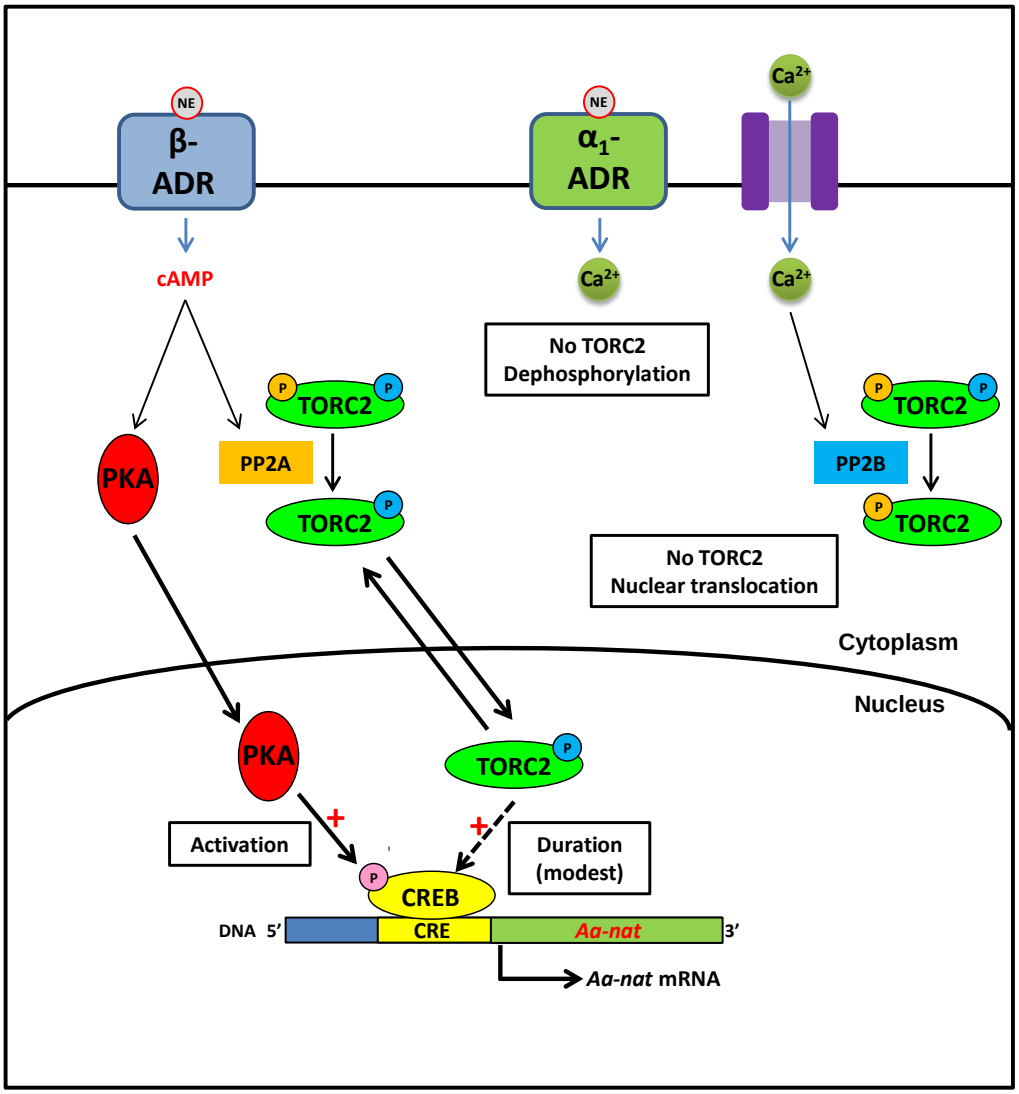

Figure 2: Regulation and function of the transducer of regulated CREB-activity 2 (TORC2) in the rat pineal gland. NE stimulates β-adrenergic receptor (ADR), which leads to an intracellular elevation of cAMP. cAMP in turn activates protein kinase A (PKA) and protein phosphatase 2A (PP2A). PP2A will dephosphorylate TORC2 which in turn causes the nuclear translocation of TORC2. Stimulation of the α_1-ADR which increases intracellular Ca^{2+} levels has no effect on TORC2 dephosphorylation or nuclear translocation. Intracellular elevation of Ca^{2+} mediated through voltage-gated L-type Ca^{2+} channels (purple) leads to sufficient increase in PP2B activity to dephosphorylate TORC2. However, PP2B-mediated TORC2 dephosphorylation does not cause nuclear translocation. PP2A and PP2B have a different effect on TORC2 nuclear translocation by targeting different phosphorylation sites. In the nucleus, PKA phosphorylates and activates CREB-dependent *Aa-nat* transcription. TORC2 enhances the duration of *Aa-nat* transcription through CREB, but its effect is small (dashed arrow).

4.3 The SIK1/TORC2-pathway in the rat pineal gland

Studies from other cell types suggest that SIK may exert its action by phosphorylating TORC, a CREB-specific coactivator (Takemori *et al.* 2002, 2007; Conkright *et al.* 2003). This leads to the export of TORC from the nucleus to the cytoplasm where it is sequestered via phosphorylation-dependent association with the 14-3-3 protein and results in the reduction of CREB-targeted transcriptional activity (Screaton *et al.* 2004).

In the rat pineal gland, besides *Aa-nat*, other CREB-target genes tested, including *Icer*, *Dio2* and *Mkp-1*, also respond in a similar manner to changes in SIK1 levels (Kanyo *et al.* 2009). As discussed in Chapter 4.1, our results support an important role of SIK1 in determining the time profile of the adrenergic induction of *Aa-nat* expression in the rat pineal gland. Given that SIK1 has been shown to mediate the nuclear export of TORC in other tissues (Koo et al., 2005), we determined the role of SIK1 in the phosphorylation and intracellular localization of TORC2 in the rat pinealocyte by using recombinant adenovirus either over-expressing the full-length *Sik1* transcript (*Sik1*-fl) or with shRNA against *Sik1* (*Sik1*-sh). In general, although overexpressing *Sik1* has a significant effect on TORC2 protein, the effect of *Sik1* knockdown is minimal. This is similar to what we have observed regarding the effects of manipulating TORC2 on *Aa-nat* transcription.

Focusing first on the effects of knocking down *Sik1* on TORC2 protein, our results suggest that endogenous SIK1 may not play a significant role in determining the phosphorylation state or the intracellular distribution of TORC2

in the pinealocyte under basal conditions. With TORC2 being highly phosphorylated and localized mainly in the cytoplasm under basal conditions, we show that knockdown of *Sik1* has no effect on the phosphorylation status of TORC2 monitored by both SDS and PhosTag gels or the intracellular distribution of this coactivator under basal conditions. Considering also that in the absence of NE stimulation, the level of SIK1 protein under basal conditions is likely low, these results suggest that SIK1 is not the kinase responsible for phosphorylating and therefore retaining TORC2 in the cytoplasm under basal conditions. Other kinases must therefore be responsible for the basal TORC2 phosphorylation in the rat pinealocyte.

Although the transcription of *Sik1* can be induced by NE stimulation and likely leading to elevated endogenous SIK1 level, our results also indicate that endogenous SIK1 may not play a major role in modulating the time profile of NE-stimulated TORC2 dephosphorylation or nuclear localization. This is based on the observation that *Sik1* knockdown has no effect on the peak level of dephosphorylated TORC2 in the nucleus during the early phase of NE stimulation. Moreover, it also has no effect on the gradual decline of nuclear TORC2 between 2 and 4 h after NE stimulation or the low level of nuclear TORC2 8 h after NE stimulation. Therefore, it is unlikely that, in the rat pinealocyte, the rephosphorylation-dependent nuclear export of TORC2 is regulated by SIK1 and suggests the involvement of other kinases.

Previous studies have shown that kinases besides SIK1 can phosphorylate TORC2. These include SIK2 (Screaton et al., 2004), AMPK (Koo et al., 2005)

and microtubule affinity-regulating kinase 2 (MARK2) (Jansson et al., 2008). Determining the contributions of these other kinases in TORC2 phosphorylation under basal conditions and the rephosphorylation of TORC2 after NE stimulation in the rat pineal gland will be of interest. In hepatocytes, it has been shown that whereas SIK1 is inducible, SIK2 is constitutively expressed at high levels under basal conditions (Koo et al., 2005).

Our demonstration of endogenous SIK1 having no effect on TORC2 distribution suggests that SIK1 probably represses NE-stimulated *Aa-nat* transcription through pathways other than nuclear export of TORC2. This possibility is supported by the following findings. Whereas SIK1 has a potent repressive effect on NE-stimulated *Aa-nat* transcription, its effect on TORC2 distribution is only modest. Although overexpressing TORC2 clearly enhances the NE-stimulated *Aa-nat* mRNA level, the reduction mediated by TORC2 knockdown is small and not translated into changes in AA-NAT protein levels. In contrast, the effects of SIK1 knockdown or overexpression on NE-stimulated *Aa-nat* mRNA levels are paralleled with changes in protein levels. Moreover, *Sik1* knockdown, which enhances the NE-stimulated *Aa-nat* transcription at time-points up to 32 h after NE stimulation, has no effect on the NE-stimulated nuclear TORC2 levels at any time-points (0.5, 3 and 8 h) tested.

If causing nuclear export of TORC2 is not the downstream mechanism through which SIK1 represses *Aa-nat* expression, what other mechanisms may be involved? One possibility is the involvement of TORC1. SIK1 has been shown to phosphorylate TORC1 and regulates its coactivator function in developing

cortical neurons (Li et al., 2009), just like TORC2. If the downstream target of SIK1 is TORC1, and not TORC2, in rat pinealocytes, this potentially can explain the repressive effect of SIK1 on NE-induced *Aa-nat* expression in the absence of major changes in TORC2. The differences in the regulation of TORC1 and TORC2 in rat pinealocytes have recently been investigated (McTague et al., 2012). The precise contributions of these two coactivators in the regulation of NE-stimulated *Aa-nat* expression is currently under investigation in our laboratory.

An alternative explanation for a lack of effect of endogenous SIK1 on TORC2 cellular distribution and yet remains repressive toward *Aa-nat* transcription is that SIK1 may repress NE-stimulated *Aa-nat* transcription without triggering nuclear export of this coactivator. Earlier studies suggest that TORC2 functions as a coactivator by enhancing the interaction of CBP and CREB (Ravnskjaer er al 2007). This would imply that as long as SIK1-mediated phosphorylation can cause the dissociation of TORC from the PIC, the effect of this coactivator on CREB-target gene transcription can be inhibited. Moreover, the cellular distribution of TORC2 may not accurately reflect the activation status of this coactivator. It is possible that distinct phosphorylation sites on TORC2 are responsible for mediating nuclear export and triggering the dissociation from the PIC.

Another possibility is that SIK1 may repress CREB-target gene expression independent of TORC2 as TORC is not the only substrate of SIK. It is generally accepted that histone acetylation by CBP/p300 can enhance CREB-target gene

expression (Bannister and Kouzarides, 1996; Kwok et al., 1994; Martinez-Balbas et al., 1998; Ogryzko et al., 1996). Earlier reports have shown that phosphorylation of Ser89 on p300 can inhibit transcriptional activity (Yang et al., 2001; Yuan and Gambee, 2000). More recently, SIK2 has been reported to phosphorylate Ser89 of p300 (SIK consensus recognition motif also exists on CBP) (Liu et al., 2008), hence raising the possibility that SIK can inhibit CREB activity through Ser89 phosphorylation of p300.

Besides CBP/p300, SIK1 may also target other mechanisms that regulate gene expression. In cell types such as the skeletal myocyte, SIK1 can function as a class II HDAC kinase leading to cytoplasmic translocation of HDAC and suppresses histone deacetylation (Berdeaux et al., 2007). A previous study has shown that, in the rat pinealocyte, inhibition HDAC suppresses NE-stimulated expression of *Aa-nat* and *Dio2* while increasing histone acetylation (Ho et al., 2007a). However, this effect of inhibiting HDAC is gene-specific since HDAC inhibition only has a minimal effect on the transcription of *Icer* and *Mkp-1*. Therefore, we cannot exclude the possibility that part of SIK1 repressive effect on induced *Aa-nat* transcription is mediated through inhibition of HDAC.

Since SIK1 has been reported to have an enhancing effect on PP2A activity (Sjostrom et al., 2007), it is also possible that SIK1, through activating PP2A, can lead to the dephosphorylation of Ser133 on CREB and inhibits CREB-target genes. However, this seems unlikely in the pineal gland since our results also show that manipulating SIK1 levels has no effect on the NE-stimulated p-CREB levels. Hence, in spite of the potent inhibitory effect of SIK1 on *Aa-nat*

transcription in the rat pinealocyte, the downstream mechanism involved remains unclear from our studies.

In studying the function of a protein, overexpression may be less physiological than knockdown of endogenous protein. Nevertheless, our investigation using overexpression of *Sik1* reveals several interesting aspects of the relation between SIK1 and TORC2. We have shown that TORC2 protein levels are significantly reduced 4 h after NE treatment in the rat pinealocyte or 6 h after onset of darkness in the rat pineal gland. Although a role of SIK1 in promoting TORC2 degradation has been suggested in hepatocytes (Dentin et al., 2007), our results indicate that the SIK1-mediated phosphorylation of TORC2 is not the explanation of this NE-stimulated decline in TORC2 protein level in rat pinealocytes. Whereas *Sik1* knockdown has no effect on TORC2 level after NE stimulation, overexpressing *Sik1* leads to an increase in intensity of the phosphorylated TORC2 band 8 h after NE stimulation. Considering that SIK-mediated phosphorylation has been shown to promote 14-3-3 interaction with TORC2 (Dentin et al., 2007; Screaton et al., 2004), the most likely explanation for the decline in TORC2 level after NE stimulation is that only a proportion of dephosphorylated TORC2 can enter the nucleus while the remaining dephosphorylated TORC2 proteins, when not being protected by binding to 14-3-3, become susceptible to proteolytic degradation in the cytoplasm. Indeed, our finding that overexpressing *Sik1*, which causes an increase in TORC2 phosphorylation, can lead to elevated TORC2 level in the cytoplasm is consistent with this explanation.

Another interesting observation of the present study is that overexpression of SIK1 leads to phosphorylation of TORC2 protein at 3 h and 8 h after NE stimulation but this effect is not observed after 0.5 h. This implies that overexpressed SIK1 does not prevent the initial dephosphorylation of TORC2 stimulated by NE. One possible explanation is that the function of SIK1 is inhibited by PKA-mediated phosphorylation as reported previously in adrenocortical tumor cells (Takemori et al., 2002). Indeed, we have shown that PKA-phosphorylation defective SIK1 mutant has a more potent inhibitory effect than the wild type of SIK1 on the NE-stimulated *Aa-nat* expression. Another possible mechanism is that, the activity of PP2A can be increased by cAMP (Feschenko et al., 2002). We have already shown that cAMP stimulates TORC2 dephosphorylation through PP2A in rat pinealocytes and that intracellular cAMP levels peak 15 min after NE stimulation (Kim et al., 2007). This raises the possibility that higher PP2A activity during the early phase of NE stimulation can override the effect of overexpressed SIK1 on TORC2.

The inhibition of SIK1 function during the early phase of NE stimulation in rat pinealocytes may be of physiological significance. In the present study, the main function of endogenous SIK1 is to repress NE-stimulated *Aa-nat* transcription. In order for the *Aa-nat* transcription to be activated soon after NE-stimulation, it is logical that the repressive pathway should be inhibited to allow for rapid increase in the transcription of the target gene. In support of this, the corresponding PKA-phosphorylation site on SIK1 (Ser577), also exists on other members of the SNF/AMPK-kinase family, including SIK2 (Ser587) (Screaton et

al., 2004) and AMPKα (Ser485) (Hurley et al., 2006). Both SIK2 and AMPK activities can be inhibited in a cAMP-dependent manner (Hurley et al., 2006; Screaton et al., 2004).

Using the PhosTag gel we show that overexpressing SIK1 causes the TORC2 band pattern at 6 h of NE stimulation to be similar to that of control. Considering that it is likely that kinases other than SIK1 are involved in phosphorylating TORC2 at basal conditions, this suggests that SIK1 can phosphorylate the same sites on TORC2 as the other kinases. In support of this idea, it has been shown that the Ser171 residue on TORC2 can be phosphorylated by SIK1, SIK2 and AMPK (Dentin et al., 2007; Koo et al., 2005), Ser275 is phosphorylated by SIK1 (Uebi et al., 2010) and MARK2 (Jansson et al., 2008) and Ser307 primarily by SIK1, but may also be targeted by MARK2 and MARK4 (Uebi et al., 2010). Indeed, phosphorylation of distinct sites on TORC2 by different kinases may lead to distinct effects on TORC2, which can include cytoplasmic sequestering, protein degradation (Dentin et al., 2007; Screaton et al., 2004) and potentially protection from degradation. Therefore, targeting of individual phosphorylation site on TORC2 appears to be an important mean by which this coactivator is regulated. Understanding the contribution of specific phosphorylation sites of TORC2 to its function likely will enhance our understanding of this coactivator.

Our study challenges the current idea that TORC2 cellular distribution can be regulated by the sole action of SIK1 (Katoh et al., 2004b; Koo et al., 2005). Since TORC2 is phosphorylated under basal conditions after *Sik1*

knockdown, the effects of other kinases, such as SIK2, on TORC2 have to be taken into consideration. The key mechanism by which SIK1 is believed to repress CREB-driven gene expression is by phosphorylation-dependent nuclear export of TORC2 (Katoh et al., 2004b; Koo et al., 2005). However, in the present work, we show that this may not be the case in rat pinealocytes. This is based on our results showing that endogenous SIK1 has no major role in regulating NE-stimulated nuclear levels of TORC2. It is possible that the function of SIK1 is mediated through a different coactivator, such as TORC1. Alternatively, SIK1 may also function by regulating the coactivator function of both TORC isoforms, and not by causing the nuclear export of TORC, but by reducing the cooperative interaction between CBP and CREB (Ravnskjaer et al., 2007).

4.4 Future Directions

1) The role of other phosphorylation sites on TORC2

As already described, previous studies identified three other Ser residues on TORC2 (Ser171, Ser275 and Ser307) that can be phosphorylated (Jansson et al., 2008; Koo et al., 2005; Uebi et al., 2010). Dephosphorylation of different TORC2 residue(s) may have a distinct effect on TORC2. This could account for some of our findings. Our results show that cAMP-mediated dephosphorylation of TORC2 leads to nuclear translocation whereas Ca^{2+}-mediated dephosphorylation does not. Also, western blot analysis with PhosTag gel reveals a different TORC2 band-pattern after dBcAMP treatment compared to treatment with KCl. This suggests that the phosphorylation status also differs. Studies comparing different

TORC2 overexpression constructs, wild-type and mutant (selectively abolished phosphorylation sites), could give insight about the role of the specific Ser residue(s) regulating the cellular distribution and the protein level of TORC2. This could identify the specific residue(s) that need to be dephosphorylated for nuclear tranlocation allowing TORC2 to function as a coactivator. In addition, this approach may also reveal what site needs to be phosphorylated for 14-3-3 interaction, and/or regulating the stability of TORC2.

2) The role of other TORC family members in regulating *Aa-nat* expression

Our finding suggests the existence of other signalling pathways by which SIK1 can repress CREB-driven *Aa-nat* transcription. This is based on our observation that the inhibitory effect of overexpressed SIK1 on NE-stimulated *Aa-nat* expression is more potent than the effect mediated by *Torc2* knockdown. Whereas the effects of manipulating SIK1 on *Aa-nat* were translated to the AA-NAT protein level the effects of *Torc2* knockdown were not. Other pathways that need to be considered include TORC1, an isoform of TORC2, that can be also regulated by SIK1 (Altarejos et al., 2008; Li et al., 2009). Knockdown studies of TORC1 in combination with TORC2 may provide additional insight on the effect of SIK1 on *Aa-nat* transcription.

3) Role of other SNF/AMPK family members in regulating TORC2

Our results suggest that endogenous SIK1 is not the sole kinase involved in phosphorylating and regulating the cellular distribution of TORC2. Under basal

conditions, TORC2 is phosphorylated and located in the cytoplasm even after *Sik1* knockdown. As already described, TORC2 has been found to be phosphorylated by other members of the SNF/AMPK kinase family, such as SIK2 (Screaton et al., 2004). Knockdown of other SNF/AMPK kinase family members with adenoviral constructs may identify the kinase(s) that control the shutteling of TORC2 between the cytoplasm and the nucleus.

4.5 Summary

In the rat pineal gland, the melatonin-rhythm generating enzyme, AA-NAT, is induced by NE stimulation. *Aa-nat* transcription is triggered by NE-dependent activation of the β-adrenoreceptor/cAMP pathway which activates PKA (Roseboom and Klein, 1995). Although activation of CREB-target gene expression is accepted to be via PKA-mediated phosphorylation of KID within CREB, reports using other tissues show that the transcriptional activity of CREB can also be regulated by the SIK1/TORC2 pathway acting through the CREB bZIP domain (Doi et al., 2002). The recognition of SIK1/TORC2 pathway in regulating CREB activity (Doi et al., 2002) prompted our investigation of this pathway in the regulation of *Aa-nat* induction.

The main findings from the present studies are:

1) Marked nocturnal induction of *Sik1* transcription in the rat pineal gland, which precedes the induction of *Aa-nat*.

2) *Sik1* induction is mainly driven by a β-adrenoreceptor/cAMP-dependent mechanism with a minor contribution from the α_1-adrenoreceptor/Ca^{2+}-pathway.
3) Endogenous SIK1 represses the duration of NE-stimulated *Aa-nat* transcription.
4) Removal of the PKA phosphorylation-site on this kinase increases the SIK1 inhibitory effect on *Aa-nat* transcription.
5) Although there is no change in the levels of *Torc2* mRNA, TORC2 protein is dephosphorylated in the rat pineal gland with the onset of darkness.
6) TORC2 protein is dephosphorylated within 15 min of NE stimulation in the rat pinealocyte via the β-adrenoreceptor/cAMP pathway.
7) PP2A is involved in the NE-stimulated TORC2 dephosphorylation.
8) TORC2 dephosphorylation leads to the nuclear translocation of this coactivator.
9) Intracellular Ca^{2+}- elevating agents also induce dephosphorylation but not nuclear translocation of TORC2.
10) Overexpression of TORC2 enhances NE-stimulated *Aa-nat* expression while knockdown of TORC2 only has a small inhibitory effect on *Aa-nat* mRNA levels.
11) Other genes that are regulated by SIK1 and TORC2 in a similar manner include *Icer*, *Dio2* and *Mkp-1*.

12) Knockdown of the endogenous *Sik1* does not change the phosphorylation status or the cellular distribution of TORC2 under basal or stimulated conditions.

In conclusion, the β-adrenoreceptor/cAMP signalling mechanism appears to be the dominant pathway in stimulating *Sik1* transcription and nuclear translocation of TORC2. However, *Sik1* knockdown enhances NE-stimulated AA-NAT protein levels without changing the nuclear TORC2 levels. The effect of SIK1 on *Aa-nat* cannot be explained by regulating the cellular distribution of TORC2. This study also shows that the phosphorylation status of TORC2 may not reflect the activation of TORC2 since Ca^{2+}-mediated dephosphorylation of TORC2 does not cause its nuclear translocation. Finally, our study challenges the current idea that TORC2 cellular distribution can be regulated by the sole action of SIK1 (Katoh et al., 2004b; Koo et al., 2005).

References

Ali, S.A., and A. Steinkasserer. 1995. PCR-ligation-PCR mutagenesis: a protocol for creating gene fusions and mutations. *Biotechniques*. 18:746-750.

Altarejos, J.Y., N. Goebel, M.D. Conkright, H. Inoue, J. Xie, C.M. Arias, P.E. Sawchenko, and M. Montminy. 2008. The Creb1 coactivator Crtc1 is required for energy balance and fertility. *Nat Med*. 14:1112-1117.

Altarejos, J.Y., and M. Montminy. 2011. CREB and the CRTC co-activators: sensors for hormonal and metabolic signals. *Nat Rev Mol Cell Biol*. 12:141-151.

Arendt, J. 1998. Melatonin and the pineal gland: influence on mammalian seasonal and circadian physiology. *Rev Reprod*. 3:13-22.

Axelrod, J. 1974. The pineal gland: a neurochemical transducer. *Science*. 184:1341-1348.

Bailey, M.J., S.L. Coon, D.A. Carter, A. Humphries, J.S. Kim, Q. Shi, P. Gaildrat, F. Morin, S. Ganguly, J.B. Hogenesch, J.L. Weller, M.F. Rath, M. Moller, R. Baler, D. Sugden, Z.G. Rangel, P.J. Munson, and D.C. Klein. 2009. Night/day changes in pineal expression of >600 genes: central role of adrenergic/cAMP signaling. *J Biol Chem*. 284:7606-7622.

Baler, R., S. Covington, and D.C. Klein. 1997. The rat arylalkylamine N-acetyltransferase gene promoter. cAMP activation via a cAMP-responsive element-CCAAT complex. *J Biol Chem*. 272:6979-6985.

Baler, R., and D.C. Klein. 1995. Circadian expression of transcription factor Fra-2 in the rat pineal gland. *J Biol Chem*. 270:27319-27325.

Bannister, A.J., and T. Kouzarides. 1996. The CBP co-activator is a histone acetyltransferase. *Nature*. 384:641-643.

Berdeaux, R., N. Goebel, L. Banaszynski, H. Takemori, T. Wandless, G.D. Shelton, and M. Montminy. 2007. SIK1 is a class II HDAC kinase that promotes survival of skeletal myocytes. *Nat Med*. 13:597-603.

Bittinger, M.A., E. McWhinnie, J. Meltzer, V. Iourgenko, B. Latario, X. Liu, C.H. Chen, C. Song, D. Garza, and M. Labow. 2004. Activation of cAMP response element-mediated gene expression by regulated nuclear transport of TORC proteins. *Curr Biol*. 14:2156-2161.

Bourtchuladze, R., B. Frenguelli, J. Blendy, D. Cioffi, G. Schutz, and A.J. Silva. 1994. Deficient long-term memory in mice with a targeted mutation of the cAMP-responsive element-binding protein. *Cell*. 79:59-68.

Braun, A.P., and H. Schulman. 1995. The multifunctional calcium/calmodulin-dependent protein kinase: from form to function. *Annu Rev Physiol*. 57:417-445.

Carlezon, W.A., Jr., R.S. Duman, and E.J. Nestler. 2005. The many faces of CREB. *Trends Neurosci*. 28:436-445.

Chik, C.L., T.G. Arnason, W.G. Dukewich, D.M. Price, A. Ranger, and A.K. Ho. 2007a. Histone H3 phosphorylation in the rat pineal gland: adrenergic regulation and diurnal variation. *Endocrinology*. 148:1465-1472.

Chik, C.L., and A.K. Ho. 1989. Multiple receptor regulation of cyclic nucleotides in rat pinealocytes. *Prog Biophys Mol Biol*. 53:197-203.

Chik, C.L., and A.K. Ho. 1995. Pituitary adenylate cyclase-activating polypeptide: control of rat pineal cyclic AMP and melatonin but not cyclic GMP. *J Neurochem*. 64:2111-2117.

Chik, C.L., A.K. Ho, and D.C. Klein. 1988. Alpha 1-adrenergic potentiation of vasoactive intestinal peptide stimulation of rat pinealocyte adenosine 3',5'-monophosphate and guanosine 3',5'-monophosphate: evidence for a role of calcium and protein kinase-C. *Endocrinology*. 122:702-708.

Chik, C.L., Q.Y. Liu, B. Li, E. Karpinski, and A.K. Ho. 1995. cGMP inhibits L-type Ca2+ channel currents through protein phosphorylation in rat pinealocytes. *J Neurosci*. 15:3104-3109.

Chik, C.L., M.T. Wloka, D.M. Price, and A.K. Ho. 2007b. The role of repressor proteins in the adrenergic induction of type II iodothyronine deiodinase in rat pinealocytes. *Endocrinology*. 148:3523-3531.

Chin, D., and A.R. Means. 2000. Calmodulin: a prototypical calcium sensor. *Trends Cell Biol*. 10:322-328.

Choi, S., W. Kim, and J. Chung. 2011. Drosophila salt-inducible kinase (SIK) regulates starvation resistance through cAMP-response element-binding protein (CREB)-regulated transcription coactivator (CRTC). *J Biol Chem*. 286:2658-2664.

Chrivia, J.C., R.P. Kwok, N. Lamb, M. Hagiwara, M.R. Montminy, and R.H. Goodman. 1993. Phosphorylated CREB binds specifically to the nuclear protein CBP. *Nature*. 365:855-859.

Conkright, M.D., G. Canettieri, R. Screaton, E. Guzman, L. Miraglia, J.B. Hogenesch, and M. Montminy. 2003. TORCs: transducers of regulated CREB activity. *Mol Cell*. 12:413-423.

Craig, J.C., M.A. Schumacher, S.E. Mansoor, D.L. Farrens, R.G. Brennan, and R.H. Goodman. 2001. Consensus and variant cAMP-regulated enhancers have distinct CREB-binding properties. *J Biol Chem*. 276:11719-11728.

Dentin, R., Y. Liu, S.H. Koo, S. Hedrick, T. Vargas, J. Heredia, J. Yates, 3rd, and M. Montminy. 2007. Insulin modulates gluconeogenesis by inhibition of the coactivator TORC2. *Nature*. 449:366-369.

Doi, J., H. Takemori, X.Z. Lin, N. Horike, Y. Katoh, and M. Okamoto. 2002. Salt-inducible kinase represses cAMP-dependent protein kinase-mediated activation of human cholesterol side chain cleavage cytochrome P450 promoter through the CREB basic leucine zipper domain. *J Biol Chem*. 277:15629-15637.

Ebling, F.J. 1996. The role of glutamate in the photic regulation of the suprachiasmatic nucleus. *Prog Neurobiol*. 50:109-132.

Feldman, J.D., L. Vician, M. Crispino, W. Hoe, M. Baudry, and H.R. Herschman. 2000. The salt-inducible kinase, SIK, is induced by depolarization in brain. *J Neurochem*. 74:2227-2238.

Felinski, E.A., J. Kim, J. Lu, and P.G. Quinn. 2001. Recruitment of an RNA polymerase II complex is mediated by the constitutive activation domain in CREB, independently of CREB phosphorylation. *Mol Cell Biol*. 21:1001-1010.

Ferreri, K., G. Gill, and M. Montminy. 1994. The cAMP-regulated transcription factor CREB interacts with a component of the TFIID complex. *Proc Natl Acad Sci U S A*. 91:1210-1213.

Feschenko, M.S., E. Stevenson, A.C. Nairn, and K.J. Sweadner. 2002. A novel cAMP-stimulated pathway in protein phosphatase 2A activation. *J Pharmacol Exp Ther*. 302:111-118.

Figurov, A., H. Boddeke, and D. Muller. 1993. Enhancement of AMPA-mediated synaptic transmission by the protein phosphatase inhibitor calyculin A in rat hippocampal slices. *Eur J Neurosci*. 5:1035-1041.

Fimia, G.M., D. De Cesare, and P. Sassone-Corsi. 1999. CBP-independent activation of CREM and CREB by the LIM-only protein ACT. *Nature*. 398:165-169.

Fink, J.S., M. Verhave, S. Kasper, T. Tsukada, G. Mandel, and R.H. Goodman. 1988. The CGTCA sequence motif is essential for biological activity of the vasoactive intestinal peptide gene cAMP-regulated enhancer. *Proc Natl Acad Sci U S A*. 85:6662-6666.

Fisher, C.L., and G.K. Pei. 1997. Modification of a PCR-based site-directed mutagenesis method. *Biotechniques*. 23:570-571, 574.

Foulkes, N.S., J. Borjigin, S.H. Snyder, and P. Sassone-Corsi. 1996. Transcriptional control of circadian hormone synthesis via the CREM feedback loop. *Proc Natl Acad Sci U S A*. 93:14140-14145.

Foulkes, N.S., D. Whitmore, and P. Sassone-Corsi. 1997. Rhythmic transcription: the molecular basis of circadian melatonin synthesis. *Biol Cell*. 89:487-494.

Francis, S.H., and J.D. Corbin. 1999. Cyclic nucleotide-dependent protein kinases: intracellular receptors for cAMP and cGMP action. *Crit Rev Clin Lab Sci*. 36:275-328.

Ganguly, S., J.A. Gastel, J.L. Weller, C. Schwartz, H. Jaffe, M.A. Namboodiri, S.L. Coon, A.B. Hickman, M. Rollag, T. Obsil, P. Beauverger, G. Ferry, J.A. Boutin, and D.C. Klein. 2001. Role of a pineal cAMP-operated arylalkylamine N-acetyltransferase/14-3-3-binding switch in melatonin synthesis. *Proc Natl Acad Sci U S A*. 98:8083-8088.

Ganguly, S., S.L. Coon, and D.C. Klein. 2002. Control of melatonin synthesis in the mammalian pineal gland: the critical role of serotonin acetylation. *Cell Tissue Res*. 309:127-137.

Gastel, J.A., P.H. Roseboom, P.A. Rinaldi, J.L. Weller, and D.C. Klein. 1998. Melatonin production: proteasomal proteolysis in serotonin N-acetyltransferase regulation. *Science*. 279:1358-1360.

Gaston, K., and P.S. Jayaraman. 2003. Transcriptional repression in eukaryotes: repressors and repression mechanisms. *Cell Mol Life Sci*. 60:721-741.

Glauser, D.A., T. Brun, B.R. Gauthier, and W. Schlegel. 2007. Transcriptional response of pancreatic beta cells to metabolic stimulation: large scale identification of immediate-early and secondary response genes. *BMC Mol Biol*. 8:54.

Gilman, A.G. 1987. G proteins: transducers of receptor-generated signals. *Annu Rev Biochem*. 56:615-649.

Gonzalez, G.A., and M.R. Montminy. 1989. Cyclic AMP stimulates somatostatin gene transcription by phosphorylation of CREB at serine 133. *Cell*. 59:675-680.

Groblewski, G.E., A.C. Wagner, and J.A. Williams. 1994. Cyclosporin A inhibits Ca2+/calmodulin-dependent protein phosphatase and secretion in pancreatic acinar cells. *J Biol Chem*. 269:15111-15117.

Grunstein, M. 1997. Histone acetylation in chromatin structure and transcription. *Nature*. 389:349-352.

Gubina, E., X. Luo, E. Kwon, K. Sakamoto, Y.F. Shi, and R.A. Mufson. 2001. betac cytokine receptor-induced stimulation of cAMP response element binding protein phosphorylation requires protein kinase C in myeloid cells: a novel cytokine signal transduction cascade. *J Immunol*. 167:4303-4310.

Hardie, D.G. 2004. The AMP-activated protein kinase pathway--new players upstream and downstream. *J Cell Sci*. 117:5479-5487.

Hardie, D.G. 2007. AMP-activated/SNF1 protein kinases: conserved guardians of cellular energy. *Nat Rev Mol Cell Biol*. 8:774-785.

Haystead, T.A., A.T. Sim, D. Carling, R.C. Honnor, Y. Tsukitani, P. Cohen, and D.G. Hardie. 1989. Effects of the tumour promoter okadaic acid on intracellular protein phosphorylation and metabolism. *Nature*. 337:78-81.

Herzig, S., F. Long, U.S. Jhala, S. Hedrick, R. Quinn, A. Bauer, D. Rudolph, G. Schutz, C. Yoon, P. Puigserver, B. Spiegelman, and M. Montminy. 2001. CREB regulates hepatic gluconeogenesis through the coactivator PGC-1. *Nature*. 413:179-183.

Ho, A.K., J. Cheng, and M. Girard. 1992. Differential effects of intracellular calcium elevating agents on adrenergic-stimulated cyclic nucleotide and melatonin synthesis in rat pinealocytes. *Can J Physiol Pharmacol*. 70:1254-1260.

Ho, A.K., and C.L. Chik. 2000. Adrenergic regulation of mitogen-activated protein kinase in rat pinealocytes: opposing effects of protein kinase A and protein kinase G. *Endocrinology*. 141:4496-4502.

Ho, A.K., C.L. Chik, and D.C. Klein. 1987a. Protein kinase C is involved in adrenergic stimulation of pineal cGMP accumulation. *J Biol Chem*. 262:10059-10064.

Ho, A.K., C.L. Chik, and D.C. Klein. 1987b. Transmembrane receptor cross-talk: concurrent VIP and alpha 1-adrenergic activation rapidly elevates pinealocyte cGMP greater than 100-fold. *Biochem Biophys Res Commun*. 146:1478-1484.

Ho, A.K., C.L. Chik, and D.C. Klein. 1988a. Permissive role of calcium in alpha 1-adrenergic stimulation of pineal phosphatidylinositol phosphodiesterase (phospholipase C) activity. *J Pineal Res*. 5:553-564.

Ho, A.K., K. Hashimoto, and C.L. Chik. 1999. 3',5'-cyclic guanosine monophosphate activates mitogen-activated protein kinase in rat pinealocytes. *J Neurochem*. 73:598-604.

Ho, A.K., and D.C. Klein. 1987. Phosphatidylinositol phosphodiesterase (phospholipase C) activity in the pineal gland: characterization and photoneural regulation. *J Neurochem*. 48:1033-1038.

Ho, A.K., D.M. Price, W.G. Dukewich, N. Steinberg, T.G. Arnason, and C.L. Chik. 2007a. Acetylation of histone H3 and adrenergic-regulated gene transcription in rat pinealocytes. *Endocrinology*. 148:4592-4600.

Ho, A.K., D.L. Terriff, D.M. Price, M.T. Wloka, and C.L. Chik. 2007b. The role of inducible repressor proteins in the adrenergic induction of arylalkylamine-N-acetyltransferase and mitogen-activated protein kinase phosphatase-1 in rat pinealocytes. *Endocrinology*. 148:743-751.

Ho, A.K., T.P. Thomas, C.L. Chik, W.B. Anderson, and D.C. Klein. 1988b. Protein kinase C: subcellular redistribution by increased Ca2+ influx. Evidence that Ca2+-dependent subcellular redistribution of protein kinase C is involved in potentiation of beta-adrenergic stimulation of pineal cAMP and cGMP by K+ and A23187. *J Biol Chem*. 263:9292-9297.

Ho, A.K., I. Young, and C.L. Chik. 1991. Evidence for a role of calmodulin in regulation of pinealocyte cyclic nucleotides. *Biochem Pharmacol*. 41:897-903.

Ho, A.K., and C.L. Chik. 2010. Modulation of Aanat gene transcription in the rat pineal gland. *J Neurochem*. 112:321-331.

Horike, N., H. Takemori, Y. Katoh, J. Doi, L. Min, T. Asano, X.J. Sun, H. Yamamoto, S. Kasayama, M. Muraoka, Y. Nonaka, and M. Okamoto. 2003. Adipose-specific expression, phosphorylation of Ser794 in insulin receptor substrate-1, and activation in diabetic animals of salt-inducible kinase-2. *J Biol Chem*. 278:18440-18447.

Hurley, J.H. 1998. The adenylyl and guanylyl cyclase superfamily. *Curr Opin Struct Biol*. 8:770-777.

Hurley, R.L., L.K. Barre, S.D. Wood, K.A. Anderson, B.E. Kemp, A.R. Means, and L.A. Witters. 2006. Regulation of AMP-activated protein kinase by multisite phosphorylation in response to agents that elevate cellular cAMP. *J Biol Chem*. 281:36662-36672.

Iguchi, H., K.I. Kato, and H. Ibayashi. 1982. Melatonin serum levels and metabolic clearance rate in patients with liver cirrhosis. *J Clin Endocrinol Metab*. 54:1025-1027.

Illnerova, H., M. Backstrom, J. Saaf, L. Wetterberg, and B. Vangbo. 1978. Melatonin in rat pineal gland and serum; rapid parallel decline after light exposure at night. *Neurosci Lett*. 9:189-193.

Inoue, H., N. Watanabe, Y. Higashi, and Y. Fujii-Kuriyama. 1991. Structures of regulatory regions in the human cytochrome P-450scc (desmolase) gene. *Eur J Biochem*. 195:563-569.

Iourgenko, V., W. Zhang, C. Mickanin, I. Daly, C. Jiang, J.M. Hexham, A.P. Orth, L. Miraglia, J. Meltzer, D. Garza, G.W. Chirn, E. McWhinnie, D. Cohen, J. Skelton, R. Terry, Y. Yu, D. Bodian, F.P. Buxton, J. Zhu, C. Song, and M.A. Labow. 2003. Identification of a family of cAMP response element-binding protein coactivators by genome-scale functional analysis in mammalian cells. *Proc Natl Acad Sci U S A*. 100:12147-12152.

Jansson, D., A.C. Ng, A. Fu, C. Depatie, M. Al Azzabi, and R.A. Screaton. 2008. Glucose controls CREB activity in islet cells via regulated phosphorylation of TORC2. *Proc Natl Acad Sci U S A*. 105:10161-10166.

Kaang, B.K., E.R. Kandel, and S.G. Grant. 1993. Activation of cAMP-responsive genes by stimuli that produce long-term facilitation in Aplysia sensory neurons. *Neuron*. 10:427-435.

Kalsbeek, A., R.A. Cutrera, J.J. Van Heerikhuize, J. Van Der Vliet, and R.M. Buijs. 1999. GABA release from suprachiasmatic nucleus terminals is necessary for the light-induced inhibition of nocturnal melatonin release in the rat. *Neuroscience*. 91:453-461.

Kalsbeek, A., M.L. Garidou, I.F. Palm, J. Van Der Vliet, V. Simonneaux, P. Pevet, and R.M. Buijs. 2000. Melatonin sees the light: blocking GABA-ergic transmission in the paraventricular nucleus induces daytime secretion of melatonin. *Eur J Neurosci*. 12:3146-3154.

Kanyo, R., N. Amyotte, J. McTague, C.L. Chik, and A.K. Ho. 2011. Adrenergic regulation of the distribution of transducer of regulated cAMP-response element-binding protein (TORC2) in rat pinealocytes. *Endocrinology*. 152:3440-3450.

Kanyo, R., D.M. Price, C.L. Chik, and A.K. Ho. 2009. Salt-inducible kinase 1 in the rat pinealocyte: adrenergic regulation and role in arylalkylamine N-acetyltransferase gene transcription. *Endocrinology*. 150:4221-4230.

Katoh, Y., H. Takemori, N. Horike, J. Doi, M. Muraoka, L. Min, and M. Okamoto. 2004a. Salt-inducible kinase (SIK) isoforms: their involvement in steroidogenesis and adipogenesis. *Mol Cell Endocrinol*. 217:109-112.

Katoh, Y., H. Takemori, X.Z. Lin, M. Tamura, M. Muraoka, T. Satoh, Y. Tsuchiya, L. Min, J. Doi, A. Miyauchi, L.A. Witters, H. Nakamura, and M. Okamoto. 2006. Silencing the constitutive active transcription factor CREB by the LKB1-SIK signaling cascade. *FEBS J*. 273:2730-2748.

Katoh, Y., H. Takemori, L. Min, M. Muraoka, J. Doi, N. Horike, and M. Okamoto. 2004b. Salt-inducible kinase-1 represses cAMP response element-binding protein activity both in the nucleus and in the cytoplasm. *Eur J Biochem*. 271:4307-4319.

Kim, J.S., M.J. Bailey, A.K. Ho, M. Moller, P. Gaildrat, and D.C. Klein. 2007. Daily rhythm in pineal phosphodiesterase (PDE) activity reflects adrenergic/3',5'-cyclic adenosine 5'-monophosphate induction of the PDE4B2 variant. *Endocrinology*. 148:1475-1485.

Kinoshita, E., E. Kinoshita-Kikuta, and T. Koike. 2009. Separation and detection of large phosphoproteins using Phos-tag SDS-PAGE. *Nat Protoc*. 4:1513-1521.

Klein, D.C. 1985. Photoneural regulation of the mammalian pineal gland. *Ciba Found Symp*. 117:38-56.

Klein, D.C., G.R. Berg, and J. Weller. 1970a. Melatonin synthesis: adenosine 3',5'-monophosphate and norepinephrine stimulate N-acetyltransferase. *Science*. 168:979-980.

Klein, D.C., G.R. Berg, J. Weller, and W. Glinsmann. 1970b. Pineal gland: dibutyryl cyclic adenosine monophosphate stimulation of labeled melatonin production. *Science*. 167:1738-1740.

Klein, D.C., R. Smoot, J.L. Weller, S. Higa, S.P. Markey, G.J. Creed, and D.M. Jacobowitz. 1983. Lesions of the paraventricular nucleus area of the hypothalamus disrupt the suprachiasmatic leads to spinal cord circuit in the melatonin rhythm generating system. *Brain Res Bull*. 10:647-652.

Klein, D.C., and J.L. Weller. 1970. Indole metabolism in the pineal gland: a circadian rhythm in N-acetyltransferase. *Science*. 169:1093-1095.

Koo, S.H., L. Flechner, L. Qi, X. Zhang, R.A. Screaton, S. Jeffries, S. Hedrick, W. Xu, F. Boussouar, P. Brindle, H. Takemori, and M. Montminy. 2005. The CREB coactivator TORC2 is a key regulator of fasting glucose metabolism. *Nature*. 437:1109-1111.

Korf, H.W., C. Schomerus, and J.H. Stehle. 1998. The pineal organ, its hormone melatonin, and the photoneuroendocrine system. *Adv Anat Embryol Cell Biol*. 146:1-100.

Kopin, I.J., J. Axelrod, and E. Gordon. 1961. The metabolic fate of H3-epinephrine and C14-metanephrine in the rat. *J Biol Chem*. 236:2109-2113.

Kwok, R.P., J.R. Lundblad, J.C. Chrivia, J.P. Richards, H.P. Bachinger, R.G. Brennan, S.G. Roberts, M.R. Green, and R.H. Goodman. 1994. Nuclear protein CBP is a coactivator for the transcription factor CREB. *Nature*. 370:223-226.

Kyriakis, J.M., and J. Avruch. 2001. Mammalian mitogen-activated protein kinase signal transduction pathways activated by stress and inflammation. *Physiol Rev*. 81:807-869.

Laemmli, U.K. 1970. Cleavage of structural proteins during the assembly of the head of bacteriophage T4. *Nature*. 227:680-685.

Lee, S.Y., B.H. Choi, E.M. Hur, J.H. Lee, S.J. Lee, C.O. Lee, and K.T. Kim. 2006. Norepinephrine activates store-operated Ca2+ entry coupled to large-conductance Ca2+-activated K+ channels in rat pinealocytes. *Am J Physiol Cell Physiol*. 290:C1060-1066.

Lee, T.I., and R.A. Young. 2000. Transcription of eukaryotic protein-coding genes. *Annu Rev Genet*. 34:77-137.

Lerner, A.B., J.D. Case, and Y. Takahashi. 1960. Isolation of melatonin and 5-methoxyindole-3-acetic acid from bovine pineal glands. *J Biol Chem*. 235:1992-1997.

Letz, B., C. Schomerus, E. Maronde, H.W. Korf, and C. Korbmacher. 1997. Stimulation of a nicotinic ACh receptor causes depolarization and activation of L-type Ca2+ channels in rat pinealocytes. *J Physiol*. 499 (Pt 2):329-340.

Li, S., C. Zhang, H. Takemori, Y. Zhou, and Z.Q. Xiong. 2009. TORC1 regulates activity-dependent CREB-target gene transcription and dendritic growth of developing cortical neurons. *J Neurosci*. 29:2334-2343.

Lin, X., H. Takemori, Y. Katoh, J. Doi, N. Horike, A. Makino, Y. Nonaka, and M. Okamoto. 2001. Salt-inducible kinase is involved in the ACTH/cAMP-

dependent protein kinase signaling in Y1 mouse adrenocortical tumor cells. *Mol Endocrinol*. 15:1264-1276.

Link, W.A., F. Ledo, B. Torres, M. Palczewska, T.M. Madsen, M. Savignac, J.P. Albar, B. Mellstrom, and J.R. Naranjo. 2004. Day-night changes in downstream regulatory element antagonist modulator/potassium channel interacting protein activity contribute to circadian gene expression in pineal gland. *J Neurosci*. 24:5346-5355.

Liu, Y., R. Dentin, D. Chen, S. Hedrick, K. Ravnskjaer, S. Schenk, J. Milne, D.J. Meyers, P. Cole, J. Yates, 3rd, J. Olefsky, L. Guarente, and M. Montminy. 2008. A fasting inducible switch modulates gluconeogenesis via activator/coactivator exchange. *Nature*. 456:269-273.

Longin, S., J. Jordens, E. Martens, I. Stevens, V. Janssens, E. Rondelez, I. De Baere, R. Derua, E. Waelkens, J. Goris, and C. Van Hoof. 2004. An inactive protein phosphatase 2A population is associated with methylesterase and can be re-activated by the phosphotyrosyl phosphatase activator. *Biochem J*. 380:111-119.

MacKintosh, C., and S. Klumpp. 1990. Tautomycin from the bacterium Streptomyces verticillatus. Another potent and specific inhibitor of protein phosphatases 1 and 2A. *FEBS Lett*. 277:137-140.

Mair, W., I. Morantte, A.P. Rodrigues, G. Manning, M. Montminy, R.J. Shaw, and A. Dillin. 2011. Lifespan extension induced by AMPK and calcineurin is mediated by CRTC-1 and CREB. *Nature*. 470:404-408.

Man, J.R., S. Rustaeus, D.M. Price, C.L. Chik, and A.K. Ho. 2004. Inhibition of p38 mitogen-activated protein kinase enhances adrenergic-stimulated arylalkylamine N-acetyltransferase activity in rat pinealocytes. *Endocrinology*. 145:1167-1174.

Manna, P.R., M.T. Dyson, D.W. Eubank, B.J. Clark, E. Lalli, P. Sassone-Corsi, A.J. Zeleznik, and D.M. Stocco. 2002. Regulation of steroidogenesis and the steroidogenic acute regulatory protein by a member of the cAMP response-element binding protein family. *Mol Endocrinol*. 16:184-199.

Maronde, E., M. Pfeffer, J. Olcese, C.A. Molina, F. Schlotter, F. Dehghani, H.W. Korf, and J.H. Stehle. 1999. Transcription factors in neuroendocrine regulation: rhythmic changes in pCREB and ICER levels frame melatonin synthesis. *J Neurosci*. 19:3326-3336.

Maronde, E., and J.H. Stehle. 2007. The mammalian pineal gland: known facts, unknown facets. *Trends Endocrinol Metab*. 18:142-149.

Martinez-Balbas, M.A., A.J. Bannister, K. Martin, P. Haus-Seuffert, M. Meisterernst, and T. Kouzarides. 1998. The acetyltransferase activity of CBP stimulates transcription. *EMBO J*. 17:2886-2893.

Mayr, B., and M. Montminy. 2001. Transcriptional regulation by the phosphorylation-dependent factor CREB. *Nat Rev Mol Cell Biol*. 2:599-609.

McTague, J., N. Amyotte, R. Kanyo, M. Ferguson, C.L. Chik, and A.K. Ho. 2012. Different Signaling Mechanisms Are Involved in the Norepinephrine-Stimulated TORC1 and TORC2 Nuclear Translocation in Rat Pinealocytes. *Endocrinology*. 153:3839-49.

Montminy, M.R., K.A. Sevarino, J.A. Wagner, G. Mandel, and R.H. Goodman. 1986. Identification of a cyclic-AMP-responsive element within the rat somatostatin gene. *Proc Natl Acad Sci U S A*. 83:6682-6686.

Moore, R.Y., and D.C. Klein. 1974. Visual pathways and the central neural control of a circadian rhythm in pineal serotonin N-acetyltransferase activity. *Brain Res*. 71:17-33.

Murakami, N., N. Sakai, K. Nei, S. Matsuyama, N. Saito, and C. Tanaka. 1994. Potassium and calcium channel involvement in induction of long-lasting synaptic enhancement by calyculin A, a protein phosphatase inhibitor, in rat hippocampal CA1 region. *Neurosci Lett*. 176:181-184.

Nishizuka, Y. 1995. Protein kinase C and lipid signaling for sustained cellular responses. *FASEB J*. 9:484-496.

Nomura, M., J.T. Stull, K.E. Kamm, and M.C. Mumby. 1992. Site-specific dephosphorylation of smooth muscle myosin light chain kinase by protein phosphatases 1 and 2A. *Biochemistry*. 31:11915-11920.

Ogris, E., X. Du, K.C. Nelson, E.K. Mak, X.X. Yu, W.S. Lane, and D.C. Pallas. 1999. A protein phosphatase methylesterase (PME-1) is one of several novel proteins stably associating with two inactive mutants of protein phosphatase 2A. *J Biol Chem*. 274:14382-14391.

Ogryzko, V.V., R.L. Schiltz, V. Russanova, B.H. Howard, and Y. Nakatani. 1996. The transcriptional coactivators p300 and CBP are histone acetyltransferases. *Cell*. 87:953-959.

Okamoto, M., H. Takemori, and Y. Katoh. 2004. Salt-inducible kinase in steroidogenesis and adipogenesis. *Trends Endocrinol Metab*. 15:21-26.

Oliver, C.J., and S. Shenolikar. 1998. Physiologic importance of protein phosphatase inhibitors. *Front Biosci*. 3:D961-972.

Perreau-Lenz, S., A. Kalsbeek, M.L. Garidou, J. Wortel, J. van der Vliet, C. van Heijningen, V. Simonneaux, P. Pevet, and R.M. Buijs. 2003. Suprachiasmatic control of melatonin synthesis in rats: inhibitory and stimulatory mechanisms. *Eur J Neurosci*. 17:221-228.

Perreau-Lenz, S., A. Kalsbeek, P. Pevet, and R.M. Buijs. 2004. Glutamatergic clock output stimulates melatonin synthesis at night. *Eur J Neurosci*. 19:318-324.

Price, D.M., C.L. Chik, and A.K. Ho. 2004a. Norepinephrine induction of mitogen-activated protein kinase phosphatase-1 expression in rat pinealocytes: distinct roles of alpha- and beta-adrenergic receptors. *Endocrinology*. 145:5723-5733.

Price, D.M., C.L. Chik, D. Terriff, J. Weller, A. Humphries, D.A. Carter, D.C. Klein, and A.K. Ho. 2004b. Mitogen-activated protein kinase phosphatase-1 (MKP-1): >100-fold nocturnal and norepinephrine-induced changes in the rat pineal gland. *FEBS Lett*. 577:220-226.

Price, D.M., R. Kanyo, N. Steinberg, C.L. Chik, and A.K. Ho. 2009. Nocturnal activation of aurora C in rat pineal gland: its role in the norepinephrine-induced phosphorylation of histone H3 and gene expression. *Endocrinology*. 150:2334-2341.

Price, D.M., M.T. Wloka, C.L. Chik, and A.K. Ho. 2007. Mitogen-activated protein kinase phosphatase-1 (MKP-1) preferentially dephosphorylates p42/44MAPK but not p38MAPK in rat pinealocytes. *J Neurochem*. 101:1685-1693.

Quinn, P.G., and D.K. Granner. 1990. Cyclic AMP-dependent protein kinase regulates transcription of the phosphoenolpyruvate carboxykinase gene but not binding of nuclear factors to the cyclic AMP regulatory element. *Mol Cell Biol*. 10:3357-3364.

Radhakrishnan, I., G.C. Perez-Alvarado, D. Parker, H.J. Dyson, M.R. Montminy, and P.E. Wright. 1997. Solution structure of the KIX domain of CBP bound to the transactivation domain of CREB: a model for activator:coactivator interactions. *Cell*. 91:741-752.

Ravnskjaer, K., H. Kester, Y. Liu, X. Zhang, D. Lee, J.R. Yates, 3rd, and M. Montminy. 2007. Cooperative interactions between CBP and TORC2 confer selectivity to CREB target gene expression. *EMBO J*. 26:2880-2889.

Rhee, S.G. 2001. Regulation of phosphoinositide-specific phospholipase C. *Annu Rev Biochem*. 70:281-312.

Reppert, S.M., C. Godson, C.D. Mahle, D.R. Weaver, S.A. Slaugenhaupt, and J.F. Gusella. 1995. Molecular characterization of a second melatonin receptor expressed in human retina and brain: the Mel1b melatonin receptor. *Proc Natl Acad Sci U S A*. 92:8734-8738.

Roca, A.L., C. Godson, D.R. Weaver, and S.M. Reppert. 1996. Structure, characterization, and expression of the gene encoding the mouse Mel1a melatonin receptor. *Endocrinology*. 137:3469-3477.

Roseboom, P.H., S.L. Coon, R. Baler, S.K. McCune, J.L. Weller, and D.C. Klein. 1996. Melatonin synthesis: analysis of the more than 150-fold nocturnal increase in serotonin N-acetyltransferase messenger ribonucleic acid in the rat pineal gland. *Endocrinology*. 137:3033-3045.

Roseboom, P.H., and D.C. Klein. 1995. Norepinephrine stimulation of pineal cyclic AMP response element-binding protein phosphorylation: primary role of a beta-adrenergic receptor/cyclic AMP mechanism. *Mol Pharmacol*. 47:439-449.

Rozen, S., and H. Skaletsky. 2000. Primer3 on the WWW for general users and for biologist programmers. *Methods Mol Biol*. 132:365-386.

Saez, J.C., A.P. Moreno, and D.C. Spray. 1994. Norepinephrine induces Ca2+ release from intracellular stores in rat pinealocytes. *J Pineal Res*. 16:57-64.

Saluja, D., M.F. Vassallo, and N. Tanese. 1998. Distinct subdomains of human TAFII130 are required for interactions with glutamine-rich transcriptional activators. *Mol Cell Biol*. 18:5734-5743.

Schomerus, C., E. Laedtke, and H.W. Korf. 1995. Calcium responses of isolated, immunocytochemically identified rat pinealocytes to noradrenergic, cholinergic and vasopressinergic stimulations. *Neurochem Int*. 27:163-175.

Schumacher, M.A., R.H. Goodman, and R.G. Brennan. 2000. The structure of a CREB bZIP.somatostatin CRE complex reveals the basis for selective dimerization and divalent cation-enhanced DNA binding. *J Biol Chem*. 275:35242-35247.

Screaton, R.A., M.D. Conkright, Y. Katoh, J.L. Best, G. Canettieri, S. Jeffries, E. Guzman, S. Niessen, J.R. Yates, 3rd, H. Takemori, M. Okamoto, and M. Montminy. 2004. The CREB coactivator TORC2 functions as a calcium- and cAMP-sensitive coincidence detector. *Cell*. 119:61-74.

Sheng, M., and M.E. Greenberg. 1990. The regulation and function of c-fos and other immediate early genes in the nervous system. *Neuron*. 4:477-485.

Shi, Y. 2009. Serine/threonine phosphatases: mechanism through structure. *Cell*. 139:468-484.

Sjostrom, M., K. Stenstrom, K. Eneling, J. Zwiller, A.I. Katz, H. Takemori, and A.M. Bertorello. 2007. SIK1 is part of a cell sodium-sensing network that regulates active sodium transport through a calcium-dependent process. *Proc Natl Acad Sci U S A*. 104:16922-16927.

Smale, S.T., and J.T. Kadonaga. 2003. The RNA polymerase II core promoter. *Annu Rev Biochem*. 72:449-479.

Smith, M., Z. Burke, A. Humphries, T. Wells, D. Klein, D. Carter, and R. Baler. 2001. Tissue-specific transgenic knockdown of Fos-related antigen 2 (Fra-2) expression mediated by dominant negative Fra-2. *Mol Cell Biol*. 21:3704-3713.

Song, Y., J. Altarejos, M.O. Goodarzi, H. Inoue, X. Guo, R. Berdeaux, J.H. Kim, J. Goode, M. Igata, J.C. Paz, M.F. Hogan, P.K. Singh, N. Goebel, L. Vera, N. Miller, J. Cui, M.R. Jones, Y.D. Chen, K.D. Taylor, W.A. Hsueh, J.I. Rotter, and M. Montminy. 2010. CRTC3 links catecholamine signalling to energy balance. *Nature*. 468:933-939.

Stehle, J.H., N.S. Foulkes, C.A. Molina, V. Simonneaux, P. Pevet, and P. Sassone-Corsi. 1993. Adrenergic signals direct rhythmic expression of transcriptional repressor CREM in the pineal gland. *Nature*. 365:314-320.

Sugden, D., and D.C. Klein. 1987. A cholera toxin substrate regulates cyclic GMP content of rat pinealocytes. *J Biol Chem*. 262:7447-7450.

Sugden, D., J. Vanecek, D.C. Klein, T.P. Thomas, and W.B. Anderson. 1985. Activation of protein kinase C potentiates isoprenaline-induced cyclic AMP accumulation in rat pinealocytes. *Nature*. 314:359-361.

Sugden, L.A., D. Sugden, and D.C. Klein. 1987. Alpha 1-adrenoceptor activation elevates cytosolic calcium in rat pinealocytes by increasing net influx. *J Biol Chem*. 262:741-745.

Sun, P., H. Enslen, P.S. Myung, and R.A. Maurer. 1994. Differential activation of CREB by Ca2+/calmodulin-dependent protein kinases type II and type IV involves phosphorylation of a site that negatively regulates activity. *Genes Dev*. 8:2527-2539.

Takemori, H., J. Kajimura, and M. Okamoto. 2007. TORC-SIK cascade regulates CREB activity through the basic leucine zipper domain. *FEBS J*. 274:3202-3209.

Takemori, H., Y. Katoh, N. Horike, J. Doi, and M. Okamoto. 2002. ACTH-induced nucleocytoplasmic translocation of salt-inducible kinase. Implication in the protein kinase A-activated gene transcription in mouse adrenocortical tumor cells. *J Biol Chem*. 277:42334-42343.

Terriff, D.L., C.L. Chik, D.M. Price, and A.K. Ho. 2005. Proteasomal proteolysis in the adrenergic induction of arylalkylamine-N-acetyltransferase in rat pinealocytes. *Endocrinology*. 146:4795-4803.

Uebi, T., M. Tamura, N. Horike, Y.K. Hashimoto, and H. Takemori. 2010. Phosphorylation of the CREB-specific coactivator TORC2 at Ser(307) regulates its intracellular localization in COS-7 cells and in the mouse liver. *Am J Physiol Endocrinol Metab*. 299:E413-425.

van der Linden, A.M., S. Wiener, Y.J. You, K. Kim, L. Avery, and P. Sengupta. 2008. The EGL-4 PKG acts with KIN-29 salt-inducible kinase and protein kinase A to regulate chemoreceptor gene expression and sensory behaviors in Caenorhabditis elegans. *Genetics*. 180:1475-1491.

Vanecek, J., D. Sugden, J. Weller, and D.C. Klein. 1985. Atypical synergistic alpha 1- and beta-adrenergic regulation of adenosine 3',5'-monophosphate and guanosine 3',5'-monophosphate in rat pinealocytes. *Endocrinology*. 116:2167-2173.

Wagner, B.L., A. Bauer, G. Schutz, and M. Montminy. 2000. Stimulus-specific interaction between activator-coactivator cognates revealed with a novel complex-specific antiserum. *J Biol Chem*. 275:8263-8266.

Wang, B., J. Goode, J. Best, J. Meltzer, P.E. Schilman, J. Chen, D. Garza, J.B. Thomas, and M. Montminy. 2008. The insulin-regulated CREB coactivator TORC promotes stress resistance in Drosophila. *Cell Metab*. 7:434-444.

Wang, Z., H. Takemori, S.K. Halder, Y. Nonaka, and M. Okamoto. 1999. Cloning of a novel kinase (SIK) of the SNF1/AMPK family from high salt diet-treated rat adrenal. *FEBS Lett*. 453:135-139.

Webb, B.L., S.J. Hirst, and M.A. Giembycz. 2000. Protein kinase C isoenzymes: a review of their structure, regulation and role in regulating airways smooth muscle tone and mitogenesis. *Br J Pharmacol*. 130:1433-1452.

Weissbach, H., B.G. Redfield, and J. Axelrod. 1960. Biosynthesis of melatonin: enzymic conversion of serotonin to N-acetylserotonin. *Biochim Biophys Acta*. 43:352-353.

Wen, A.Y., K.M. Sakamoto, and L.S. Miller. 2010. The role of the transcription factor CREB in immune function. *J Immunol*. 185:6413-6419.

Wettschureck, N., and S. Offermanns. 2005. Mammalian G proteins and their cell type specific functions. *Physiol Rev*. 85:1159-1204.

Wu, Z., X. Huang, Y. Feng, C. Handschin, P.S. Gullicksen, O. Bare, M. Labow, B. Spiegelman, and S.C. Stevenson. 2006. Transducer of regulated CREB-binding proteins (TORCs) induce PGC-1alpha transcription and mitochondrial biogenesis in muscle cells. *Proc Natl Acad Sci U S A*. 103:14379-14384.

Wynshaw-Boris, A., J.M. Short, D.S. Loose, and R.W. Hanson. 1986. Characterization of the phosphoenolpyruvate carboxykinase (GTP)

promoter-regulatory region. I. Multiple hormone regulatory elements and the effects of enhancers. *J Biol Chem*. 261:9714-9720.

Xu, W., L.H. Kasper, S. Lerach, T. Jeevan, and P.K. Brindle. 2007. Individual CREB-target genes dictate usage of distinct cAMP-responsive coactivation mechanisms. *EMBO J*. 26:2890-2903.

Yamamoto, K.K., G.A. Gonzalez, W.H. Biggs, 3rd, and M.R. Montminy. 1988. Phosphorylation-induced binding and transcriptional efficacy of nuclear factor CREB. *Nature*. 334:494-498.

Yang, W., Y.H. Hong, X.Q. Shen, C. Frankowski, H.S. Camp, and T. Leff. 2001. Regulation of transcription by AMP-activated protein kinase: phosphorylation of p300 blocks its interaction with nuclear receptors. *J Biol Chem*. 276:38341-38344.

Yin, J.C., J.S. Wallach, M. Del Vecchio, E.L. Wilder, H. Zhou, W.G. Quinn, and T. Tully. 1994. Induction of a dominant negative CREB transgene specifically blocks long-term memory in Drosophila. *Cell*. 79:49-58.

Yuan, L.W., and J.E. Gambee. 2000. Phosphorylation of p300 at serine 89 by protein kinase C. *J Biol Chem*. 275:40946-40951.

Zatz, M. 1985. Phorbol esters mimic alpha-Adrenergic potentiation of serotonin N-acetyltransferase induction in the rat pineal. *J Neurochem*. 45:637-639.

Zemkova, H., S.S. Stojilkovic, and D.C. Klein. 2011. Norepinephrine causes a biphasic change in mammalian pinealocye membrane potential: role of alpha1B-adrenoreceptors, phospholipase C, and Ca2+. *Endocrinology*. 152:3842-3851.

Zhang, L., W. Zhou, V.E. Velculescu, S.E. Kern, R.H. Hruban, S.R. Hamilton, B. Vogelstein, and K.W. Kinzler. 1997. Gene expression profiles in normal and cancer cells. *Science*. 276:1268-1272.